ISTANBUL TECHNICAL UNIVERSITY ★ GRADUATE SCHOOL OF SCIENCE ENGINEERING AND TECHNOLOGY

THERMO-ELASTIC ANALYSIS AND MULTI OBJECTIVE OPTIMAL DESIGN OF FUNCTIONALLY GRADED FLYWHEEL FOR ENERGY STORAGE SYSTEMS

M.Sc. THESIS

Alper UYAR

Department of Aeronautics and Astronautics Engineering

Aeronautics and Asgtronautics Engineering Programme

JUNE 2018

ISTANBUL TECHNICAL UNIVERSITY ★ GRADUATE SCHOOL OF SCIENCE ENGINEERING AND TECHNOLOGY

THERMO-ELASTIC ANALYSIS AND MULTI OBJECTIVE OPTIMAL DESIGN OF FUNCTIONALLY GRADED FLYWHEEL FOR ENERGY STORAGE SYSTEMS

M.Sc. THESIS

Alper UYAR
(511091122)

Department of Aeronautics and Astronautics Engineering

Aeronautics and Astronautics Engineering Programme

Thesis Advisor: Prof. Dr. İbrahim ÖZKOL

JUNE 2018

ISTANBUL TEKNİK ÜNİVERSİTESİ ★ FEN BİLİMLERİ ENSTİTÜSÜ

ENERJİ DEPOLAMA SİSTEMLERİ İÇİN FONKSİYONEL DERECELENDİRİLMİŞ VOLAN TERMOELASTİK ANALİZİ VE ÇOK PARAMETRELİ OPTİMİZASYONU

YÜKSEK LİSANS TEZİ

Alper UYAR
(511091122)

Uçak ve Uzay Mühendisliği Anabilim Dalı

Uçak ve Uzay Mühendisliği Programı

Tez Danışmanı: Prof. Dr. İbrahim ÖZKOL

HAZİRAN 2018

Alper Uyar, a M.Sc. student of İTU Graduate School of Science Engineering and Technology student ID 511091122, successfully defended the thesis entitled "**THERMO-ELASTIC ANALYSIS AND MULTI OBJECTIVE OPTIMAL DESIGN OF FUNCTIONALLY GRADED FLYWHEEL FOR ENERGY STORAGE SYSTEMS**", which he prepared after fulfilling the requirements specified in the associated legislations, before the jury whose signatures are below.

Thesis Advisor :	**Prof. Dr. İbrahim Özkol** İstanbul Technical University	.....
Jury Members :	**Prof. Dr. Erol Uzal** İstanbul University	.....
	Assoc. Prof. Dr. Aytaç Arıkoğlu İstanbul Technical University	.....

Date of Submission : 03 May 2018
Date of Defense : 01 June 2018

To my loves Emel and Mehmet Alp,

FOREWORD

I would like to express my sincere gratitudes to my thesis supervisor Professor İbrahim Özkol for his guidance and valuable advices during this study.
I am so grateful to Associate Professor Güven Kömürgöz as well for her support and encouragements.
Deepest thanks to Associate Professor Aytaç Arıkoğlu for his close friendship and precious support during the development and completion of this study.
With this opportunity, I also would like to express deepest regards and appreciation to my parents for all the sacrifices they made while raising me.
Finally, my most sincere gratitudes are for my wife and my son for whom I have always been thankful to God for their presence. They felt the challenge at least as much as me during this study. It is impossible to find a proper word to express my appreciation for their endless love, passion and support!

June 2018

Alper UYAR
Aeronautical Engineer

TABLE OF CONTENTS

Page

ABBREVIATIONS

AMB **:** Active Magnetic Bearing
AC **:** Alternative Current
DC **:** Direct Current
DQM **:** Differential Quadrature Method
FESS **:** Flywheel Energy Storage System
FEM **:** Finite Element Method
FGM **:** Functionally Graded Material
GA **:** Genetic Algorithm
GDQM **:** Generalized Differential Quadrature Method
IM **:** Induction Machine
NSGA **:** Non Dominated Sorting Algorithm
PMB **:** Passive Magnetic Bearing
PMSM **:** Permanent Magnet Synchronous Machine
RES **:** Renewable Energy Sources
SMB **:** Superconducting Magnetic Bearing
SRM **:** Switched Reluctance Machine
UPS **:** Uninterruptable Power Supply

SYMBOLS

ω	: Angular velocity
u	: Displacement vector component
σ_r, σ_θ	: Normal stress components in radial and hoop direction
σ_{VM}	: Von Misses equivalent stress
ε_r, ε_θ	: Normal **s**train components in radial and hoop direction
h	: Thickness
I	: Mass moment of inertia
T	: Temperature
ρ	: Density
α	: Thermal expansion coefficient
k	: Thermal conductivity coefficient
ν	: Poisson ratio
α	: Angle of deviation from the direction of the principal stresses
c_{ij}	: Weighting coefficients for the derivatives
P_m	: Mutation probability
P_c	: Crossover probability

LIST OF TABLES

Page

LIST OF FIGURES

Page

THERMO-ELASTIC ANALYSIS AND MULTI OBJECTIVE OPTIMAL DESIGN OF FUNCTIONALLY GRADED FLYWHEEL FOR ENERGY STORAGE SYSTEMS

SUMMARY

In this study, thermo-elastic analysis and a multi objective optimal design of a functionally graded Flywheel rotor that can be used in a Flywheel Energy Storage System (FESS) has been investigated. Due to the rapid mechanization and technological innovations that have taken place since the industrial revolution, our energy need has been increasing at an unprecedented rate. On the other hand, limited availability of known energy resources makes it necessary to find solutions that enables more efficient use of energy. One of the solutions to enhance energy efficiency is to store excess production for future usage. In this context, Flywheel energy storage applications for storing electrical energy have gained a great interest in recent years.

Flywheel energy storage systems are in favorable position among others due to their strengths in high energy capacity, fast response, long life, low maintenance and environmentally friendly characteristics. Recent advancements in lightweight high strength materials, power electronics and magnetic bearings have made high speed FESS applications possible today. Obviously, those high speed applications such as turbo machinery components, high speed compressors, brake disks, gears, pumps, generators are of practical interest in engineering. Therefore, development of FESS systems has become a popular research topic for scientists and engineers nowadays.

Flywheel energy systems are based on a rotating mass principle. In a FESS, electrical energy is converted into the mechanical energy and stored in the Flywheel rotor as rotational kinetic energy. Energy conversion is achieved by means of an electric motor and a bi-directional power converter. Flywheel rotor is the key element to determine the overall performance and capacity of the system. Energy capacity of a Flywheel rotor can be increased by using materials that is capable of resisting loads at high rotational speeds. Functionally graded materials which is a special kind of composites can be used for this purpose.

For this reason, the subjected Flywheel rotor in this study has been assumed to be made of a functional graded material. For the thermo elastic analysis, a complex nonlinear differential equilibrium equation has been established. The complexity came from several factors such as non uniform thickness Flywheel geometry, non homogenous material content and by taking into account of the thermal effects on material properties. The governing equation of motion solved numerically by using generalized differential quadrature method (GDQM). Results of numerical solution has been validate by comparison with an axisymmetric two dimensional finite element model. A perfect correlation of both approaches has been demonstrated.

Flywheel shape optimization task has been carried by using non dominated sorting genetic algorithm (NSGA II). Optimal designs have been searched for 18 design spaces having different speed, thickness and radius limits. Depending on the bearing type, maximum speed of the flywheel can be two types such as low speed and high speed. In 9 of the design spaces it has been assumed that conventional mechanical

bearings were used. Hence, these designs had a maximum rotational speed limit of 10000 rpm. The other 9 design spaces assumed to have magnetic bearings. Therefore, those designs had a maximum rotational speed limit of 100000 rpm.
The optimization problem is defined to maximize the average kinetic energy that the flywheel can store between an ambient temperature range without failure and without exceeding rotational speeds allowed by the bearings while minimizing the mass. The genotype of individuals have been constructed by a mixed type encoding such that thickness (h) and volume fraction coeffficient (m) has been encoded by 15 bit Gray coding and materials are encoded by value encoding. For generating child populations a multi point crossover has been used. Additionally, bit invertion and value changing mutations has been applied to the chromosomes. Genetic algorithm code have generated 1000 populations each of them having 1000 individuals. Therefore 1 million potential candidates have been evaluated for each design space. For the material content, random combinations of two materials out of three possibles (Ti-6Al-4V, Inconel 718, AISI 4340) have been selected for each designs. Optimization results have been achieved by using the Numerical solver and the Genetic algorithm code simultaneously and iteratively for each solution.

Optimization study has presented following results,

- At constant speed, size of the outer radius is the most effective design parameter in terms of the energy capacity. For reaching a higher energy capacity a bigger Flywheel size is reqiured. However, as the size gets bigger the stresses induced due to the centrifugal force increases proportional to the square of the radius of the Flywheel.
- At high speeds the stress concerns becomes more evident such that, maximum design speed can not be achieved due to the violation of the stress limit. In such cases, algorithm starts another loop to determine the maximum allowable speed before continuing the other steps. In other words at high speed designs maximum rotational speed becomes another design variable. Therefore, computational efforts highly increases for high speed design searches. Consequently the convergence speed substantially decreases.
- For low speed designs, maximum design speed (10000rpm) is achievable without violating any optimization criteria. Whereas, for the high speed applications, maximum achievable speed can not be attained due to stress constrains. For high speed designs maximum achievable speed depends on the Flywheel material and geometry considered.
- For the optimal shape, the algorithm tries to increase the mass near the outer edge to increase the energy capacity. Whereas, near the inner edge mass has been increased in order to reduce stresses. In middle sections, algorithm has kept as minimum thickness as possible to reduce the weight of the design.
- For material composition, algorithm allocates the lighter materials near outer radius. Whereas, the heavier materials are placed as possible as at the inner radius region in order to reduce stresses caused by the centrifugal loads. Additionally, algorithm tends to allocate AISI4340 to increase the stored energy due to its high density and strength. Whereas, for low energy capacity designs Ti-6Al-4V has been used to minimize the mass. Inco 718 has been used together with these materials to fine tune the designs with its medium properties. Some of the designs seem to have only one material content instead of a mixed FGM structure. Therefore, it can be said for some optimal designs

homogenous material structure is the best choice to provide the optimal energy storage.

- Some of the designs seem unrealistic due to very thin web sections. For such solutions the study may be developed further to take into account of resonance vibration effects.

ENERJİ DEPOLAMA SİSTEMLERİ İÇİN FONKSİYONEL DERECELENDİRİLMİŞ VOLAN TERMOELASTİK ANALİZİ VE ÇOK PARAMETRELİ OPTİMİZASYONU

ÖZET

Bu çalışmada enerji depolama sistemlerinde kullanılabilecek, fonksiyonel derecelendirilmiş bir volanın termoelastik analizi ve çok parametreli optimizasyonu gerçekleştirilmiştir. Sanayi devriminden bu yana gerçekleşen teknik ilerlemeler hızlı bir makineleşme sürecini beraberinde getirmiştir. Bu sayede, insanoğlu geçmişte el yordamıyla yaptığı pek çok işi günümüzde makinelere yaptırır hale gelmiştir. Gelinen noktada insanoğlunun hayat standartlarını yükselten teknolojik gelişmeler modern hayatımızın vazgeçilmez bir parçası haline gelmiştir. Bu durum ise, bir makine veya makine sistemin temel girdisi olan elektrik enerjisini günümüzde en çok ihtiyaç duyulan değerlerden biri haline getirmiştir. Ekonomik ve teknik gelişmelere paralel olarak gittikçe daha fazla sayıda insanın endüstriyelleşme ve teknolojik nimetlerden faydalanmaya başlayacağı gözönüne alındığında, gelecekte enerjiye olan ihtiyacımızın bugünki ihtiyaçtan çok daha fazla olacağı açıktır.

Öte yandan, kullanılabilir enerji kaynaklarının mevcut tüketim hızıyla bile ancak birkaç yüzyıl yeteceği öngörüsü göz önüne alındığında, enerji üretiminde alternatif kaynaklara yönelim ve daha önemlisi üretilen enerjinin daha verimli kullanılmasını sağlayan çözümler bulmak bir zorunluluk olarak karşımıza çıkmaktadır. Bu yönelimin bir sonucu olarak, elektrik üretimi havuzunda fosil yakıtların yanında rüzgar ve güneş enerjisi gibi yenilenebilir enerji kaynaklarından elde edilen enerjinin payı gün geçtikçe artmaktadır. Ancak yine de, yenilebilir enerji sistemlerinin enerji üretiminin birincil elemanı haline gelebilmesi için çözülmesi gereken bazı zayıflıkları bulunmaktadir. Bu zayıflıkların en başta gelenlerinden bir tanesi sözkonusu sistemlerin çıktılarının hava koşullarına ve mevsimsel değişimlere bağımlı oluşu ve dolayısıyla enerji üretiminin kesintili yada dalgalı bir profile çizmesidir. Bu karakteristik nedeniyle arz ve talebi eşleştirmek çoğu durumda mümkün olmamaktadır. Talebin yüksek olduğu zamanlarda üretim düşük kalabilmekte veya üretim yüksek olduğunda talep yetersiz gelebilmektedir. Bu durum sözkonusu sistemlerin tek başına kullanılması halinde verimlerinin düşük kalmasında veya verimi yüksek tutabilmek için mutlaka gas türbini gibi yan sistemlerle desteklenmesini gerekli kılmaktadır.

Bu noktada, ihtiyaçtan fazla üretilen enerjinin gelecekteki kullanımlar için depolanmasi fikri enerji verimliliğini artıracak çözümlerden biri olarak ortaya çıkmaktadır. Bu bağlamda, elektrik enerjisini depolamak için kullanılan Volan Enerji Depolama Sistemi (VEDS) uygulamaları son yıllarda büyük ilgi uyandırmaktadır. Volan enerji depolama sistemleri yüksek depolama kapasitesi, hızlı cevap verebilme, uzun ömür, düşük bakım gereksinimi ve çevresel etkisinin sıfıra yakın olması gibi avantajları sebebiyle diğer alternatif çözümlere kıyasla daha iyi bir konumda bulunmaktadır. Son yıllarda yüksek mukavemetli hafif malzemelerin üretim ve kullanımının yaygınlaşmasının yanı sıra, güç elektroniği ve manyetik rulman teknolojisi alanlarındaki gelişmeler de yüksek hızlı VEDS uygulamalarına imkan vermiştir. Günümüzde VEDS uygulamaları büyük ölçekteki enerji üretim hatlarından

bireysel kulllanıcı seviyesindeki kesintisiz güç kaynağı uygulamalarına, hatta otomotiv, uzay araçları ve askeri uygulamalara kadar pek çok yerde karşımıza çıkmaktadır. Buna benzer uygulamaların daha da yaygınlaşması için sözkonusu enerji depolama sistemlerinin daha detaylı incelenmesi ve sınırlarının anlaşılması gerekmektedir. Bu nedenle, VEDS sistemlerinin geliştirilmesi günümüzde bilim adamları ve mühendisler için popüler bir araştırma konusu haline gelmiştir.

Volanlı enerji sistemleri, elektrik enerjisinin dönen bir kütle bünyesinde dönme kinetik enerjisi şeklinde depolanması prensibine dayanmaktadır. Bir VES'de, elektrik enerjisi kinetik enerjiye dönüştürülürek Volan rotorunda depolanır. Enerji dönüşümü, bir elektrik motoru/jeneratörü ve çift yönlü bir güç dönüştürücü aracılığıyla sağlanır. Enerji depolama sırasında elektrik motoru Volan rotorun hızını artırırken; depolanan enerjinin harcanması sırasında Volan rotoru jeneratörü besler ve hızını kaybeder. Volan rotoru, sistemin genel performansını ve kapasitesini belirleyen temel elemandır. Sistemin enerji depolama kapasitesini arttırmak için Volan rotorunun yüksek hızlara çıkabilmesi gerekmektedir. Bunun içinse, Volan rotorunun, yüksek dönme hızlarında ortaya çıkan yüklere direnç gösterebilen malzemelerden üretilmesi gerekmektedir. Özel bir tür kompozit malzeme olan fonksiyonel dereceli malzemeler böyle bir amaç için kullanılabilir.

Fonksiyonel dereceli malzemeler, birden fazla ana malzemenin mekanik özelliklerinin bir doğrultu boyunca sürekli bir fonksiyon şeklinde değişmesiyle elde edilen bir tür komposit malzemedir. Bu sayede farklı malzemelerin üstün özelliklerini bünyesinde barındıran heterojen yapılı malzemeler elde edilebilmek amaçlanmaktadır. Fonksiyonel dereceli malzemeler, mühendislik uygulamalarında sıklıkla karşılaşılan yüksek mukavemetli, yüksek ısıl dayanıma sahip aynı zamanda da son derece hafif yapılı malzeme ihtiyacına güçlü bir çözüm sunmaktadır. Bu nedenle bu çalışma sırasında fonksiyonel derecelendirilmiş malzeme yapısına sahip bir Volan diski ele alınmıştır. Ana malzeme tipleri, özellikle turbomakinelerde yaygın kullanılan, Ti-6Al-4V, Inconel 718 ve AISI 4340 olarak belirlenmiş ve herbir tasarımda bu malzemelerin rastgele seçilmiş ikili kombinasyonları değerlendirilmiştir. Fonksiyonel dereceleme için malzeme kompozisyonun Volan diskinin iç çapından dış çapına doğru radyal yönde bir üstel fonksiyona uygun şekilde değiştiği varsayılmıştır.

Termoelastik analiz çalışması için, öncelikle değişkn kalınlıklı dönen bir disk için denge denklemi genel halde elde edilmiş, ardından sözkonusu denklem, foksiyonel dereceli malzeme yapısı ve sıcaklığa bağlı değişkenleri gösterecek şekilde düzenlenmiştir. Benzer şekilde sınır koşulları için de denge denklemleri bulunmuştur. Ortaya çıkan lineer olmayan diferansiyel denklemler elle çözülemeyecek kadar karmaşık yapıda olduğundan denklem çözümü için sayısal bir metod olan diferansiyel kuadratür metodu uygulanmıştır. Diferansiyel kuadratür metodu, verilen bir aralığın her noktasında sürekli ve türevli olan bir fonksiyonun bilinmeyen bir türev ifadesine, fonksiyonun bir grid hattı boyunca tüm fonksiyonel değerlerinin ağırlıklandırılmış bir toplamı şeklinde yaklaşım yapılabileceği temeline dayanan bir sayısal yöntemdir. Sonlu elemanlar, sonlu farklar yada sonlu hacimler gibi diğer sayısal metodlara göre çok daha az sayıda nokta kullanarak yeterince doğru sonuçlar vermesi nedeniyle DKM metodu son yıllarda parçalı diferansiyel denklem çözümü gerektiren problemler sözkonusu oldugunda gittikçe artan bir uygulama alanı bulmaktadır. Ele alınan termoelastik analiz problemi DKM metodu ile çözülerek, Volan diski boyunca sıcaklık dağılımı, radyal deplasmanlar, gerinme ve gerilme değerleri elde edilmiştir.

Matematiksel model ve varsayımların doğruluğu, sayısal çözüm sonuçlarının iki boyutlu eksenel simetrik bir sonlu elemanlar modeli çözümleriyle kıyaslanarak yapılmıştır. Termal ve mekanik analiz sonuçları incelendiğinde, diferansiyel kuadratür

ve sonlu elemanlar metodlarının birbiyle son derece uyumlu sonuçlar verdiği gösterilmiştir.
Optimizasyon problemi, -20 ile +40 santigrad derece arasındaki bir ortam sıcaklığında dayanım şartlarını aşmaksızın ve rulmanların izin verdiği maksimum hız limitleri dahilinde ortalama kinetik enerjiyi maksimum yaparken kütleyi de mimimum yapacak bir Volan geometrisini elde etmek olarak belirlenmiştir. Optimizasyon çalışması içim özel bir tür evrimsel algoritma olan NSGA II metodu izlenmiştir. Tasarım adayları için karma kodlama yapılmış, eşleşme ve mutasyonlar yoluyla yeni nesiller türetilerek toplamda 18 farklı tasarım tipindeki Volan diskleri için en iyi geometriler aranmıştır. Tasarım tipleri kullanılan rulman çeşidine bağlı olarak yüksek hızlı ve düşük hızlı olmak üzere iki gruba ayrılmıştır. Düşük hızlı tasarımlar icin maksimum hız limiti 10000 rpm, yüksek hızlı tasarımlar içinse 100000 rpm olarak belirlenmiştir. Her bir tasarım tipi için, toplam 1000 iterasyon sonunda birer milyon aday çözüm oluşturulmuş ve değerlendirilmiştir. Optimizasyon çalışması aşağıdaki sonuçları ortaya koymuştur.

- Hız sabit iken, enerji kapasitesini etkiyelen en önemli parametre disk çapıdır. Enerji kapasitesini arttırmak için büyük çaplı disk kullanmak gerekmektedir. Ancak disk çapı büyüdükçe merkez kaç kuvveti nedeniyle oluşan stress te disk yarıçapının karesiyle orantılı olarak artmaktadır.
- Yüksek hızlarda stress etkileri tasarımı limitleyen bir hale gelmektedir, öyle ki izin verilen maksimum hızlara çıkmak mümkün olmamakta bu nedenle algoritma, stress koşullarını sağlayabilecek bir maksimum hız aramaya başlamaktadır. Yüksek hızlı çözümler için elde edilebilecek en yüksek hız 60000 rpm civarı olarak görülmektedir.
- Optimum Volan geometrisi genel olarak iç ve dış kenarlarda malzeme miktarını arttırırken orta kesimlerde azaltacak şekilde oluşmaktadir.
- Malzeme komposizyonu, Volan dış kenarına doğru daha hafif malzemeler kullanırken iç kenarlara doğru daha yoğun malzemelerin kullanılması gerektigini göstermektedir.
- Elde edilen bazı geometriler son derece ince kesitli profiller vermiştir. Bu çözümler optimizasyon algoritmasının ince kesitlerdeki titreşim etkilerinin de gözönüne alınarak geliştirilmesi gerektiği konusunda fikir vermektedir.

1. INTRODUCTION

After industrial revolution in mid 18th century, energy has become one of the main need of our modern society. As the population of the world increases and people strive for a higher standard of living, the amount of energy to sustain our society is ever increasing [1]. According to International Energy Agency reports the world's energy demand will increase from about 12 billion tonne oil equivalents (t.o.e.) in 2009 to either 18 billion t.o.e. or 17 billion t.o.e. by 2035 [2]. On the other hand, availability of known energy resources such as fossil fuels are rapidly shrinking. Therefore, efficient use of limited energy resources is becoming an important issue day after day.

The efficiency in energy consumption can be achieved by reducing losses. One method of reducing losses is to store excessive energy production for later usage. Energy can be stored in several way such as electrical, mechanical and chemical. The idea of energy storage is based on transforming the energy into a more suitable and economical form, reserve, and re-transfom for usage when needed. For example, Electirical energy can be stored as chemical or mechanical forms. Chemical batteries have long been using to store electrical energy. However, they are inadequate in responding to the demand for long-life applications. Furthermore, chemical batteries have a limited energy capacity depending on its size. Hence, chemical batteries are not suitable for high energy density applications. Another major drawback associated with the chemical batteries is the disposal of dangerous chemical content.

On the other hand, the need for reliable, economical and environmentally friendly systems are increasing, especially for high scale energy production applications such as an electrical network or a grid. This is mainly due to the increasing contribution from renewable energy resources in the electric energy production mix. Power output of renewable energy resources (RES) such as Solar and Wind energy has intermittent characteristics due to their strict dependence on the weather conditions. Also, it is possible to happen seasonal or monthly variations in the production of energy because of the weather conditions [3]. Therefore, it is difficult to match the supply and demand. For example, when the high rate of production is available, the energy demand can be

low; or when availability is low demand can be high. At a time when RES are supplying energy, there may be low demand, but when the energy is demanded, it may exceed RES energy production [4]. Additionally, peak demands may result disturbances in the power network. Although it may last only a few seconds such disturbances may cause very high costs to the end users. Therefore, it is very important to increase the reliability of these sources to become as primary sources of energy. Flywheel energy storage systems (FESS) is a promising technology to answer this need. Recently, flywheel energy storage systems (FESS) have gained considerable attention among other alternatives due to several advantages such as high power density and high energy efficiency. With these attributes, flywheel energy storage systems compete with other storage technologies in electrical energy storage applications, as well as in transportation, military services, and space satellites [5]. Main advantages of FESS can be listed as below.

a) High power densities
b) Fast response times
c) Long cyclic life
d) No capacity degradation
e) Easy monitoring of the state of charge
f) Need for very little maintenance
g) No environmental impact

1.1 Flyhweel Energy Storage Systems

Flywheel is one of the oldest mechanical energy storage devices. It stores mechanical energy based on the rotating mass principle. Potters wheel in Figre 1.1 and stone grinders are some of the historical samples of flywheels. In early applications flywheel were made of wooden discs connected to an axle and driven by manually. In 18th century, with the advancement of casting technology steel flywheels started to appear on mechanical devices for smooth operation. However it took until the early 20th century before flywheel rotor shapes and rotational stresses were thoroughly analysed by Stodola A [6]. After 70's composite flywheels started to be used on high speed applications due to their high energy storage capacity. Recent developments in materials technology, magnetic bearings and power electronics makes it possible to operate at higher speeds and increases capacity of the flywheels even higher levels.

Figure 1.1 A Potter's wheel

1.1.1 Structure of a FESS

In a Flywheel energy storage system amount of the energy stored is a function of inertia of the mass (I), and the rotational speed (ω). Flywheel's speed increases when storing energy and reduces when delivering the stored energy. A modern flywheel energy storage system consists of five major components.

a) Flywheel rotor
b) Bearings
c) Generator/motor
d) Bi-directional power converter
e) Containment Housing (Enclosure)

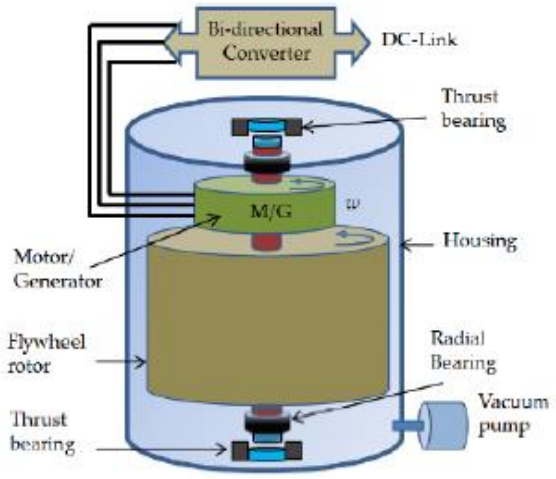

Figure 1.2 Structure of a FESS

1.1.1.1 Flywheel rotor

Energy is stored in the form of rotating kinetic energy in a flywheel. Amount of the energy is determined by the rotational speed, mass and the geometry of the flywheel rotor.

$$E_k = \frac{1}{2} I\omega^2 \left[J \right] \tag{1.1}$$

where,
$$I = \frac{1}{2} mr^2 \left[kg.m^2 \right] \tag{1.2}$$

Hence, for a hollow cylindrical flywheel of inner radius r_i and outer radius r_o the moment of inertia is,

$$I = \frac{1}{2} m\left(r_o^2 + r_i^2 \right) \tag{1.3}$$

For a flywheel shown in Figure 1.3 below, density ρ and the height of h the moment of inertia and the stored kinetic energy is,

$$I = \frac{1}{2} \pi\rho h\left(r_o^4 - r_i^4 \right) \tag{1.4}$$

$$E = \frac{1}{4} \pi\rho h\omega^2 \left(r_o^4 - r_i^4 \right) \tag{1.5}$$

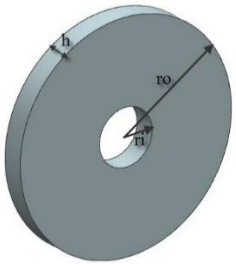

Figure 1.3 An annular disc

1.1.1.2 Bearings

Bearings support flywheel rotor and keep other components in the right position on the shaft to allow for rotation freely. Flywheel energy storage systems typically classified into two types depending on the speed of the application. In current technology level, FES up to 10,000 rpm is accepted as low speed applications whereas, beyond this speed is accepted as high speed application. Low speed applications allow for using conventional mechanical bearings whereas due to high friction losses and cyclic life concerns they are not suitable for high speed applications. High speed applications require magnetic bearings instead. Magnetic bearing is a fairly new technology and provides several advantages over conventional bearings. In a magnetic bearing there is no contact between shaft and the bearing. Shaft is supported by the repelling forces dynamically. Additionally, no lubrication is needed for the magnetic bearings. Hence, magnetic bearings can speed up to 100,000 rpms with minimum losses. There are mainly three types of magnetic bearings as Active Magnetic Bearing (AMB), Passive Magnetic Bearing (PMB) and Superconducting Magnetic Bearing (SMB). AMB uses controlled magnetic fields, where the force on the bearing axes is varied to compensate the movements of the wheel away from the equilibrium position [7]. PMB consist of permanent magnets and must be combined with another type of bearings as they are inherently unstable [8]. SMB takes the advantage of dia-magnetic behavior of superconductors therefore needs cyrogenic cooling system.

1.1.1.3 Generator / Motor

Generator/motor (GM) is the electrical machine in a FESS. GM provides an interface between Flywheel and the Bi-directional electric converter. GM has dual function. When functioning as a motor, GM drives the Flywheel by appling a Torque and causing it to accelerate. Hence Flywheel gains rotating kinetic energy. During stand-by mode, Flywheel maintains most of this energy due to its mass inertia. When functioning as a generator, GM receives mechanical torque from the Flywheel and causing it to slowdown, therefore consuming its kinetic energy.

In current applications several type of GM machines are being used. Some of the most common types are Permanent Magnet Synchronous Machine (PMSM), Switched Reluctance Machine (SRM) and Induction Machine (IM). . Main properties of these machines are briefly given in Table 1.1 below.

Table 1.1 Advantages and disadvantages of common electrical machines [9]**.**

	Advantages	Disadvantages
PMSM	No need for excitation	Risk of demagnetization
	No need for electrical wiring	Electromagnetic spinning losses at zero torque
	High overal efficiency	Low strength of PM material require structural support against centrifugal forces
	Highest power density	Sensitive to heating
IM	Demagnetization impossible	Poor overload capability
	No electromagnetic spinning losses	High maintenance
	Can be built low cost, high strength matierials	Add complexity to the rotor design due to the need of wiring
SR	Very robust	Low power density

1.1.1.4 Bi-directional power converter

Bi-directional power converter established the electrical interface of a FESS. Together with the GM, it makes the electrical/mechanical or mechanical/electrical energy conversion. Bi-directional power converter provides a means to connect Flywheel to the electrical machine via a DC-link. By swithcing, power converter also controls the electrical machine to function as either a motor or as a generator. For connecting to the AC grid, FESS needs another bi-directional power converter (DC/AC). The electrical machine is usually controlled to vary the torque as needed in order to keep the DC-link voltage constant. This is achieved by ordering motor/brake torque to accelerate/decelerate flywheel when the DC-link voltage rises/falls. Hence, the constant voltage DC-link behaves as an ideal DC voltage source analogous to a conventional electrochemical battery [8].

1.1.1.5 Containment housing

Flywheels operate at rotational speed of up to 100,000 rpm. At such speed aerodynamic friction becomes an important factor effecting the performance of the system since it is proportional to the speed and the density of the gas. For this reason, flywheel needs to operate in a controlled environment. Main function of the containment housing in a FESS is to provide a vacuum (or low pressure) enclosure in order to reduce aerodynamics friction losses coming from the surrounding gases. Due to its high speed, energy stored in a flywheel can be in the order of Million joules. In case of a failure, this energy has to be retained without impacting the safety around.

For this matter, Flywheel housing has to be carefully designed so that it is able to keep fragments of the flywheel in case of any catastrophic failure such as disc burst.

1.1.2 Applications of FESS

Flywheels have been used in wide range of field applications including Electrical network, UPS, Vehicle traction, Space and Military. In large scale, FESS can be used for grid stability and Voltage Sag control of electrical networks. As with the increasing contribution from renewable energy resources in the electricity production, power quality and stability issues becomes more important. Therefore, flywheel energy storage systems can smooth out interruptions in energy production and can help balancing the supply and demand. On the other hand, in small scale uninterrupted power supply applications Flywheels provides better cost efficiency due to their long service life of more than 20 years [7]. For the UPS applications FESS can be used as power backup devices from low to medium power range. On vehicles, FESS can either be used for improving traction or to provide hybrid power. Additionally, for space applications FESS can be used for satelite altitude control and power backup. In military, energy demand of marine based systems can be met by using FESS due to their long service life.

1.2 Functionally Graded Materials

Functionally graded materials are a kind of composites that allows to obtain hybrid materials having a smooth combination of base materials in any arbitrary partition. This is achieved by changing material properties continuosly along the spatial directions. In this way, material microstructure can be designed to gain benefit from desired mechanical or physical properties of different materials. The concept of FGM was proposed in 1984 by a group of material scientist in Sendai, Japan[10]. There are many advantages of functionally graded materials. For example, low density, high strength and in the meantime high thermal resistant materials can be produced which is of importance for space vehicle applications. Local stress concentrations on an iterrupted designs can be alleviated or residual stresses can be minimized, fatigue life of a rotating disc can be increased or dynamic stability of a plate can be improved. Additionally, combination of different material which is difficult or impossible with

the current manufacturing technologies can get together with this method. Metal and ceramic bonded applications can be done.

Because of these advantages FGMs have been attracting a great interest by the researchers in recent years. Althoguh it can be applied in various applications, recent studies on this topic mostly focused on improving the performance of high speed rotating discs due to practical concerns in many engineering applications such as high speed compressors, gas turbine engines, brake disks, gears, pumps, generators and flywheels.

One of the major inhibiting factors that limit the interest in Functionally graded materials has been the lack of economical fabrication processes [11]. However, recent developments in manufacturing technologies such as layered manufacturing or additive technology makes it possible to produce such non homogenous structures for various applications.

1.3 Literature Review

Flywheel is the key element to determine the performance and capacity of Flywheel energy storage system. For this reason, there have been several studies focused on the optimization of flywheels in literature. For the optimal flywheel design, earliest studies goes back to late nineteenth century when Stodola [6] first analysed the stress distribution in an arbitrary shaped rotating disk thorougly. He then, studied different disc configurations in an effort to find the best geometry to give the unifrom stress distribution. His idea was that, maximum achieveable energy of the disk can be achieved when all pieces of the disc reaches its maximum allowable stress without failure. Since then a vast number of studies have been presented in literature. In one of the earlier studies, Sandgren and Ragsdell [12] provided a general solution procedure to obtain optimal flywheel profile. They applied Fourier sine series approach to obtain a continuously differentiable thickness function along the radius and derived the differential equation for the stress components. Then they formulated the two point boundary value problem as a nonlinear programming problem and solved for various objectives such as maximum energy and minimum volume. Later, Ebrahimi [13] represented the thickness function as a polynomial expansion and formulated the nonlinear optimization problem for maximizing the ratio of inertia over volume. By applying a multiple shooting technique he was able to prove that the optimum flywheel

geometry has significantly more energy storage capacity comparing to its uniform thickness counterpart. Additionally, he demonstrated that carefully defined objective functions yield as much as 55% increased kinetic energy in the flywheel. Kress et al [14] created a two dimensional axisymmetric FEM to achieve best thickness distribution along the radius that yields an evenly stressed flywheel design with a central hole. In their study, Huang and Fadel [15] demonstrated a methodology for a heterogeneous flywheel design. Uniqe side of this study is that both shape and the material distribution are considered when optimizing the flywheel geometry. They investigated two configurations one consist of finite number distinct materials and the other consisting of two primary materials with a volume fraction grading. Profile of the flywheel were approached by Bezier curves in both designs to get smooth height distribution along the radius. For multi objective optimization, they defined the two objective functions as maximizing the kinetic energy and minimizing the difference between minimum and maximum Von Mises equivalent stresses subjected to the thickness upper and lower thickness limits together with the maximum mass and stress constraints. Results of this study demonstrated that, both heterogenous and homogenous flywheels have similar optimum profiles although heterogenous designs can store much more energy than homogenous flywheel designs. In another study, Huang and Fadel [16] presented a procedure for bi-objective optimal design of a functionally graded flywheel whose material microstructure consists of a combination of two primary materials. For material distribution, they used a generic distribution function instead of a commonly accepted power law function. Then, they provided a micromechanical analysis method for calculation of material properties. For material gradation authors selected Tin (Sn) and Aluminium Alloy 2124_T851. Former was selected due to its high density to favour maximizing the energy storage, whereas latter was selected due to its high strength. Flywheel geometry and material distribution were represented by Bezier curves. Two design criteria for the optimal Flywheel form were deteremined as maximizing kinetic energy and minimizing maximum equivalent stress. Bi objective optimization was reduced to single objective optimization by applying weighted Tchebycheff method. Analysis results showed that, thickness of the optimal geometry was highest at the inner diameter and smallest close to the middle of inner and outer radiuses. Arslan et al.[17] studied different flywheel geometries to investigate its impact on energy storage capacity. To do this, he created finite element models for six flywheel configuration and analyze them against maximum specific

energy objective function. Results proved that, Flywheel geometry has significant effect on energy sotrage capacity per unit mass. Another multi objective flywheel design study was presented by Krack and Secanell [18] for cost optimisation of flywheels. By using a scaling technique they reduced the problem into single objective aimed for maximizing energy per cost ratio. For finding optimal rim thicknes and rotational speed they employed a nonliner interior point method. The flywheel model they analyzed was having a split type hub instead of a ring. Purpose of this selection was to relief interference stresses at the shaft/hub joint and eliminate need for addhessives by facilitating the radial expansion during rotation. Analyse results demonstrated that, energy per cost value was 3.7% higher for the split type hub flywheel than the ring type. Mahdi et al. [19] investigated optimal solid flywheel disk profiles that gives maximum stored kinetic energy per unit mass subjected to maximum allowable equivalent stress. He represented flywheel geometries by using cubic spline curves and applied finite element method for numerical analyses. Results of this study was similar to those previosuly performed that maximum stresses occured near the center of the flywheel and thickness of the optimal geometry should be maximum in this region. In a novel approach for investigating the effect of flywheel profile on specific energy Aghaları and Kafiabad [20] used a combination of genetic algorithm and finite element method. Optimal flywheel geometry with this apporach showed a good correlation to the previous studies indicating a smaller thickness at the middle section and thicker sections at the edges. Additionally, for uniform tihckness flywheel maximum effective stress occured close to the center. Jiang and Zhang [21] conducted another shape optimization study to with the objective of maximizing energy density. They investigated two configurations, one was integrated shaft design the other one was interference fit flywheel design. For the analyses, they created a parametric finite element model where flywheel profile was obtained by spline curve fitting method. Then adopted a Downhill simplex algorithm to solve the nonlinear optimization problem under stress and size limits. Results of this study indicated that optimal shape design significantly improves the energy storage capacity of a flywheel. Later, in an effort to find the optimal structural layout of a flywheel Jiang and Wu [22] presented a topology optimization study by applying variable density method. Design objective was selected as maximizing the flywheel inertia. Optimization was carried under manufacturing constraints, stress constraints and volume fraction constraints.

Results of the study demonstrated that, a proper volume grading not only provides a high mass inertia but also results in a high energy density in the flywheel.

1.4 Purpose of the Thesis

In order to meet the ever-increasing need for energy, the human being has to try all the ways in his hand. For the continuation of the development of our civilization and for more people to live in more prosperity it is necessary to focus on the efficiency of supply and consumption of the energy.

On the production side, the trend towards alternative energy sources also brings with some weaknesses. For example, a wind power plant is extremely inefficient on days when the weather is stagnant or, can not respond to instantenous increases or decreases in the demand.

On consumption side, world atmosphere has been polluted increasingly by the carbon emissions of fossil fuels. Given the fact that one third of the carbon emissions in United States is from vehicles, it is even more frightening to predict the future pollution of the atmosphere when other developing countries completes their economical development.

On the storage side, it is obvious that conventional methods such as electrochemical batteries are insufficient to store the amount of energy to backup an energy grid network and cannot operatre on high cycle life. Furthermore, size and weight implications limited their vehicle applications. For example, a solar energry system of space satellite needs a light weight and long lasting power back up system when travelling on the dark side of its trajectory.

When all these issues are taken into account, it can not be ignored to importance of searching for system that increase energy efficiency.

Flywheels energy storage systems (FESS) can be a great supplement to energy production, consumption and conservation due to their advantages such as high capacity, fast response, high cycle life and low operation and maintenance costs over conventional methods. Flywheels can be used from power generation and transmission lines to personal cars, trains, data servers, backup power units, space vehicles almost everywhere that has a relation with energy. Therefore it has practical importance of focusing on the development of these systems. Flywheel rotor is the main element that

determines the performance of a Flywheel energy storage system. For example, a FESS system can be further improved by using composite flywheel rotor. On the other hand, recent studies in materials and manufacturing technologies are dealing with Functionally graded materials which is a special type of composite materials.

Under the light of all these considerations, the purpose of this thesis has been determined as investigating the multi objective optimal design of a variable thickness FGM Flywheel rotor disc that can be used in a Flywheel energy storage application.

1.5 Methodology

In this study, thermo elastic analysis and a multi objective optimal design of a Flywheel rotor has been studied. Flywheel geometry has been constructed by the thickness values at 12 locations along the radius. End points of those 12 locations have been connected to each other by cubic spline curves to establish the shape of the Flywheel. Design optimality is based on finding the best flywheel geometry to maximize energy storage capacity in a minimal mass without failing to withstand thermal and mechanical loads. In order to accomplish this, below steps have been followed.

Mathematical model construction: At first step, mathematical model of the Flywheel has been established. To do this, governing equation of motion for a rotating disc has been obtained in general form. Then, functionally graded and temperature dependent material variables have been adopted to obtain the differential equation. Boundary conditions have been obtained in a similar way.

GDQM discretization and solution: The resulting differential equations then dicretized by the generalized differential quadrature method (GDQM). With this method, the governing differential equations have become a set of linear equations with known boundary conditions. Obtained set of linear equations are solved by using Mathematica software.

Validation of results: For the validation of numerical results an axisymmetric finite element model has been built by using Ansys program. Thermal conductivity and stress analysis have been performed with the same boundary conditions as numerical solutions. Resulting stress and displacements from both solutions have been compared to make sure the accuracy of mathematical model and assumptions.

Optimization via Genetic Algorithm: Optimization has been carried by using Nondominated sorting genetic algortihm (NSGA II). For keeping the generality, it has not been focused on any specific size or application. Instead, 18 different design spaces that are categorized by the Flywheel size and operating speeds have been investigated during the optimization. Design space size have been kept large to make sure the space is searched thoroughly and we are not stuck at any sub optimal solution.

2. MATHEMATICAL MODEL

In developing the mathematical model, firstly governing force equilibrium equation and boundary conditions for a uniform thickness rotating disc is obtained in general form. Then, these equations are adopted to reflect functional graded material property variation and the thermal effects on a non-uniform thickness rotor disc. In order to obtain thermal effects, temperature distribution on the Flywheel geometry needs to be calculated. For calculation of temperature distribution, on each design a thermal conduction analysis are performed. As the boundary conditions for the thermal analysis, it is asssumed that the temperature is higher at the inner radius to take into account of the heat generation by the bearings and electrical motor on the shaft. On the other hand, temperature is equal to the ambient at the outer radius. Then, derived thermal and force equilibrium equations are solved respectively to obtain displacement and stress components. Numerical results are compared with a two dimensional axisymmetric Finite element model results.

2.1 FGM Properties

This study considers an axially symmetrical FGM flywheel rotor, where the composition of two materials between the flywheel root and tip are changed along the radial direction by a power law presented below [23].

$$P = P_i + \left(P_o - P_i\right)\left(\frac{r - r_i}{r_0 - r_i}\right)^m \tag{2.1}$$

where P is a mechanical or thermal property of interest, Pi and Po are the magnitude of this property at the inner radius rin and the outer radius rout, respectively and m is the volume fraction exponent that is a real number between zero and infinity. Figure 2.1 below shows material property distribution for different m values.

The effects of temperature not only on the mechanical and thermal properties of the flywheel material but also on the stress components are considered. Therefore,

Young's modulus (E), the Yield strength (σy), Thermal expansion coefficient (α) and Thermal conductivity coefficient (k) that show significant dependence on the temperature are considered as temperature varying while the Poisson's ratio (ν) and the Density (ρ) are assumed to be temperature invariant.

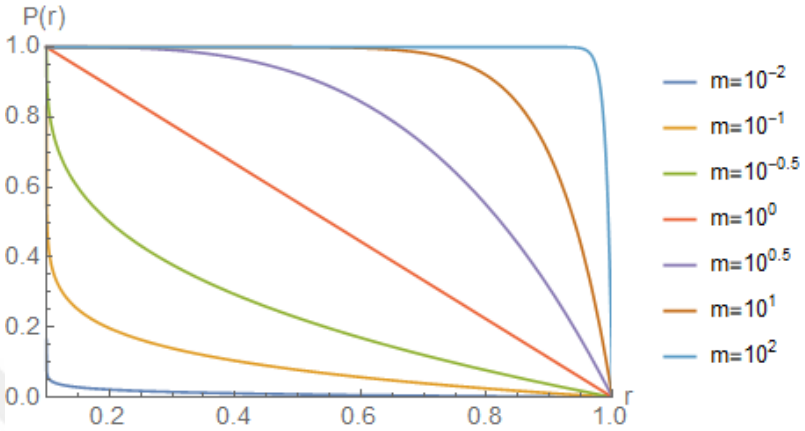

Figure 2.1 FGM material distribution

Functionally gradation of Ti-6Al-4V alloy, Inconel 718 and AISI 4340 steels are considered in the optimization analysis. The variation of material properties with respect to temperature (T) for these metals are extracted from Figures 2.2 to 2.5 available in [24]. Third order polynomials are fitted to these data as presented in Table2.1. Temperature dependent material properties in table below are third order polynomials in the form of:

$$P(T) = a_0 + a_1 T + a_2 T^2 + a_3 T^3 \qquad (2.2)$$

Table 2.1 Coefficients of fitted polynomials to the material data for 250K<T<500K

		a_0	a_1	a_2	a_3
Ti-6Al-4V	E_1 (GPa)	107.918	0.153378	-5.35879×10^{-4}	4.06819×10^{-7}
	$\sigma_{y,1}$ (MPa)	1414.87	-2.38389	1.43476×10^{-3}	-7.19190×10^{-8}
	α_1 (10^{-6} K^{-1})	7.70796	3.57776×10^{-3}	1.45392×10^{-6}	-3.16972×10^{-9}
	k_1 ($Wm^{-1}K^{-1}$)	-7.43730×10^{-2}	4.78728×10^{-2}	-1.08840×10^{-4}	9.92854×10^{-8}
	ρ_1 (kg/m^3)	4429	-	-	-
	ν_1	0.31	-	-	-
Inconel 718	E_2 (GPa)	220.962	-5.56780×10^{-2}	2.92575×10^{-5}	-3.42199×10^{-8}
	$\sigma_{y,2}$ (MPa)	1315.92	-1.47577	2.12002×10^{-3}	-1.06071×10^{-6}
	α_2 (10^{-6} K^{-1})	8.86433	1.65453×10^{-2}	-1.85187×10^{-5}	8.34362×10^{-9}
	k_2 ($Wm^{-1}K^{-1}$)	7.17170	1.62246×10^{-2}	-3.59047×10^{-6}	1.90972×10^{-9}
	ρ_2 (kg/m^3)	8221	-	-	-
	ν_2	0.29	-	-	-
AISI 4340	E_3 (GPa)	225.010	-0.131490	2.24956×10^{-4}	-2.18217×10^{-7}
	$\sigma_{y,3}$ (MPa)	1818.03	-1.05391	-4.41370×10^{-5}	2.56761×10^{-8}
	α_3 (10^{-6} K^{-1})	5.74645	2.66572×10^{-2}	-2.73622×10^{-5}	8.83699×10^{-9}
	k_3 ($Wm^{-1}K^{-1}$)	9.32328	0.144129	-2.21897×10^{-4}	9.86446×10^{-8}
	ρ_3 (kg/m^3)	7833	-	-	-
	ν_3	0.32	-	-	-

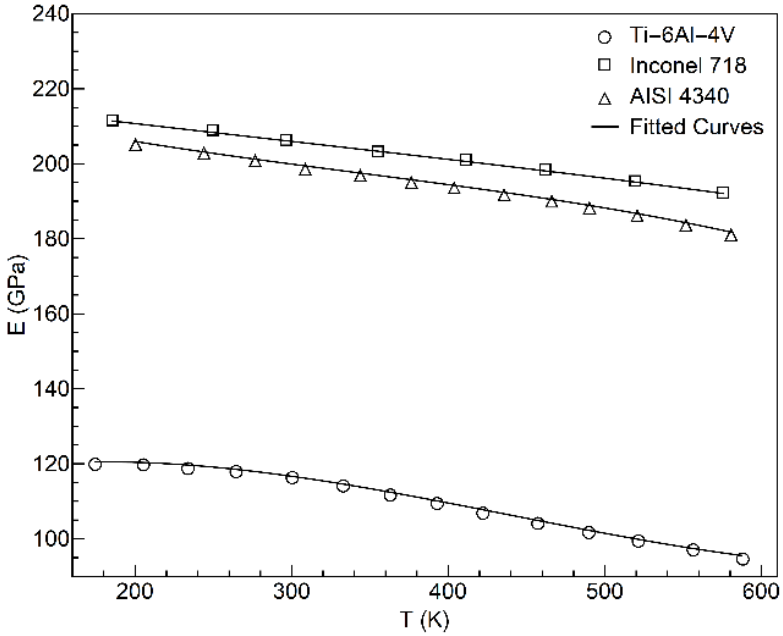

Figure 2.2 Temperature dependent Young modulus.

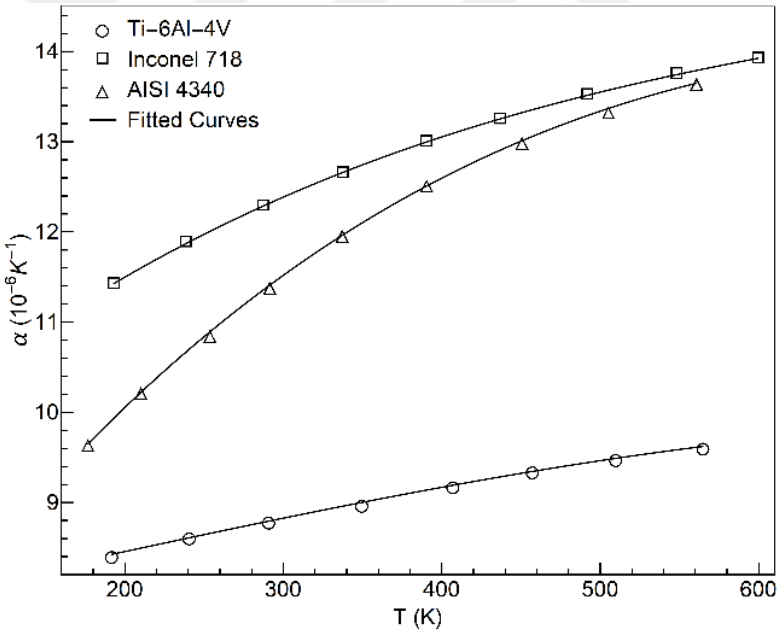

Figure 2.3 Temperature dependent Thermal expansion coefficients.

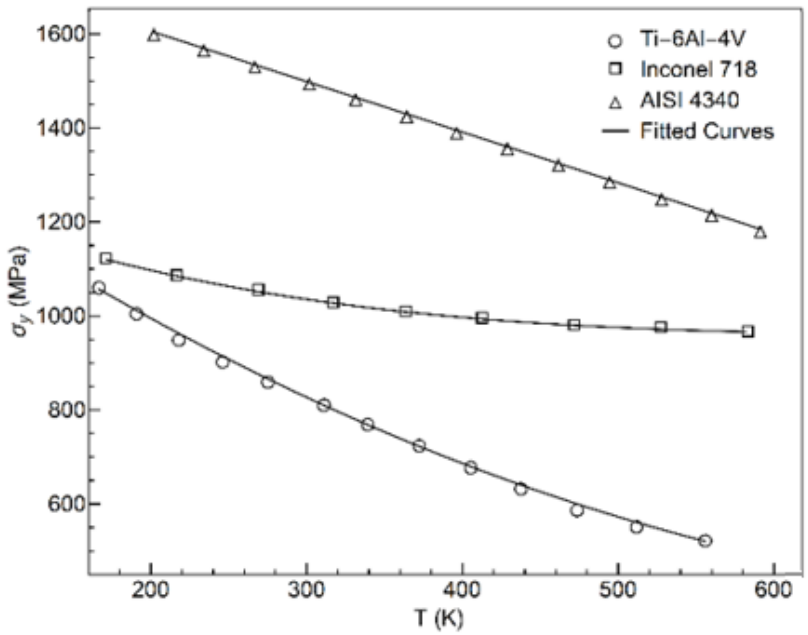

Figure 2.4 Temperature dependent Tensile yield strengths.

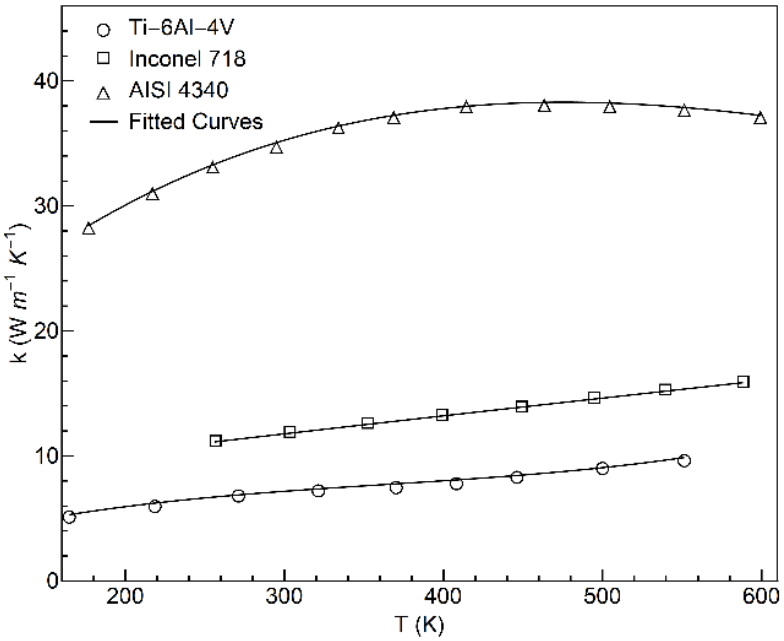

Figure 2.5 Temperature dependent Thermal conductivity coefficients.

2.2 Thermal Analysis

Thermal conductivity equation for a rotating disc of variable thickness can be derived by considering an annular ring depicted below in Figure 2.6.

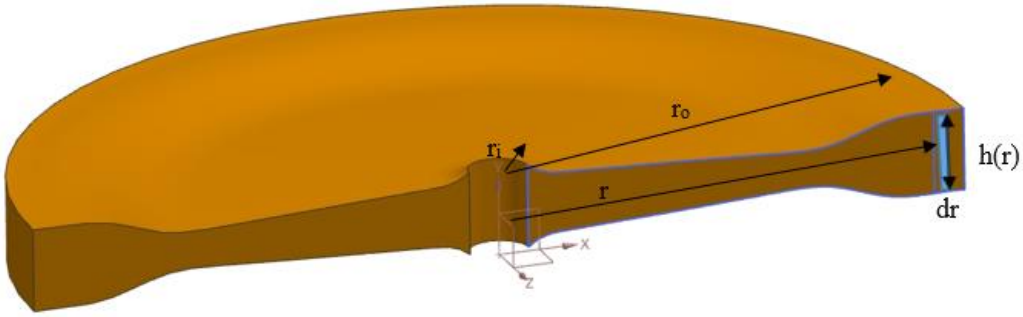

Figure 2.6 A nonuniform thickness annular disc section.

On inner ring surface;

$$\begin{aligned} r_i &= r \\ k_i &= k(r,T) \\ h_i &= h(r) \end{aligned} \tag{2.3}$$

On outer ring surface;

$$\begin{aligned} r_o &= r + dr \\ k_o &= k(r+dr,T) \\ h_o &= h(r+dr) \end{aligned} \tag{2.4}$$

Assuming that, inner surface is hotter than the outer surface, heat transfer from inner surface to outer surface can be formulated as follows,

$$-rh(r)k(r,T)\frac{dT}{dr}(r)+\left[(r+dr)h(r+dr)k(r+dr,T)\frac{dT}{dr}(\mathrm{r+dr})\right]=0 \tag{2.5}$$

Hence,

$$\frac{d}{dr}\left(rh(r)k(r,T)\frac{dT}{dr} \right) = 0 \tag{2.6}$$

2.3 Stress Analysis

As discussed in previous chapters, problem of calculating stress and displacements of a rotating disc is necessary due to the commons use of such structures in many practical applications. In order to establish the theoritical foundation, it is meaningful to start with a unifom thickness homogenous disc due to its simplicity. Timoshenko [25] was the first who provided the closed form analytical solution of the stress and displacements for a uniform thickness homogenous isotropic rotating disc.

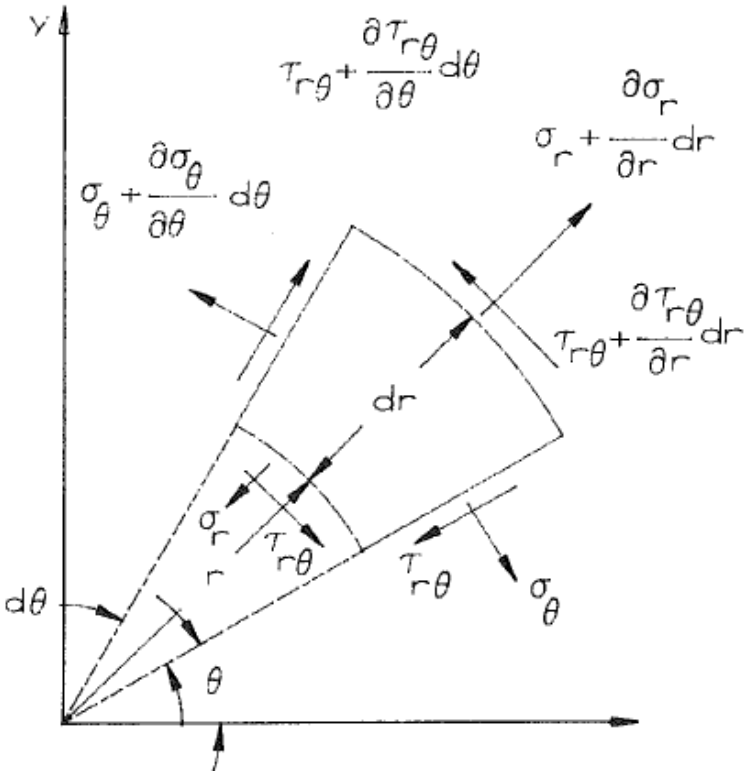

Figure 2.7 Stress components of an annular ring piece.

Figure 2.7 shows an annular disc element of $rdrd\theta$ in polar coordinates. Stress components normal to the surfaces in radial and circumferential directions are denoted as σ_r and σ_θ respectively. Sharing stress components are denoted as $\tau_{r\theta}$. The element is assuming to rotate at a speed of ω. The dimensions of the element are dr

in radial direction, $rd\theta$ on inner surface, $(r+dr)d\theta$ on outer surface. Equilibrium equation in radial direction can be written as follows.

$$\sum F_r = \left(\sigma_r + \frac{\partial \sigma_r}{\partial r} dr\right)(r+dr)d\theta - \sigma_r r d\theta - \left(\sigma_\theta + \frac{\partial \sigma_\theta}{\partial \theta} d\theta\right)\sin\frac{d\theta}{2} dr - \sigma_\theta \sin\frac{d\theta}{2} dr$$
$$+\left(\tau_{r\theta} + \frac{\tau_{r\theta}}{\partial \theta} d\theta\right)\cos\frac{d\theta}{2} dr - \tau_{r\theta}\cos\frac{d\theta}{2} dr + \omega^2 r^2 \rho dr d\theta = 0 \tag{2.7}$$

For a small element, sinθ ≈ θ, cosθ ≈ 1. After summing up all the terms, making necessary elimiation, and dividing through by drdθ,

$$\frac{\partial \sigma_r}{\partial r} + \frac{1}{r}\frac{\partial \tau_{r\theta}}{\partial \theta} + \frac{\sigma_r - \sigma_\theta}{r} + \rho\omega^2 r = 0 \tag{2.8}$$

Shear terms in this equation can be neglected due to symmetry. Additionally σ_r and σ_θ are independent of θ. Hence, the equilibrium equation for a unifrom thickness rotating disc can be written as follows.

$$\frac{d}{dr}(r\sigma_r) - \sigma_\theta + \rho\omega^2 r^2 = 0 \tag{2.9}$$

For a variable thickness rotating disks, all terms in the equilibrium equation should be multiplied by h. Thus, equilibrium equation for a variable thickness rotating annular disc can be obtained as follows.

$$\frac{d}{dr}(hr\sigma_r) - h\sigma_\theta + h\rho\omega^2 r^2 = 0 \tag{2.10}$$

Strain components in the case of symmetry can be written as follows.

$$\varepsilon_r = \frac{du}{dr} \tag{2.11}$$

$$\varepsilon_\theta = \frac{u}{r} \tag{2.12}$$

By using Hooke's law, radial and tangential (hoop) stress components for a plane stress condition can be written respectively as follows.

$$\sigma_r = \frac{E}{1-\nu^2}\left[\left(\varepsilon_r + \nu\varepsilon_\theta\right) - \left(1+\nu\right)\alpha\Delta T\right] \tag{2.13}$$

$$\sigma_\theta = \frac{E}{1-\nu^2}\left[\left(\varepsilon_\theta + \nu\varepsilon_r\right) - \left(1+\nu\right)\alpha\Delta T\right] \tag{2.14}$$

2.4 Problem Definition

After derivations above, the force equilibrium in radial direction for an axially symmetrical, variable thickness FGM flywheel under centrifugal and thermal loads can be stated as follows [26]:

$$\frac{d}{dr}\left[rh(r)\sigma_r(r,T)\right] - h(r)\sigma_\theta(r,T) + h(r)\rho(r)\omega^2 r^2 = 0 \tag{2.15}$$

where, r is the radial coordinate, h is the thickness and ω is the angular velocity of the flywheel. In addition, σ_r and σ_θ are the radial and circumferential components of the stress that are related to the strains and thermal effects as follows:

$$\sigma_r = \frac{E(r,T)}{1-\nu(r)^2}\left\{\left[\epsilon_r + \nu(r)\epsilon_\theta\right] - \left[1+\nu(r)\right]\alpha(r,T)\left[T(r) - T_0\right]\right\} \tag{2.16}$$

and,

$$\sigma_\theta = \frac{E(r,T)}{1-\nu(r)^2}\left\{\left[\epsilon_\theta + \nu(r)\epsilon_r\right] - \left[1+\nu(r)\right]\alpha(r,T)\left[T(r) - T_0\right]\right\} \tag{2.17}$$

Where T_0 is a reference temperature. On the other hand, the linear strain-displacement relations are:

$$\varepsilon_r = \frac{du(r)}{dr} \tag{2.18}$$

and,

$$\varepsilon_\theta = \frac{u(r)}{r} \tag{2.19}$$

Where u is the radial displacement. Using Eqs. (2.16-2.19) in Equation (2.15) the force equilibrium equation is obtained as follows:

$$\left\{\frac{d}{dr}\left[\frac{h(r)\nu(r)E(r,T)}{1-\nu(r)^2}\right]-\frac{E(r,T)h(r)}{r\left[1-\nu(r)^2\right]}\right\}u(r)+\frac{d}{dr}\left[\frac{rh(r)E(r,T)}{1-\nu(r)^2}\right]\frac{du(r)}{dr}+$$

$$\frac{rE(r,T)h(r)}{1-\nu(r)^2}\frac{d^2u(r)}{dr^2}+\left\{\frac{E(r,T)h(r)\alpha(r,T)}{1-\nu(r)}-\frac{d}{dr}\left[\frac{rE(r,T)\alpha(r,T)h(r)}{1-\nu(r)}\right]\right\}\left[T(r)-T_0\right] \tag{2.20}$$

$$-\frac{rE(r,T)h(r)\alpha(r,T)}{1-\nu(r)}\frac{dT(r)}{dr}+h(r)\rho(r)\omega^2r^2=0$$

Note that, the reference temperature is selected as T_0=20 °C throughout this study. The radial stress at flywheel tip is equal to zero and the radial displacement at the point where flywheel and the shaft intersect can be assumed zero, therefore, the boundary conditions can be written from Eq. (2.16), and (2.18-2.19) as follows:

$$u(r_{in})=0 \tag{2.21}$$

$$\nu(r_{out})\frac{u(r_{out})}{r_{out}}+\frac{du}{dr}(r_{out})-\left[1+\nu(r_{out})\right]\alpha(r_{out},T(r_{out}))\left[T(r_{out})-T_0\right]=0 \tag{2.22}$$

On the other hand, the steady-state heat transfer equation for a variable thickness FGM flywheel can be written as follows:

$$\frac{d}{dr}\left[rk\left(r,T\right)h\left(r\right)\right]\frac{dT\left(r\right)}{dr}+rk\left(r,T\right)h\left(r\right)\frac{d^2T\left(r\right)}{dr^2}=0 \qquad (2.23)$$

If there is a heat source or heat sink over the flywheel, one should first solve Eq. (2.23) and obtain the spatial variation of the temperature and then solve the force equilibrium in Eq. (2.20) with material properties corresponding to this temperature distribution. One may expect that the temperature at the flywheel hub should be larger than the flywheel tip due to the heat generated by the electric motor and the bearings located over the flywheel shaft. Therefore, the boundary conditions for the heat transfer equation are given as follows:

$$T\left(r_{in}\right)=T_{in} \quad , \quad T\left(r_{out}\right)=T_{out} \qquad (2.24)$$

with,

$$T_{in}=T_{out}+\Delta T \qquad (2.25)$$

$$\Delta T>0 \qquad (2.26)$$

The thermal conductivity coefficient is not assumed constant and depends on the temperature as presented in Table 1, therefore, Eq. (2.23) is non-linear and should be solved iteratively.

3. DIFFERENTIAL QUADRATURE METHOD

In engineering, physical problems of the real world is represented by a set of differential equations. In most of the cases, these equations can be very complicated that it is so difficult to obtain exact solutions if not impossible. In such situations, the solutions can be approximated by some numerical techniques that utilizes from known discrete values so called functionals of the unknown functions. Differential quadrature method (DQM) is one of a numerical discretization technique for the approximation of derivatives of a function. Method was proposed by Bellman et al. [27] in early 70's as a result of efforts for searching a rapid solution technique for the nonlinear partial differential equations. In DQM, derivate of a function at a point is approached by a weighted linear summation of functional values at all discrete points along a mesh line. Therefore, solution of a nonlinear partial differential equation problem becomes solution of a set of ordinary differenital equations with specified initial conditions. When comparing with other low order numerical solution techniques such as finite element and finite difference methods, DQM provides highly accurate results by using considerably small grid points.

Key procedure of the method is to obtain weighting coefficients. Bellman and his colleauges proposed two methods for computing the coefficients. First method was to have a matrix of algebric equations. But this matrix was becoming ill conditioned as the number of grid points increased. Therefore, applications were limited in this method. On the other hand, second method was using a simple algebraic formulation. But this formulation was based on grid points who were the roots of Legendre polynomial. Due to these drawbacks, it took until the late 80's when high speed computing became readily available to see a rapid development of applications of this method. Another major development was achieved by Shu et al. [28] when he applied a linear vector space and Lagrange polynomial approximation for determination of weighting coefficients. Shu's method was enabling to choose grid points without any restriction for the first order derivatives. Additionally, for the weighting coefficients of higher order derivatives his method was suggesting a recurrence relationship.

3.1 GDQM Governing Equations

In generalized differential quadrature (GDQ), derivative of m'th order of a single variable function u(r) represented as follows [29].

$$u^{(m)}(\mathrm{r}_i) = \sum_{j=1}^{N} c_{ij}^{(m)} u(\mathrm{r}_j) \ , \ i = 1,2,...,N \tag{3.1}$$

Where, $c_{ij}^{(m)}$ is the weighting coefficient of the m'th order derivative and N is the number of total sampling points of the grid line. The weighting coefficients for the first order derivative can be represented as written below:

$$c_{ij}^{(1)} = \begin{cases} \dfrac{M^{(1)}(r_i)}{(r_i - r_j)M^{(1)}(r_j)} & for \ \ i \neq j \ and \ i, j = 1,2,...,N \\ -\sum\limits_{s=1, s\neq i}^{N} c_{is}^{(1)} & for \ \ i = j \ and \ i, j = 1,2,...,N \end{cases} \tag{3.2}$$

Where the function $M^{(1)}$ is,

$$M^{(1)}(r_k) = \prod_{s=1, s\neq k}^{N} (r_k - r_s) \tag{3.3}$$

On the other hand, weighting coefficients of higher order derivatives obey below recurrence relation:

$$c_{ij}^{(m)} = \begin{cases} m\left(c_{ii}^{(m-1)} c_{ij}^{(1)} - \dfrac{c_{ij}^{(m-1)}}{r_i - r_j} \right) & for \ \ i \neq j \ and \ i, j = 1,2,...,N \\ -\sum\limits_{s=1, s\neq i}^{N} c_{is}^{(m)} & for \ \ i = j \ and \ i, j = 1,2,...,N \end{cases} \tag{3.4}$$

In DQM, it is a common practice to use a frequent grid point distribution on the boundaries instead of a uniform distribution. This mainly due to avoid from oscillations at the edges of the mesh interval so called Runge's phenomenon. Hence,

a special grid distribution so called Chebyshev-Gauss-Labatto is utilized to discretize the spatial coordinate.

$$r_i = r_{in} + \frac{r_{out} - r_{in}}{2}\left[1 - \cos\left(\frac{i-1}{N-1}\pi\right)\right], \; i = 1, 2, ..., N \tag{3.5}$$

Note that, for the design optimization, N is taken as 200 in this study.

3.2 GDQM Formulation

When applying the GDQ method, Eq. (2.20) and Eq. (2.23) are discretized in the following form:

$$\begin{aligned} &A_0(r_i, T_i)u_i + A_1(r_i, T_i)\sum_{j=1}^{N} c_{ij}^{(1)} u_j + A_2(r_i, T_i)\sum_{j=1}^{N} c_{ij}^{(2)} u_j \\ &+B_0(r_i, T_i)(T_i - T_0) + B_1(r_i, T_i)\sum_{j=1}^{N} c_{ij}^{(1)} T_j \qquad , \; i = 2, 3, ..., N-1 \\ &+h(r_i)\rho(r_i)\omega^2 r_i^2 = 0 \end{aligned} \tag{3.6}$$

and,

$$C_1(r_i, T_i)\sum_{j=1}^{N} c_{ij}^{(1)} T_j + C_2(r_i, T_i)\sum_{j=1}^{N} c_{ij}^{(2)} T_j = 0 \qquad , \; i = 2, 3, ..., N-1 \tag{3.7}$$

where,

$$A_0(r, T) = \frac{d}{dr}\left[\frac{h(r)\nu(r)E(r, T)}{1 - \nu(r)^2}\right] - \frac{E(r, T)h(r)}{r\left[1 - \nu(r)^2\right]} \tag{3.8}$$

$$A_1(r, T) = \frac{d}{dr}\left[\frac{rh(r)E(r, T)}{1 - \nu(r)^2}\right] \tag{3.9}$$

$$A_2(r,T)=\frac{rE(r,T)h(r)}{1-\nu(r)^2} \tag{3.10}$$

$$B_0(r,T)=\frac{E(r,T)h(r)\alpha(r,T)}{1-\nu(r)}-\frac{d}{dr}\left[\frac{rE(r,T)\alpha(r,T)h(r)}{1-\nu(r)}\right] \tag{3.11}$$

$$B_1(r,T)=-\frac{rE(r,T)h(r)\alpha(r,T)}{1-\nu(r)} \tag{3.12}$$

$$C_1(r,T)=\frac{d}{dr}\left[rk(r,T)h(r)\right] \tag{3.13}$$

$$C_2(r,T)=rk(r,T)h(r) \tag{3.14}$$

Additionally, the GDQM discretization of boundary conditions in Eqs.(2.21), (2.22) and Eqs (2.24) can be represented as follows:

$$u_1=0 \tag{3.15}$$

$$\frac{\nu(r_N)}{r_N}u_N+\sum_{j=1}^{N}c_{Nj}^{(1)}u_j-\left[1+\nu(r_N)\right]\alpha(r_N,T_N)\left[T_N-T_0\right]=0 \tag{3.16}$$

and,

$$T_1=T_{in}\ ,\quad T_N=T_{out} \tag{3.17}$$

As explained previously, Eq. (2.23) and its discretization presented in Eq. (3.13) to Eq. (3.14) are nonlinear in terms of T(r). Therefore, it will be solved iteratively. For this purpose, the discretized heat equation is obtained from the global assembling of Eqs. (3.7), (3.13), (3.14) and Eq.(3.17). The first iteration is started with the assumption that the variation of temperature between the inner and outer radii is linear:

$$T_i^0 = T_{in} + \frac{r_i - r_{in}}{r_{out} - r_{in}}\left(T_{out} - T_{in}\right) \quad \text{for} \quad i = 1, 2, ..., N \tag{3.18}$$

The heat equation is solved with the thermal conductivity coefficient corresponding to this initial temperature distribution. The next iteration is carried out with the thermal conductivity coefficient corresponding to the previously obtained temperature. The procedure is repeated until the results converge. For the convergence criteria following rule is established:

$$\max\left|\frac{T_i^{j+1} - T_i^j}{T_i^{j+1}}\right| \leq 0.01\% \quad \text{for } i = 1, 2, ..., N \text{ and } j = 0, 1, 2... \tag{3.19}$$

In the last step, Eqs.(3.6), (3.15) and (3.16) are assembled and solved for the radial displacement over the flywheel considered with the material properties corresponding to the temperature obtained in the final iteration.

Solutions of thermal and stress analysis of have been performed in Mathematica software.

3.3 Validation

In order to validate results from the numerical solution, a finite element model (FEM) is used. Ansys commercial finite element tool has been used for model creation and solution. Regarding to the symmetry in flywheel geometry, a two dimensional axisymmetric model is preferred for this analysis. FEM solution has been taken in two steps. At first step, a steady state thermal conductivity analysis carried on to get the temperature distribution along the radius of the flywheel. At the second step, resulting temperatures of previous thermal analysis has been mapped on the flywheel and then stress analysis has been performed to get the stress and displacement results.

3.3.1 Model built

First step in FEM creation is to establish the flywheel geometry. In numerical model, continuous profile of the flywheel is represented by cubic spline curves. However, creating such splines seems a tedious task if not impossible in Ansys. Hence, flywheel

geometry is established in Unigraphics (NX10) solid modelling tool than exported into the Ansys for discretization. Unigraphics representation of the flywheel is shown in Figures 3.1 and 3.2.

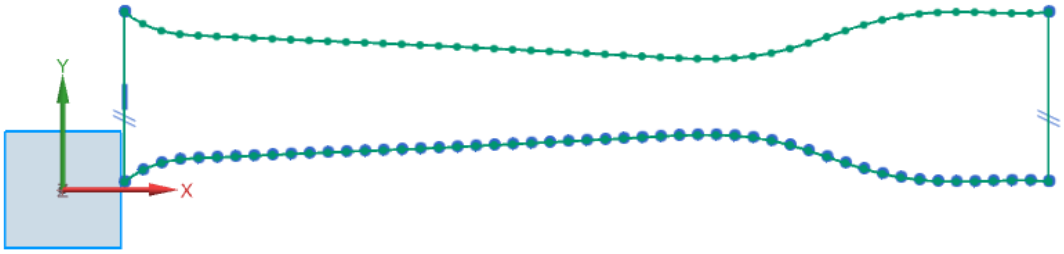

Figure 3.1 Spline curve definition at stations.

Figure 3.2 Flywheel geometry representation by cubic splines

In next step, Flywheel geometry has been divided into areas to reflect material gradation effects in the model. It is important to make sure that number of areas are sufficient to represent material grading effects. Trials demonstrated that for the flywheel considered in this study 50 sections were sufficient to provide a smooth transition contour to represent material grading effects. See below figure 3.3.

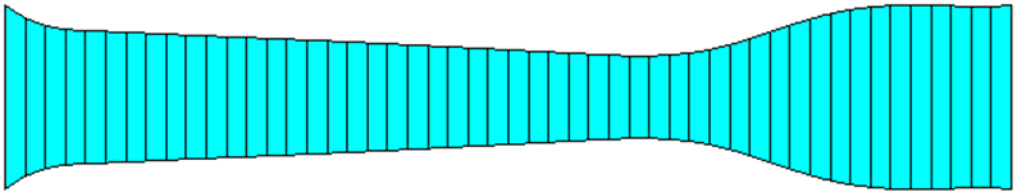

Figure 3.3 Flywheel sections in Ansys model

After flywheel geometry is established, its continuous form is discretized into small areas by means of finite elements. This is called meshing. In meshing, it is impoertant to use proper elements as there are several different elements exist for different analysis purposes. In this study, two types of elements has been used for meshing. For the thermal analysis, PLANE 55 element has been used due to its two dimensional thermal conductivity capability. PLANE 55 has 4 nodes each having single degree of freedom which is temperature. See below Figure 3.4.

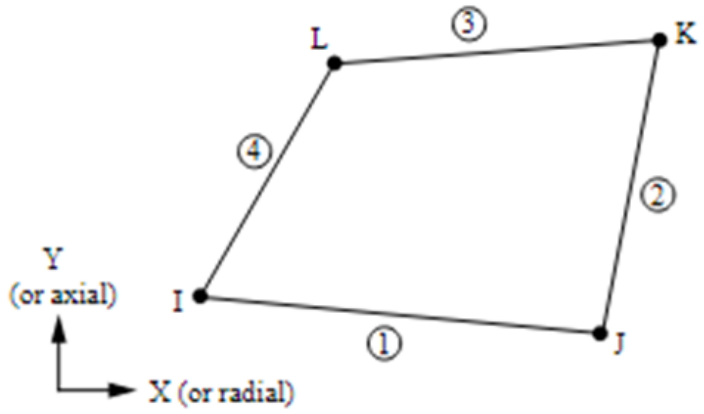

Figure 3.4 Representation of Ansys Plane 55 element.

In finite element mesh, there are in total 2869 nodes and 2700 elements. See Figure3.5.

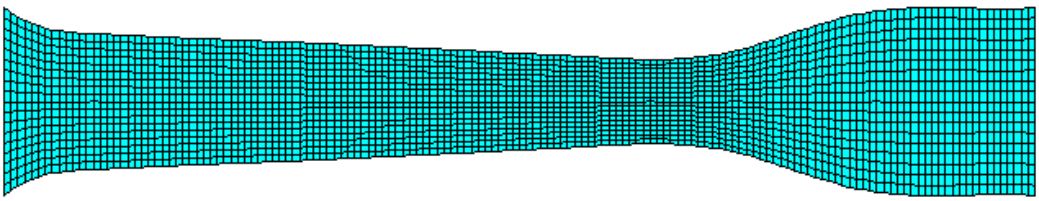

Figure 3.5 Finite element mesh model of the 2D Flywheel.

3.3.2 Thermal analysis

A Steady state thermal analysis has been conducted to determine thermal conductivity coefficient and temperature distribution along the radius of the flywheel for a given design parameters and ambient temperature. In order to do this, temperature values on inner and outer surfaces of the flywheel are given as boundary conditions (BCs). See Figure 3.6 below. Temperature distribution results is demonstretad below Figure 3.7

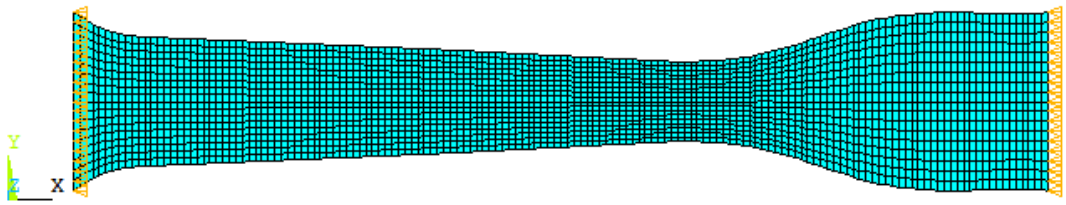

Figure 3.6 Boundary conditions for thermal analysis.

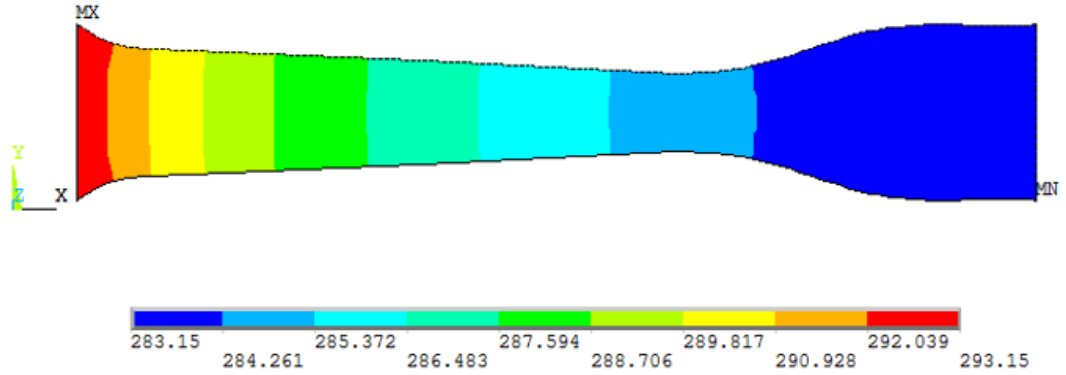

Figure 3.7 Temperature distribution results.

3.3.3 Stress analysis

Stress analysis has been performed with the same model by simply converting the element type from thermal element (PLANE 55) to structural element (PLANE 42). PLANE 42 is defined by four nodes having two degrees of freedom at each node: translations in the nodal x and y directions as depicted below Figures 3.8 and 3.9.

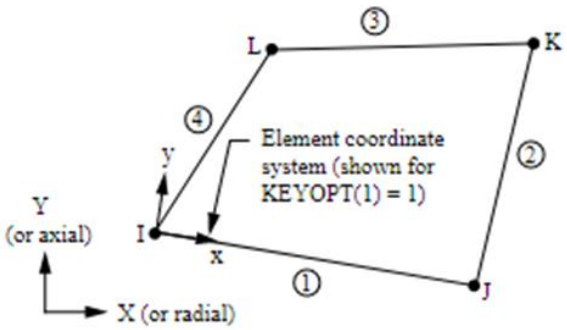

Figure 3.8 Representation of Ansys Plane 42 element.

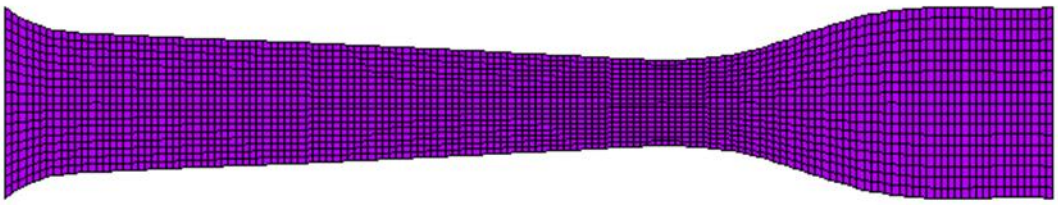

Figure 3.9 Model mesh with Plane 42 element

3.3.4 Comparison of numerical and FEM results

In this step, numerical results obtained by using generalized differential quadrature method have been compared with a finite element model results in order to make sure that, mathematical formulations, assumptions and boundary conditions are defined correctly. For this comparison an arbitrary flywheel geometry has been seleceted from the design pool. Geometry parameters, ambient temperatures and material types and volume fraction grading coefficient of that Flywheel are listed as below Table 3.1.

Table 3.1 Flywheel parameters for comparison model.

h1(m)	*h2(m)*	*h3(m)*	*h4(m)*	*h5(m)*	*h6(m)*	*h7(m)*	*h8(m)*	*h9(m)*
.05495	.047135	0.039559	0.037145	0.034186	0.030284	0.025883	0.029292	0.05060

h10(m)	*h11(m)*	*h12(m)*	*m*	*Mat_in*	*Mat_out*	*T_in*(K)	*T_out*(K)	*ω*
.05470	.05404	0.05471	13.2596	Inco_718	AISI_4340	293.15	283.15	*2094.11*

In finite element analysis, Flywheel is loaded with thermal and mechanical loads and boundary conditions such as body temperatures, rotational speed and displacement constraints. Temperature values at the inner and outer edges are given as inputs to the model. Then, by performing thermal conductivity analysis temperature distribution over the whole Flywheel domain has been obtained as indicated below Figure 3.10. Rotational speed has been given in Z direction as inertial load in rad/s units. Furthermore, displacement constraints have been given to the nodes at the inner edge of the Flywheel in X direction. In Y direction, model has been constrained from only one node to prevent any rigid body motion.

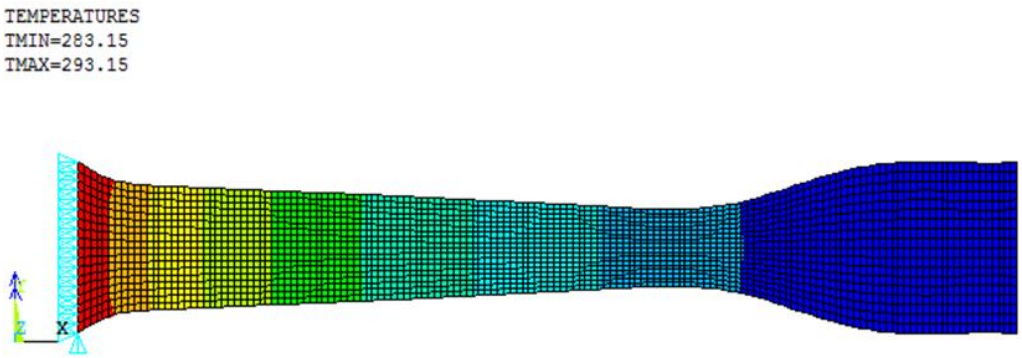

Figure 3.10 Loading and BCs for FE model

Results of the finite element analysis in radial displacement (UX) and Von Misses Equivalent stress (SEQV) have been obtained as shown in Figures 3.11 and 3.12.

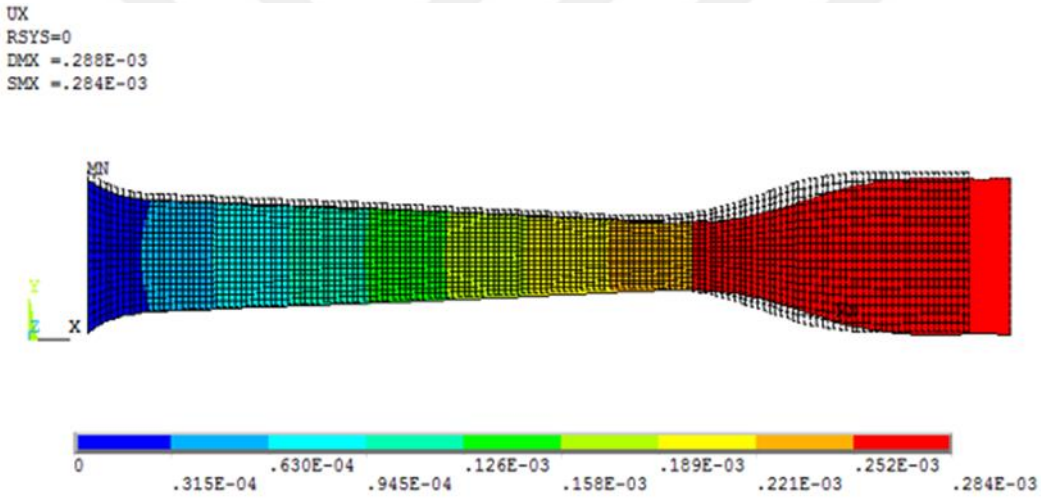

Figure 3.11 Radial displacement result.

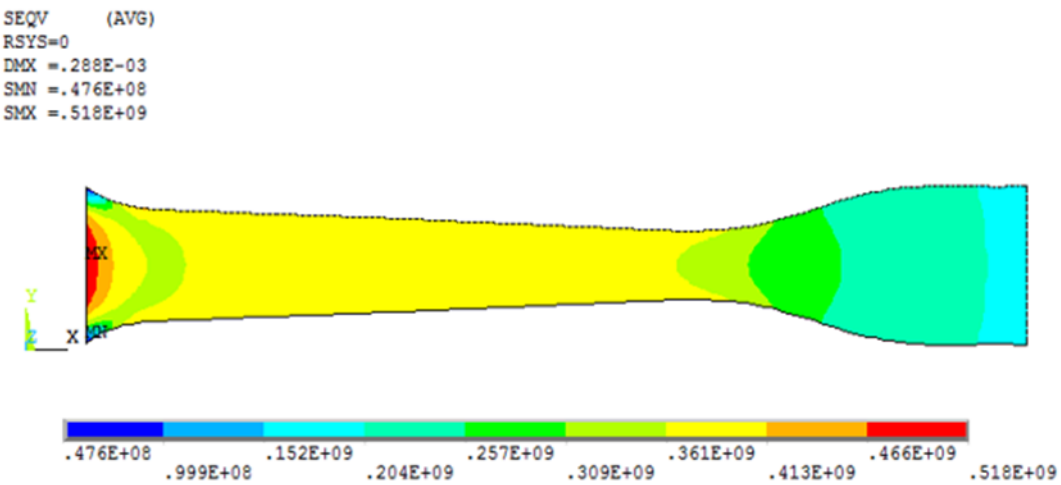

Figure 3.12 Von Mises equivalent stress results.

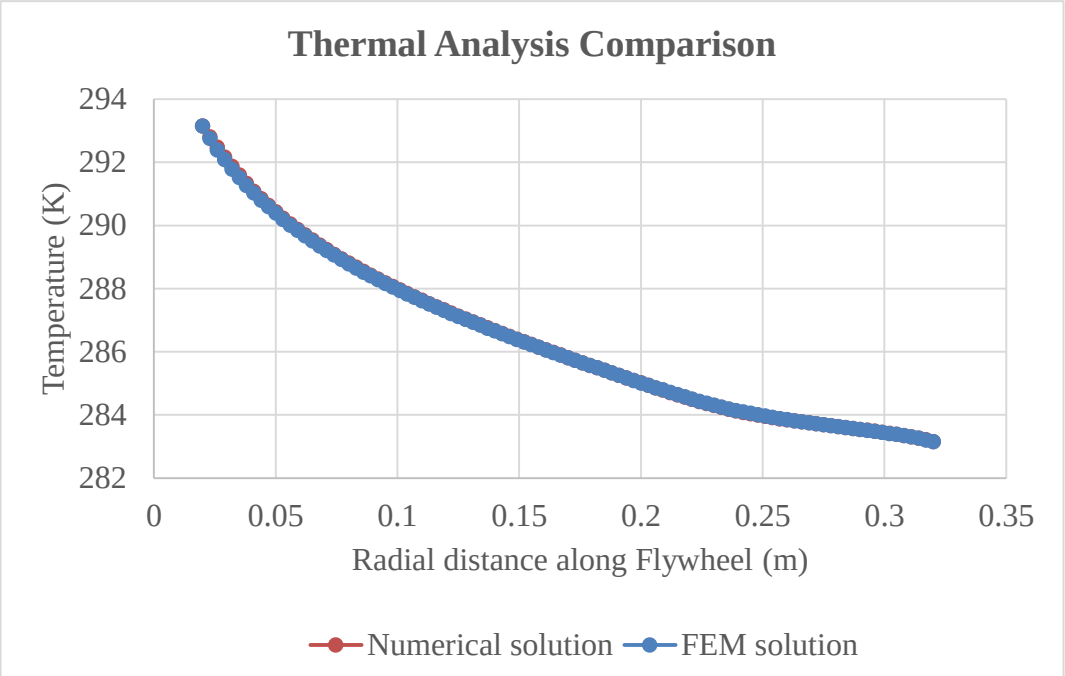

Figure 3.13 Thermal analysis result comparison.

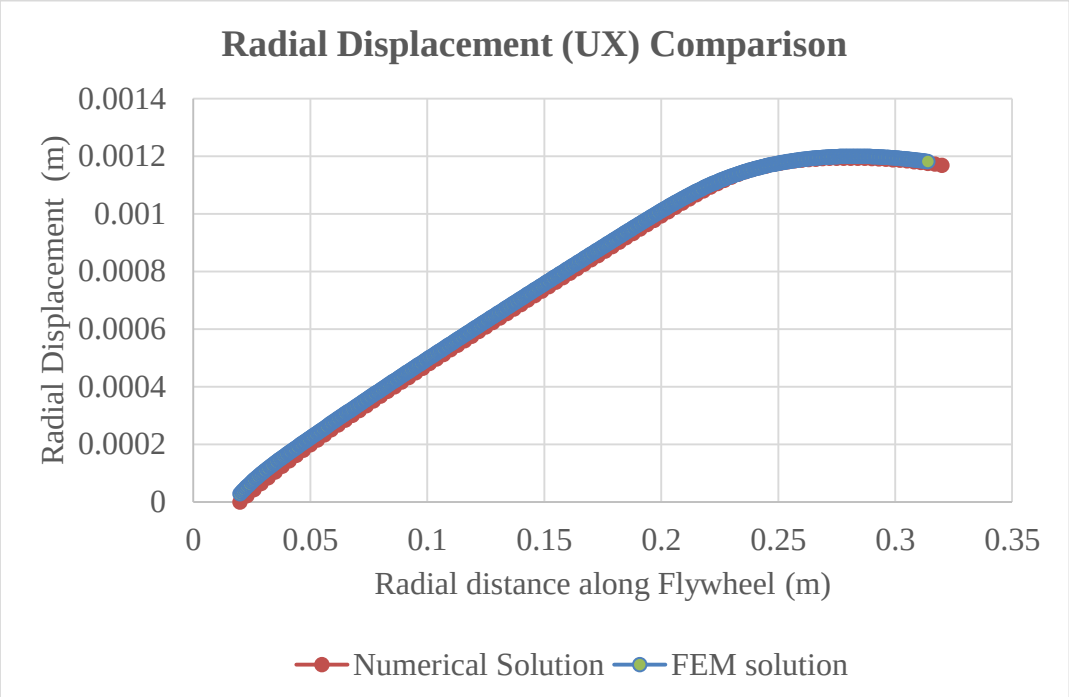

Figure 3.14 Radial displacement result comparison.

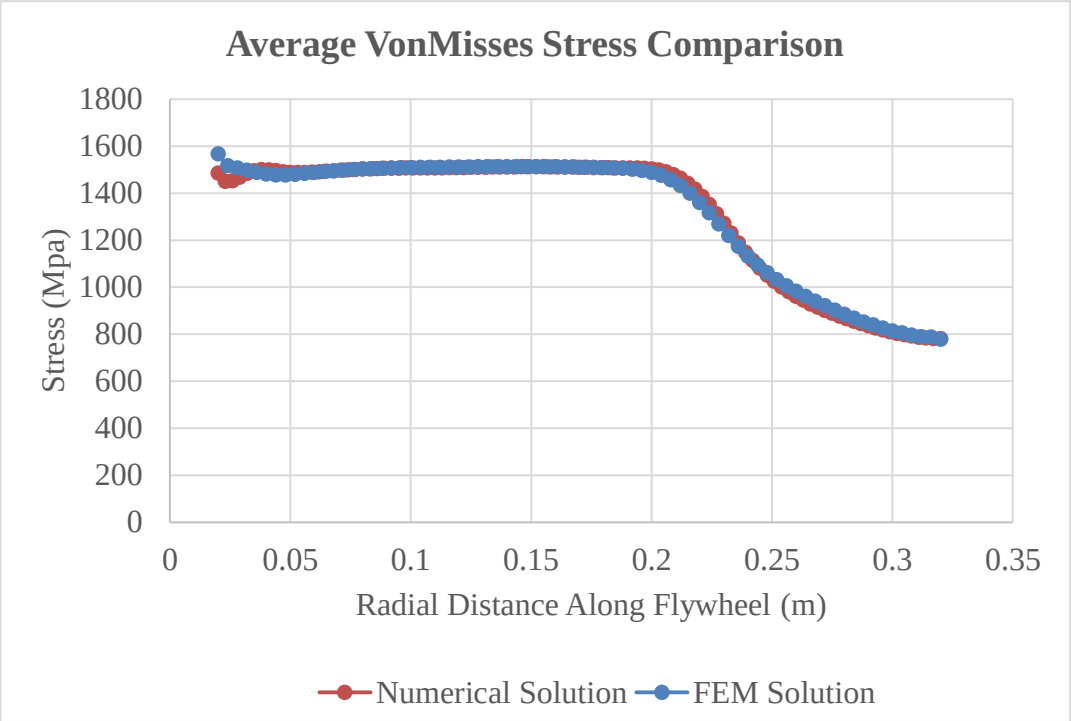

Figure 3.15 Von Misses stress result comparion.

Thermal and Stress analysis comparison plots in Figures 3.13-3.15 indicated a perfect matching between numerical and finite element results. With this results, the mathematical model formulation, DQM discretization, boundary conditions and assumptions has been validated. Then, study has been continued with the optimization step.

4. OPTIMIZATION

For finding the optimal shape of a Flywheel disc, several studies have been published in literature with different objective functions. One of the most common objective function investigated has been “maximizing specific kinetic energy” which is defined as the ratio of energy over mass [30], [31], [32], [33], [21]. In some studies, “maximizing kinetic energy”, “minimizing volume” or “minimizing mass” of the Flywheel was taken as the objective function [12], [34]. Some other studies selected “minimizing stress deviations” along the Flywheel as their objective functions [35], [12]. In one of the study, “maximizing energy density” which is the ratio of energy over volume was taken as objective [13]. Then, in one other study, “maximizing energy per cost” was used as the objective function [18].

Furthermore, in one of the study, [15] a multi objective has been used such as “maximizing kinetic energy” and “minimizing the difference between maximum and minimum Von Mises stresses”. In another multi objective study [16], “maximizing the kinetic energy storage” and “minimizing the maximum equivalent stresses” within the Flywheel was investigated. Both multi objective studies, used weighting method to reduce multi objective optimization problem into a single objective problem.

In this study, apart from the rest of the studies in literature, a Multi objective optimization for a variable thickness FGM Flywheel has been carried out via a Genetic Algortihm. Objective functions have been determined as “maximizing kinetic energy” and “minimizing mass” simultaneously. Therefore, the optimization algorithm is expected to provide a Pareto optimal solution instead of a single optimum solution.

4.1 Optimization with Genetic Algorithm

Genetic algortihm (GA) is a stochastic and iterative search method often applied to optimization and machine learning problems. The process depends on generating better solutions at each iteration. Method was first introduced by Holland in 1975 in his book Adaptation in Natural and Artificial systems [36]. Genetic algorithms are a

member of evolutionary algorithms (EA) family. Like other evolutionary algorithms, method is based on the genetic coding and natural selection principles. The idea behind evolutionary algorithms is to simulate biological evolution process in nature. Every creature in nature has a genetic information coded in its so called chromosomes. Encoding of this genetic information establishes the physical existance of that creature. Evolution process, takes place continuously on individuals's chromosomes in order to obtain better and better offtsprings. Whereas, natural selection allows good individuals to appear more and keep existing for future populations, while others that do not properly fit to its environment to dissappear. After applying these principles over the long period, final population is to be expected a better population than previos ones.

The natural principle of continuously changing to achieve for better individuals finds its provision in engineering when searching for the optimal solutions of a problem. Genetic algorithms can be used for complex nonlinear problems that are desired due to practical importance but can not be solved exactly. In fact, Genetic algorithms have found great applications due to their advantages over gradient based methods [37]. First of all, method can be applied to any kind of optimization problem no matter if it is continuous or discrete as long as it can be formulated as an objective function [38]. Secondly, in conventional methods especially for the applications having a nonlinear design space it is likely to stick around a local mimina. Genetic algorithm eliminates this problem by applying several operators such as Mutation, Cross over and Selection. Another great advantage of this method is permit parallel computations.

As a result of advancements in high computing capabilities and availability of parallel working today, genetic algorithms has become one of the widely accepted and used method for solution of nonlinear problems.

4.2 Basic Principles

In genetic algorithm, individual solutions are named as chromosomes as an analogy to the biological evoluation. Chromosomes are the main structure that genetic algrothim operates on. Each chromosome represents a candidate solution to the problem being investigated. Proposed solution is stored as set of decision variables in a Chromosome. These variables can be represented as bits, numerical values, arrays or objects. A group of bits establishes genes. Genes can have different lengths. Genetic structure that represent an individual is called genotype and the observed characteristic of it as an

organism is called fenotype [37]. A chromosome and its elements are shown in Figure 4.1 below.

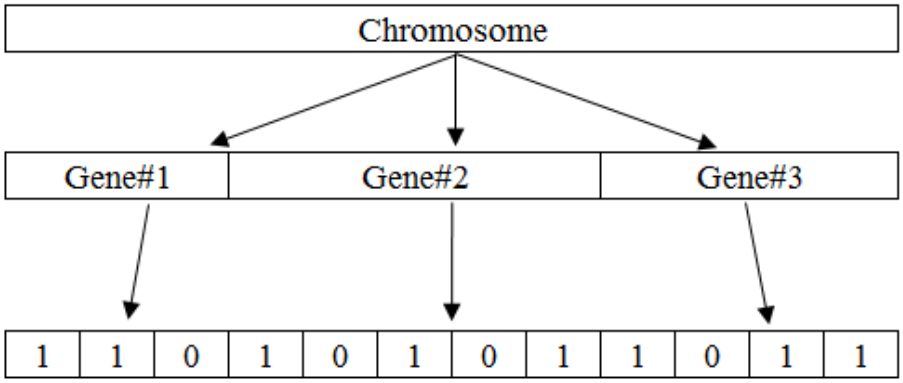

Figure 4.1 Representation of a Chromose in GA

Success of each solutions is called fitness and measured by calculating the corresponding objective function of the problem. Individual solutions are then ranked based on their fitness value and undergoes reproduction. By reproduction initial population transforms into a new one. Fitness is the guide during this transformation by directing the evolution algorithm based on the defined criteria. Evolution of populations are performed by several genetic algorithm operators. Most common operators are mutation, crossover and selection. Iterations continue untill a defined limit number is reached or the solution is converged within tolerances.

4.3 Encoding

Encoding is representing decision variables of a solutions as a string of bits. There are several methods for encoding. However most commonly used method is binary coding. In a binary code chromosome are respresented by 1 and 0. For example a proposed solution for a 12-bit string can be described as Figure 4.2 follows.

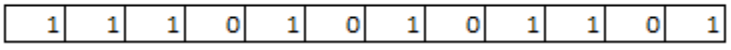

Figure 4.2 Encoding for a 12 bit string.

Number of bits in a string defines how many intervals a decision variable is to be divided. For an N number of bits, size of each interval is

$$\Delta = \left(x_{upper} - x_{lower} \right) \Big/ (2^N - 1) \tag{4.1}$$

One of the weakness of binary coding is called Hamming Cliff phenomena which can be explained as, for some of the neigboring fenotypes there may be a very different genotypes. Figure 4.3 is depicting this phenomena. In order to change 6 to 7 only one mutation is needed. However, changing 7 to 8 needs all of the bits to be changed.

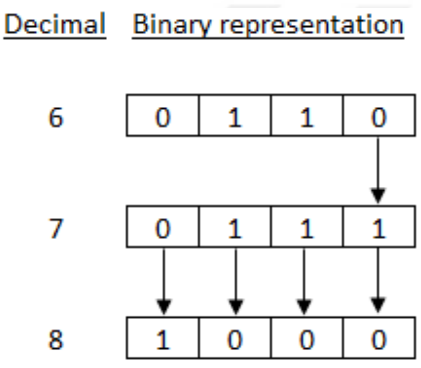

Figure 4.3 Hamming Cliff phenomena.

To avoid from this phenomena Gray proposed a method [39] that enables to change only one bit flip between neighbours. See Figure 4.4.

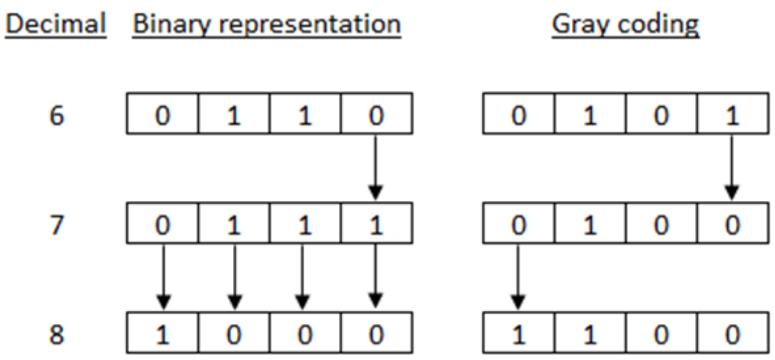

Figure 4.4 Binary coding vs. Gray coding.

4.3.1 Size of the initial population

In genetic algorithm, determinig the initial population size is a major question. Although it depends on the complexity of the problem. It can be intuitively felt that there should be an optimal population size to give a chance to explore whole design space in a reasonable amount of time. Ideally, the initial population should have a gene pool as large as possible in order to be able to explore the whole search space [38]. It is preferrable to search design space with larger populations. However, it requires more computational effort and memory. There is actually a tradeoff between the effectiveness of the method and the efficiency of the results. Hence, the correct question is to find minimum initial pouplation of size to for meaningful search to take place. According to Reeves [40] at least, every point in the search space should be reachable from the initial population by crossover only. To ensure this requirement, there should be at least one instance of every allele at each locus in the whole population of strings. Assuming that the initial population is generated by a random sample with replacement (which is a conservative assumption in this context), the probability that at least one allele is present at each locus can be found for binary strings as follows [40].

$$P = \left(1 - \left(1/2\right)^{N-1}\right)^{l} \tag{4.2}$$

Here P is the probability, N is the number individuals in the population and l is the string size. Reeves et al [40] indicated that, a population size of N=17 is sufficient to ensure that the required probability exceed 99.9% for a string of length 50.

4.3.2 Selection

Selection is the process of choosing two parents from the population for crossing [38]. After initial population is generated, each individual has been assigned a fitness value basen on the objective function. The next step is to decide which individuals to select for reproducing next generations. The purpose of the selection process is to eliminate unfit solutions and to keep better fit individuals in the population in the hope of reaching better offsprings. Selection decision is based on the fitness value of individuals. The fittest individuals has a higher chance for being selected. There are several methods for parent selection. Among others more popular methods are

Roulette wheel selection which was proposed by Holland [36], Rank selection and the Random selection.

- Roulette wheel selection: In this method a string is selected from the mating pool with a probability proportional to its fitness. The selection probabilities of individuals are related to their fitness with following equation.

$$p_i = \frac{f_i}{\sum_{j=1}^{N} f_j} \tag{4.3}$$

As can be implied from this formula, Roulette wheel selection does not guarantee for selecting fitter individuals. Instead, it offers a higher chance of being selected. As a result, method is only a moderately strong selection technique. In this method, it is essential that the population is not sorted by fitness, since this would dramatically bias the selection.

- Rank selection: In rank selection, individuals are ranked based on their fitness values. Ranking is starting from the worst one to have a fitness value of 1 and the best one to have a fitness of N. This method preserves diversity by giving weak individuals a more chance to be selected than the Roulette wheel selection. Therefore, it is preferrable to use rank selection over Roulette selection when fitness values of individuals differ very much.
- Tournament selection: This method, randomly selects k number of solutions from the population and pick the fittest one (the winner) for reproduction. The winner of the tournament is inserted to the mating pool. The tournament competition is repeated until the mating pool for generating new offspring is filled.

4.3.3 Crossover

Crossover, occurs between two parent chromosomes to produce offsprings having a different genetic code from their parents. Parent strings can be split randomly from one or more locations. Cut away pieces then swapped. This approach is valid for single point and multiple point crossovers. In fact, multiple point crossover can be considered as the generalized version of the single point crossover. Whereas, another method

called uniform crossover works quite differently. In this method, bit changes are performed based on the criteria directed by a randomly generated binary mask string. For example, in a mask string, 1 can be used to indicate that gene should be taken from first parent while 0 can be used to indicate that gene should be taken from the second parent. Figures 4.5-4.7 below depicted these crossover techniques.

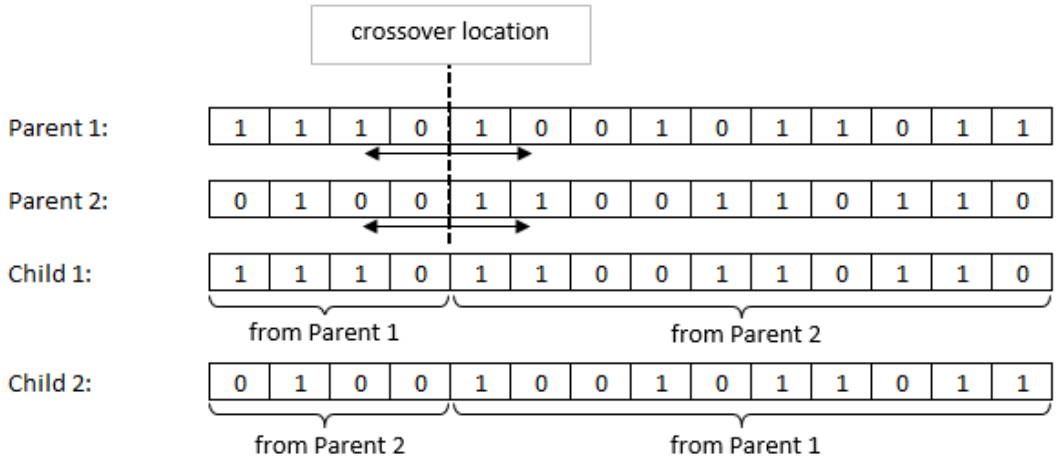

Figure 4.5 Single point crossover.

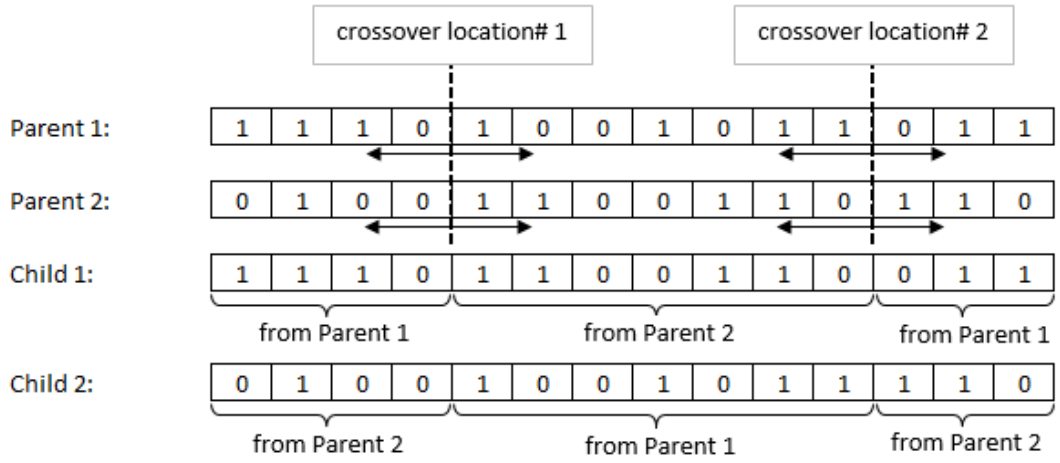

Figure 4.6 Multi point crosssover.

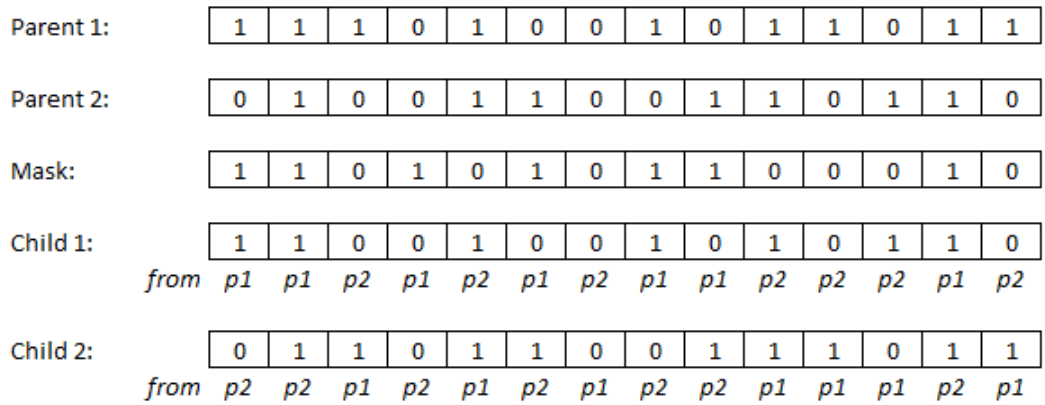

Figure 4.7 Uniform crossover.

It is important to note that there is a trade off between computation time and the number of crossover locations. As crossover location increases the effectiveness of design space search is improved and local minima is avoided.

However, the computation time is also increased. For this tradeoff, a parameter called crossover probability P_c which may take values from 0 to 1 is used. When P_c is equal to 1, all individuals in the new population is produced by the crossover. On the other hand, when P_c is equal to 0, members of the new population are to be identical to the previous generation.

4.3.4 Mutation

Mutation is applied to the childs after crossover. The purpose of mutation is to maintain a diversity in the population and therefore to avoid from local extremums. This is achieved by randomly changing the genes of an individual to obtain the new ones with the hope of having better individuals. Some of the common mutation techniques are Flipping, Interchanging and Reversing.

In flipping, a bit in the chromosome is toggled to the other bit according to the rule defined by the mask. Interchanging is simply exchanging the values of randomly selected two bits. Reversing is replacing the neighbouring bits of a location with the reversed bits. Samples of these techniques can be seen in Figures 4.8-4.10 below.

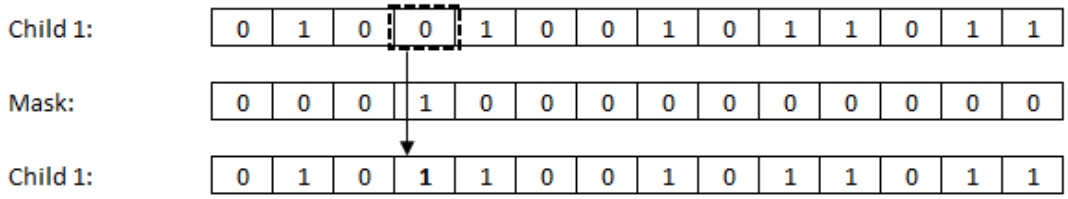

Figure 4.8 Flipping mutation.

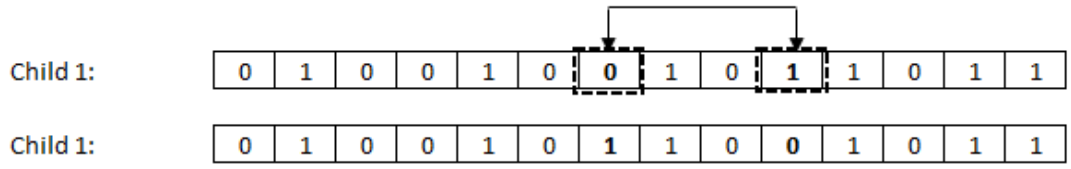

Figure 4.9 Interchanging mutation.

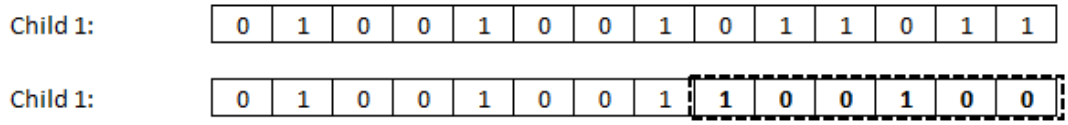

Figure 4.10 Reversing mutation.

When applying mutation operator to the generations, a possibility value called P_m is considered. P_m is traditionally chosen as a small number (P_m <<1) otherwise the algorithm will behave like a random search which is not desirable. When P_m is equal to zero, it means that offspring generation is produced with only crossover and there is no mutation.

4.3.5 Replacement

Replacement is the final step of creating new generations. After two child breed by mutation and crossovers from the two parent, there are four individuals currently. At this point, it is necessary to have a method to figure out which members are to stay with the new population. Some of the widely used replacement method are,

- Random replacement: The children replace two randomly chosen individuals in the population. The parents are also candidates for selection.

- Generational replacement: This technique simply replaces the entire population with its descendants. From an optimization stand point, this method may cause undesirable results since successful individuals of the previous population can be thrown away.
- Elitism: In elitism method, best individuals of the previous population are kept in the new population instead of elimination. Elitism can be used to remove the risk of any undesired loss of information during the mutation stage.
- Tournament replacement: In similar to tournament selection, tournament replacement relies on competitions between individuals from the last and actual generations. Again, the winners become a member of the new generation.

4.3.6 Termination

In contrary to the conventional gradient-based methods, genetic algorithms can run forever unless a termination criteria is introduced. Some of the possible termination criteria can be,

- Maximum number of generations: The genetic algorithm stops when the specified number of generation's have evolved.
- Maximum computation time: The genetic algorithm ends when a specified time is elapsed.
- Population convergence: The genetic algorithm ends when no change is observed to the population's best fitness for a specified number of generations.

In lights of the aformentioned concepts, a basic flowchart of a genetic algorithm can be as follows in Figure 4.11

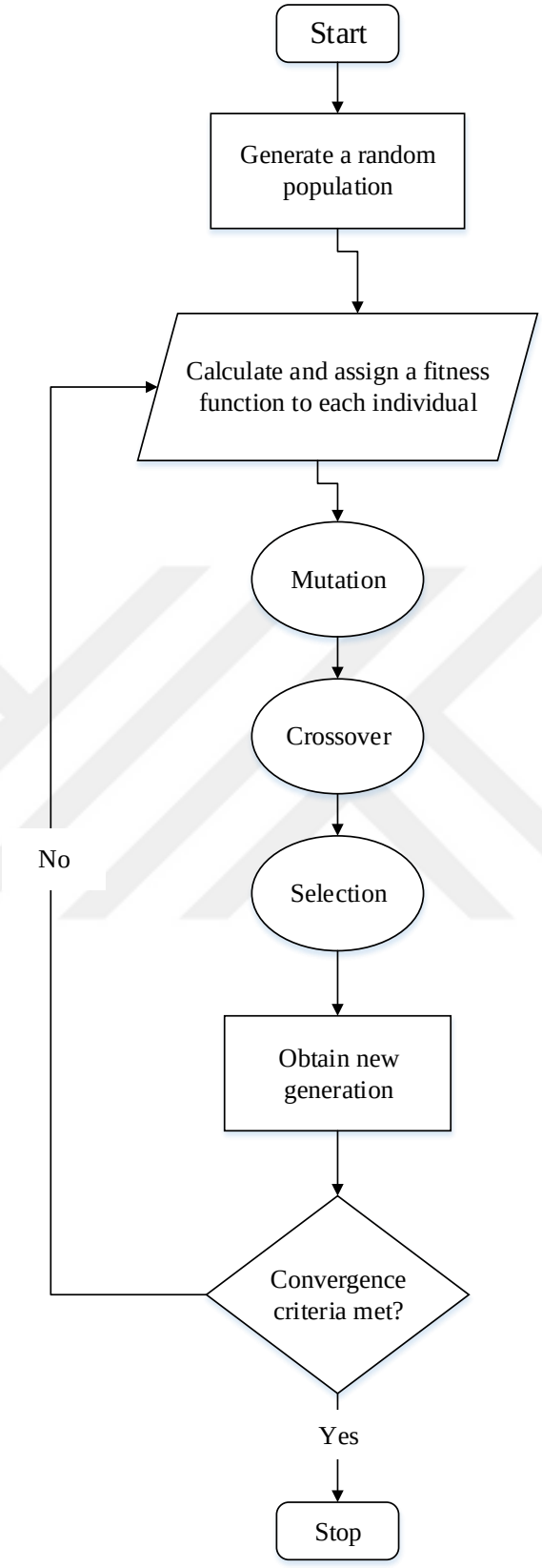

Figure 4.11 Flowchart of a Genetic Algorithm.

4.4 NSGA II

In the solution of multi objective optimization problems there are a set of optimal solutions so called Pareto optimal solutions instead of a only one optimal solution. In this case, it is not possible to decide which one of the pareto optimal solution is the best solution. Furthermore, problem becomes more challenging, when these objective are conflicting each other [41].

For this reason, in classical optimization techniques it is common practise to convert the multi objective problem into a single objective problem by using one of the weighted sum method. Nevertheless, when such a method is to be used for finding multiple solutions, it has to be applied many times, hopefully finding a different solution at each simulation run [42]. However, these independent solutions may not provide an evenly distribution on the Pareto optimal front. In order to address these troubles associated with the classcial optimization methods, NSGA is propsoed by Deb et al. [42] in 2002. NSGA, stands for Non dominated Sorting Genetic Algorithm. Method proposes a fast and elitist genetic algorithm approach when there are a number of objectives for optimization simultaneously.

In NSGA II, each individual solution in a population is assigned a fitness value depending on the rank of the non-dominated front it belongs to and the distance to other individuals at the same pareto front. Unique side of this method than other evolutionary algorithms is that, NSGA II favors the potential solution sets not only by means of their dominance but also, their diversity with the expectation of Pareto frontier obtained at the final iteration is both the Pareto optimal front and the solutions are evenly distributed along this frontier [43]. By using elitism, NSGA II technique also significantly increases the convergence rate for reaching the pareto optimal front. Elitism is a diversity preserving mechanism [44] that enables to make comparisons child populations with the pareto frontier of the parent population.

4.5 Formulation of the Optimization Problem

The materials considered in this study are ductile and the failure of flywheel material is characterized with the von Mises stress, which can be calculated from the following equation:

$$\sigma_{VM} = \sqrt{\sigma_r^2 - \sigma_r \sigma_\theta + \sigma_\theta^2} \tag{4.4}$$

Note that the shear stresses were neglected in our governing equations. Therefore, the radial and hoop stresses are the principal stresses in the r-θ plane.

As a result, the optimization problem is defined to maximize the average kinetic energy that the flywheel can store between an ambient temperature range without failure and without exceeding rotational speeds allowed by the bearings while minimizing the mass:

$$\begin{aligned} &\max_{\mathbf{x}} F_1 = \frac{1}{T_{a,\max} - T_{a,\min}} \int_{T_{a,\min}}^{T_{a,\max}} \left[2\pi \omega_{\max}^2 \int_{r_{in}}^{r_{out}} \rho(r) h(r) r^3 dr \right] dT_a, \\ &\min_{\mathbf{x}} F_2 = 2\pi \int_{r_{in}}^{r_{out}} \rho(r) h(r) r dr \end{aligned} \tag{4.5}$$

Subjected to,

$$\begin{aligned} &\omega_{\max} \le \omega_{design} \text{ and } \frac{\sigma_{VM}(r, T, \omega_{\max})}{\sigma_y(r, T)} \le 1 \\ &\omega_{design} \in \{10000rpm, 100000rpm\} \\ &-20\,°C \le T_a \le 40\,°C,\ T_{in} = T_a + 10\,°C \text{ and } T_{out} = T_a \\ &\{Mat_{in}, Mat_{out}\} \in \{\text{Ti-6Al-4V, Inconel 718, AISI 4340}\} \\ &0.01 \le m \le 100 \\ &r_{in} = 0.02m \text{ and } r_{out} \in \{0.12m, 0.32m, 0.52m\} \\ &h_{\min} \le h_i \le h_{\max} \text{ and } h_{\max} \in \{0.01m, 0.55m, 0.1m\},\ i = 1, 2, ..., 12 \end{aligned} \tag{4.6}$$

where, Mat_{in} and Mat_{out} correspond to the materials chosen for grading between the inner radius and the outer radius of the flywheel, respectively. T_{in} , T_{out} and T_a are temperatures at the inner and outer edges of the Flywheel rotor and the ambient temperature respectively.

In addition, **x** is the vector of design parameters that can be written as follows:

$$\mathbf{x} = \{h_1, h_2, ..., h_{12}, Mat_{in}, Mat_{out}, m\} \tag{4.7}$$

The optimal designs are obtained for different maximum rotation speeds determined by the choice of bearing for the FESS, different radii and different maximum thicknesses. This in turn allowed us to take into consideration the effect of design parameters that might be defined by the design limitations of the complete structure that the flywheel would be integrated. In addition, the ambient temperature variability is taken into consideration by c. In Figure 4.12 below a randomly generated Flywheel geometry is presented.

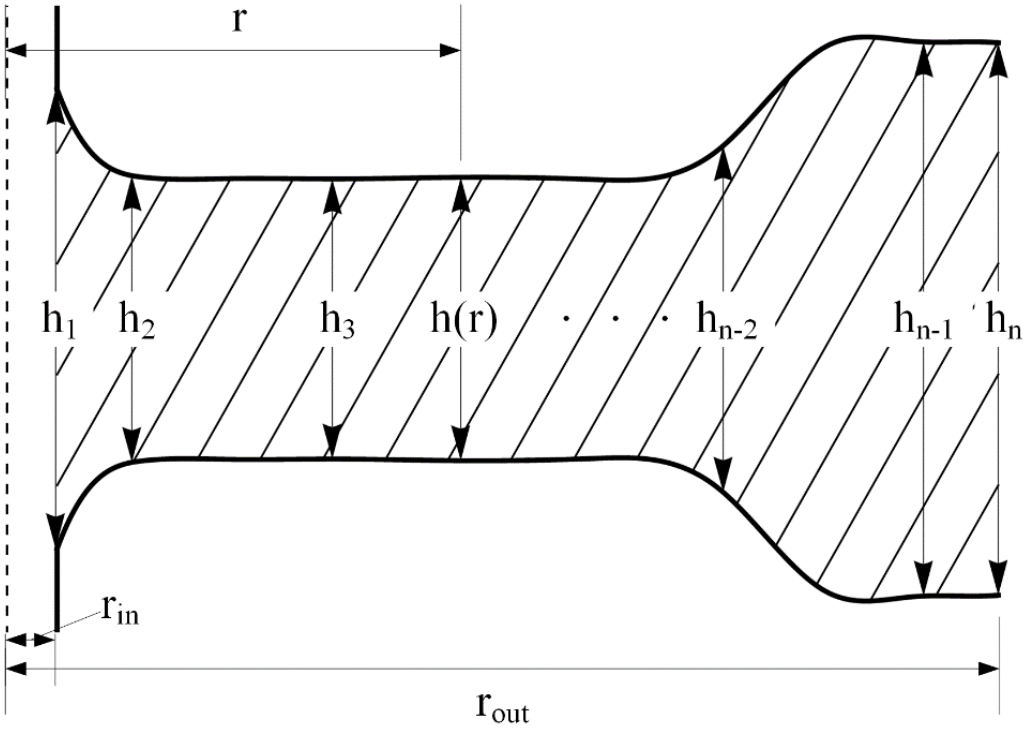

Figure 4.12 A randomly generated flywheel geometry

4.6 Optimization Algorithm Steps

Steps below have been followed in this optimization study.

- Step 1: Initial parent population randomly has been created. Size of the initial population P_0 has been decided as 1000 individuals.
- Step 2: Individuals have been assigned a rank regarding their non dominance and crowding distance
- Step 3: Offspring population Q_0 has been established from mating pool by using Roulette wheel selection, corrsover and mutation operators.
- Step 4: Combine Offspring population and the pareto front of the parent population.
- Step 5: Select best individuals of this combined population regarding to their non dominance and crowding distance to establish the next parent population P_1.
- Step 6: Continue iterations untill G=1000 generations are obtained.

The genotype of individuals have been constructed such that thickness (h) and grading coeffficient (m) has been encoded by 15 bit Gray coding and materials are encoded by value encoding. For generating child populations a multi point crossover has been used. Additionally, bit invertion and value changing mutations has been applied to the chromosomes. A flowchart of the optimization algortihm is shown in Figure 4.13.

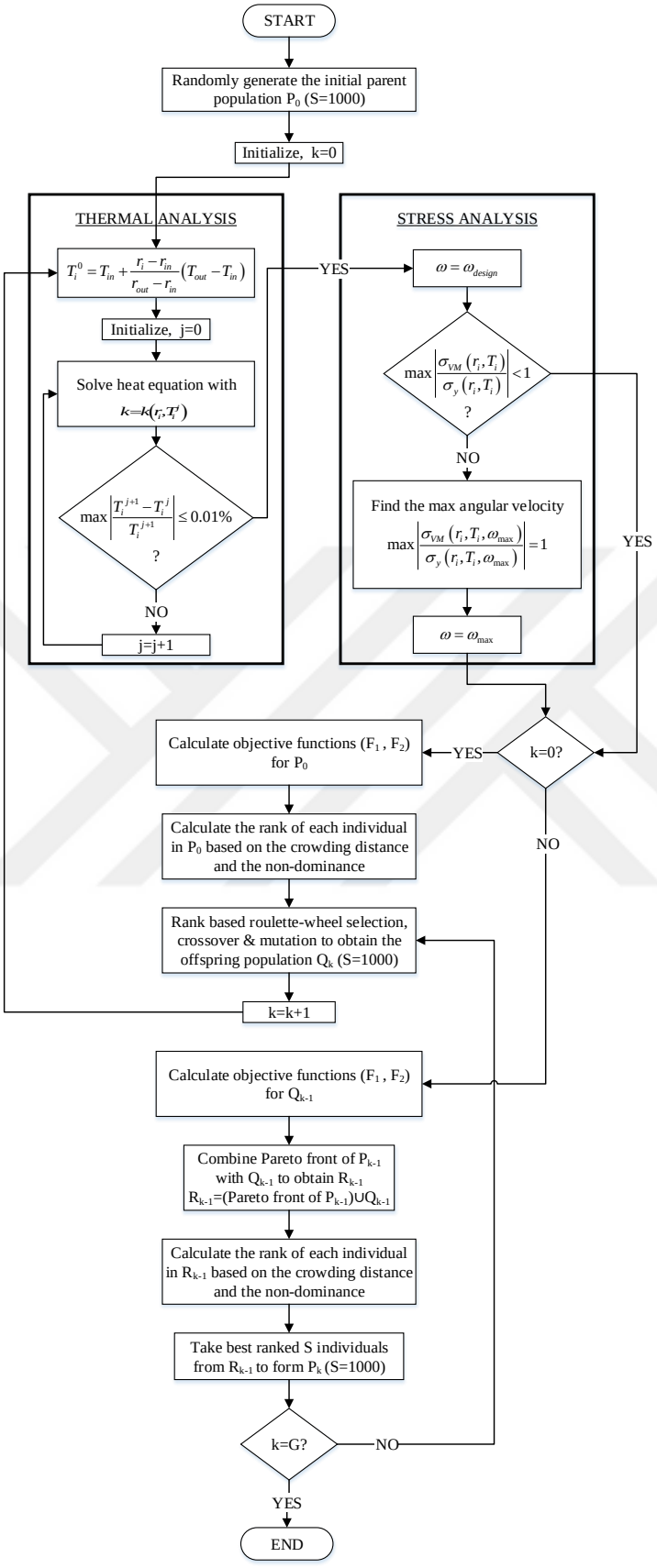

Figure 4.13 Optimization Algorithm.

5. RESULTS AND DISCUSSION

In total 18 different design space have been investigated during optimization. Table 5.1 below represents the design space parameters for 18 types.

Table 5.1 Design parameters for optimization

Design Type	ω_{max} (rpm)	h_{max} (m)	R_{thk} (m)
1	100000	0.01	0.1
2	100000	0.01	0.3
3	100000	0.01	0.5
4	100000	0.055	0.1
5	100000	0.055	0.3
6	100000	0.055	0.5
7	100000	0.1	0.1
8	100000	0.1	0.3
9	100000	0.1	0.5
10	10000	0.01	0.1
11	10000	0.01	0.3
12	10000	0.01	0.5
13	10000	0.055	0.1
14	10000	0.055	0.3
15	10000	0.055	0.5
16	10000	0.1	0.1
17	10000	0.1	0.3
18	10000	0.1	0.5

Here, ω_{max} represents maximum allowable rotational speed of the Flywheel. This parameter is determined by the maximum allowable speed of the bearings. Hence, in this optimization study we are focusing on 2 types of bearings. One is conventional mechanical bearing which is limited up to 10000 rpm, whereas the other is magnetic bearing which can operate as high as 100000 rpm.

Here,

$$R_{thk} = r_{out} - r_{in} \tag{5.1}$$

$h_{\max}$ and R_{thk} defines maximum allowable cross sectional and radial thickness of the Flywheel rotor respectively. These parameters represent physical space constraint of the system and defined in order to be more realistic as they are usually known parameters when designing such a system.

For the material content, random combinations of two materials out of three possibles (Ti-6Al-4V, Inconel 718, AISI 4340) have been selected for each designs. Mass distribution of those selected base materials have been arranged by a randomly selected volume fraction grading coefficient "m".

During optimization, genetic algorithm code have generated 1000 populations each of them has 1000 individuals. Therefore 1 million potential candidates have been evaluated for each design space. Computational time elapsed for obtaining results for one design space has been around 2000 minutes (~33.3 hours) at a cluster comprises of 4 machines with total 64 cores (CPU: Intel Xeon E5-2670 @2.6 GHz).

For this study, if we would prefer to search the same design space by hand, we would have to obtain following number of individual solutions. To give a general idea about the power of genetic algorithm search method, we can do a simple math as below.

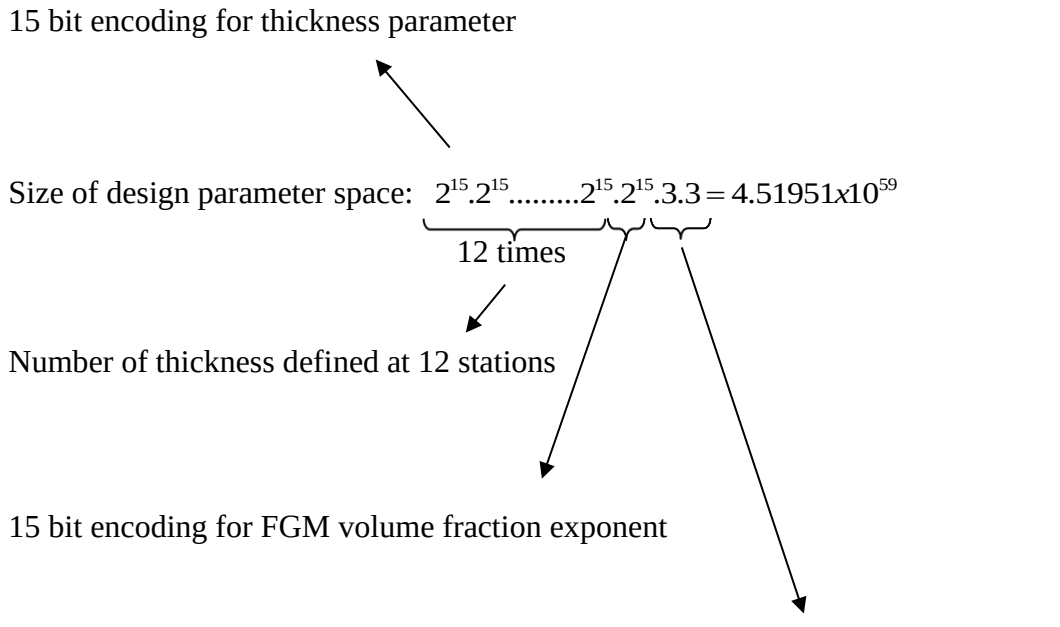

It can be clearly derived the impossibility of performing this amount of calculations by hand especially by knowing that, it is estimated that there are between 10^{78} to 10^{82} atoms in the known observable universe.

Design parameters for some of the candidate solutions have been tabulated in Appendix A. Maximum obtainable energy capacity and the minimum weight associated to that design has been also indicated.

Geometries for some of possible flywheel designs have been presented in Appendix B based on their energy storage capacities starting from the highest to the lowest. Smooth transition between parent materials can be clearly observed from these figures.

Following results can be deduced from the general behaviour of presented designs,

- For low speed designs (up to 10000rpm), it is observed that maximum design speed of 10000rpm is achievable without violating optimization criteria. Whereas, for the high speed applications (up to 100000rpm), maximum achievable speed can not be attained due to design constrains. For high speed designs maximum achievable speed is around 60000 rpm.
- The algorithm tries to increase the mass near the outer and inner edges while reducing it at the middle locations of the Flywheels. The reason for increasing the mass at the outer edge seems to increase the energy capacity. On the other hand, stress values are increasing from the outer edge to the inner edge dramatically. Thus, in order to meet stress constraints algortihm increases the mass at the inner edge. In middle sections, it can be seen that algorithm tries to keep as minimum thickness as possible to reduce the weight of the design.
- For material composition, algorithm allocates the lighter materials near outer radius whereas the heavier materials are placed as possible as at the inner radius region in order to reduce stresses caused by the centrifugal loads.
- Some of the designs seem unrealistic due to very thin web sections. For such solutions the study may be developed further to take into account of resonance vibration effects for thinner sections.

Pareto optimal fronts for all 18 design spaces have been shown in Appendix C. For the low speed designs, there is a noticeable difference in terms of the energy storage

capacity and the minimal weights between candidates. As the Flywheel size gets bigger the energy storage capacity gets higher at a remarkable rate. On the other hand, high speed results has not depicted such a noticeable difference. Though, it is still vaild that as the Flywheel size gets bigger the energy storage capacity gets higher. More iterations can be performed or mutation and crossover probability factors (P_m and P_c) may be modified to resolve this issue for high speed trials. It is also derived from figures in Appendix D, that the convergence speed is faster in low speed Flywheel designs than the high speed flywheels. This result is due to the fact that, at high speeds ω_{design} is so high that the ratio of σ_{VM}/σ_{ys} is bigger than 1. Therefore, subjected design violates stress constraint. In this case, algorithm starts another loop to find the $\omega_{\max}$ that enables the design to meet the stress constraint. Hence, the computational effort increases and speed of convergence is reduces.

6. CONCLUSION

In this study, a thermoelastic analysis and a Multi obejctive optimization of a functionally graded Flywheel that can be used on an energy storage device has been investgiated.

There have been several challenges during this study. First and foremost, the complexity of the governing differential equation of motion makes it almost impossible the exact analytical solution. One of the complexity came from the non uniform geometry of the Flywheel. The other one came from the non homogenous material content which was due to the variation of the material properties of functionally graded materials. The last complexity came due to taking into account of thermal effects on material's physical and mechanical properties. Thus, material properties such as Young modulus (E), Thermal expansion coefficient (Alpha), and Thermal conductivity coefficient (K), tensile yield strength (Sigma YS) in this study were considered temperature dependent. As a result, the governing equation and the boundary conditions became very complex nonlinear differential equations. In order to solve these complex equations the numerical methods had to be used. Therefore, one of the most favorable method for solving such problems called generalized differential quadrature method (GDQM) was used. Power of this method is to obtain sufficiently accurate results for relatively much less computational effort than other approximation methods. In order to validate the accuracy of the numerical results a finite element (FEM) test model was created. The results from both methods demonstrated a perfect correlation.

For the optimization study, non dominated sorting genetice algorithm (NSGA II) methods was used. This method is a kind of evolutionary algorithm with several advantages. Those advantages can be mentioned with three concepts: Non dominance, Crowding distance and Elitism. By applying these concepts NSGA II method provides a fast convergence while keeping diversity of the populations to avoid from sub optimal solutions. For running the genetic algorithm a computer code has been developed and used in Mathematica.

The results of the problem was achieved by using the Numerical solver and the Genetic algorithm code simultaneously and iteratively for each solution. Optimization study has also challenges itself. One of the challenges are the multi objective optimization. In this approach, optimal best solution is expected to meet both objective functions simultaneously. Hence, the optimal result is not a single solution, rather a set of solutions. Another challenge of the optimization was the number of constraints. For a realistic optimization, many design parameters were taken as design constraints. For example the yield strength of the materials were not taken as constant instead it was considered varrying by the, material grading and temperature. As a results a very complex optimization algorithm was obtained. During the optimization study, 18 Million individuals were generated and solved to search for 18 different design spaces by following this algorithm.

Results of the study demonstrated several optimal design shapes under the given physical design space and optimization constraints. Some of the common characteristics of the resultant optimal solutions are as follows.

- At constant speed, size of the outer radius is the most effective design parameter in terms of the energy capacity. For reaching a higher energy capacity a bigger Flywheel size is reqiured. However, as the size gets bigger the stresses induced due to the centrifugal force increases proportional to the square of the radius of the Flywheel.
- At high speeds the stress concerns becomes more evident such that, maximum design speed can not be achieved due to the violation of the stress limit. In such cases, algorithm starts another loop to determine the maximum allowable speed before continuing the other steps. In other words at high speed designs maximum rotational speed becomes another design variable. Therefore, computational efforts highly increases for high speed design searches. Consequently the convergence speed substantially decreases.
- For low speed designs (up to 10000rpm), it is observed that maximum design speed of 10000rpm is achievable without violating optimization criteria. Whereas, for the high speed applications (up to 100000rpm), maximum achievable speed can not be attained due to design constrains. For high speed designs maximum achievable speed depends on the flywheel material and geometry considered.

- For the optimal shape, the algorithm tries to increase the mass near the outer and inner edges while reducing it at the middle locations of the Flywheels. The reason for increasing the mass at the outer edge seems to increase the energy capacity. On the other hand, radial stress value is increasing from the outer edge to the inner edge dramatically. Thus, in order to meet stress constraints algortihm increases the mass at the inner edge. In middle sections, it can be seen that algorithm tries to keep as minimum thickness as possible to reduce the weight of the design.
- For material composition, algorithm allocates the lighter materials near outer radius. Whereas, the heavier materials are placed as possible as at the inner radius region in order to reduce stresses caused by the centrifugal loads. Additionally, algorithm tends to allocate AISI4340 to increase the stored energy due to its high density and strength. Whereas, for low energy capacity designs Ti-6Al-4V has been used to minimize the mass. Inco 718 has been used together with these materials to fine tune the designs with its medium properties. Some of the designs seem to have only one material content instead of a mixed FGM structure. Therefore, it can be said for some optimal designs homogenous material structure is the best choice to provide the optimal ebergy storage.

In conclusion, effects of the geometrical, material and environmental parameters together with the operating conditions on the performance of a Flywheel has been presented for several different designs. A very large design space consist of 18 million solutions have been searched for obtaining best Flywheel shapes under given design criteria. Different shapes has been generated regarding the optimization constraints. Some of the designs seem unrealistic due to very thin web sections. For such solutions the study may be developed further to take into account of resonance vibration effects for thinner sections.

REFERENCES

[1] **F. Kreith, and D. Y. Goswami**, *Handbook of energy efficiency and renewable energy*: Crc Press, 2007.

[2] **S. Chu, and A. Majumdar**, "Opportunities and challenges for a sustainable energy future," *nature*, vol. 488, no. 7411, pp. 294, 2012.

[3] **M. E. Amiryar, and K. R. Pullen**, "A review of flywheel energy storage system technologies and their applications," *Applied Sciences*, vol. 7, no. 3, pp. 286, 2017.

[4] **I. Hadjipaschalis, A. Poullikkas, and V. Efthimiou**, "Overview of current and future energy storage technologies for electric power applications," *Renewable and sustainable energy reviews*, vol. 13, no. 6-7, pp. 1513-1522, 2009.

[5] **R. Hebner, J. Beno, and A. Walls**, "Flywheel batteries come around again," *IEEE spectrum*, vol. 39, no. 4, pp. 46-51, 2002.

[6] **A. Stodola**, "Steam and gas turbines, 1927," *New York, NY, USA, McGrawĞ Hill*, 1945.

[7] **P. Yulong, A. Cavagnino, S. Vaschetto, C. Feng, and A. Tenconi**, "Flywheel energy storage systems for power systems application." pp. 492-501.

[8] **R. Sebastián, and R. P. Alzola**, "Flywheel energy storage systems: Review and simulation for an isolated wind power system," *Renewable and Sustainable Energy Reviews*, vol. 16, no. 9, pp. 6803-6813, 2012.

[9] **R. Östergård**, "Flywheel energy storage: a conceptucal study," 2011.

[10] **M. Damircheli, and M. Azadi**, "Temperature and thickness effects on thermal and mechanical stresses of rotating FG-disks," *Journal of mechanical science and technology*, vol. 25, no. 3, pp. 827, 2011.

[11] **J. Durodola, and O. Attia**, "Deformation and stresses in functionally graded rotating disks," *Composites Science and Technology*, vol. 60, no. 7, pp. 987-995, 2000.

[12] **E. Sandgren, and K. Ragsdell**, "Optimal flywheel design with a general thickness form representation," *Journal of Mechanisms, Transmissions, and Automation in Design*, vol. 105, no. 3, pp. 425-433, 1983.

[13] **N. D. Ebrahimi**, "Optimum design of flywheels," *Computers & Structures*, vol. 29, no. 4, pp. 681-686, 1988/01/01/, 1988.

[14] **G. R. Kress**, "Shape optimization of a flywheel," *Structural and Multidisciplinary Optimization*, vol. 19, no. 1, pp. 74-81, March 01, 2000.

[15] **J. Huang, and G. M. Fadel**, "Heterogeneous flywheel modeling and optimization," *Materials & Design*, vol. 21, no. 2, pp. 111-125, 2000/04/01/, 2000.

[16] **J. Huang, G. M. Fadel, V. Y. Blouin, and M. Grujicic**, "Bi-objective optimization design of functionally gradient materials," *Materials & Design*, vol. 23, no. 7, pp. 657-666, 2002/10/01/, 2002.

[17] **M. A. Arslan**, "Flywheel geometry design for improved energy storage using finite element analysis," *Materials & Design,* vol. 29, no. 2, pp. 514-518, 2008/01/01/, 2008.

[18] **M. Krack, M. Secanell, and P. Mertiny**, "Cost optimization of a hybrid composite flywheel rotor with a split-type hub using combined analytical/numerical models," *Structural and Multidisciplinary Optimization,* vol. 44, no. 1, pp. 57-73, July 01, 2011.

[19] **M. Mahdi**, "An optimal two-dimensional geometry of flywheel for kinetic energy storage," *Int. J. of Thermal & Environmental Engineering,* vol. 3, no. 2, pp. 67-72, 2011.

[20] **A. Aghalari, and J. Saeed**, "Optimum Design of Flywheels Using Genetic Algorithm and Finite Element Coupling," *Majlesi Journal of Mechatronic Systems,* vol. 1, no. 4, pp. ll, 2012.

[21] **L. Jiang, W. Zhang, G. J. Ma, and C. W. Wu**, "Shape optimization of energy storage flywheel rotor," *Structural and Multidisciplinary Optimization,* vol. 55, no. 2, pp. 739-750, February 01, 2017.

[22] **L. Jiang, and C. W. Wu**, "Topology optimization of energy storage flywheel," *Structural and Multidisciplinary Optimization,* vol. 55, no. 5, pp. 1917-1925, May 01, 2017.

[23] **G. N. Praveen, and J. N. Reddy**, "Nonlinear transient thermoelastic analysis of functionally graded ceramic-metal plates," *International Journal of Solids and Structures,* vol. 35, no. 33, pp. 4457-4476, Nov, 1998.

[24] **United States. Federal Aviation Administration.**, Battelle Memorial Institute. Columbus Laboratories., William J. Hughes Technical Center (U.S.), United States. Department of Defense., and United States. National Aeronautics and Space Administration., *Metallic materials properties development and standardization (MMPDS) ; MMPDS-04*, Washington, D.C.Columbus, Ohio: Federal Aviation Administration ;Battelle Memorial Institute distributor, 2008.

[25] **S. P. Timoshenko, and J. N. Goodier**, *Theory of elasticity*: McGraw-Hill, New York London, 1970.

[26] **M. Bayat, B. Sahari, M. Saleem, A. Hamouda, and J. Reddy**, "Thermo elastic analysis of functionally graded rotating disks with temperature-dependent material properties: uniform and variable thickness," *International Journal of Mechanics and Materials in Design,* vol. 5, no. 3, pp. 263-279, 2009.

[27] **R. Bellman, B. Kashef, and J. Casti**, "Differential quadrature: a technique for the rapid solution of nonlinear partial differential equations," *Journal of computational physics,* vol. 10, no. 1, pp. 40-52, 1972.

[28] **C. Shu**, *Differential quadrature and its application in engineering*: Springer Science & Business Media, 2012.

[29] **C. Shu, and H. Du**, "Implementation of clamped and simply supported boundary conditions in the GDQ free vibration analysis of beams and plates," *International Journal of Solids and Structures,* vol. 34, no. 7, pp. 819-835, Mar, 1997.

[30] **M. Berger, and I. Porat**, "Optimal design of a rotating disk for kinetic energy storage," *Journal of applied mechanics,* vol. 55, no. 1, pp. 164-170, 1988.

[31] **N. Hiroshima, H. Hatta, M. Koyama, K. Goto, and Y. Kogo**, "Optimization of flywheel rotor made of three-dimensional composites," *Composite Structures,* vol. 131, pp. 304-311, 2015.

[32] **S. K. Ha, H.-M. Jeong, and Y.-S. Cho**, "Optimum design of thick-walled composite rings for an energy storage system," *Journal of Composite Materials*, vol. 32, no. 9, pp. 851-873, 1998.
[33] **L. Jiang, and C. Wu**, "Topology optimization of energy storage flywheel," *Structural and Multidisciplinary Optimization*, vol. 55, no. 5, pp. 1917-1925, 2017.
[34] **B. Farshi, H. Jahed, and A. Mehrabian**, "Optimum design of inhomogeneous non-uniform rotating discs," *Computers & structures*, vol. 82, no. 9-10, pp. 773-779, 2004.
[35] **S. Bhavikatti, and C. Ramakrishnan**, "Optimum shape design of rotating disks," *Computers & Structures*, vol. 11, no. 5, pp. 397-401, 1980.
[36] **J. H. Holland**, *Adaptation in natural and artificial systems: an introductory analysis with applications to biology, control, and artificial intelligence*: MIT press, 1992.
[37] **A. Arikoglu, and I. Ozkol**, "Vibration analysis of composite sandwich beams with viscoelastic core by using differential transform method," *Composite Structures*, vol. 92, no. 12, pp. 3031-3039, 2010.
[38] **S. Sivanandam, and S. Deepa**, *Introduction to genetic algorithms*: Springer Science & Business Media, 2007.
[39] **G. Frank**, "Pulse code communication," Google Patents, 1953.
[40] **C. Reeves**, "Genetic algorithms," *Handbook of metaheuristics*, pp. 55-82: Springer, 2003.
[41] **K. Deb**, "Multi-objective optimization using evolutionary algorithms: an introduction," *Multi-objective evolutionary optimisation for product design and manufacturing*, pp. 1-24, 2011.
[42] **K. Deb, A. Pratap, S. Agarwal, and T. Meyarivan**, "A fast and elitist multiobjective genetic algorithm: NSGA-II," *IEEE transactions on evolutionary computation*, vol. 6, no. 2, pp. 182-197, 2002.
[43] **A. Arikoglu**, "Multi-objective optimal design of hybrid viscoelastic/composite sandwich beams by using the generalized differential quadrature method and the non-dominated sorting genetic algorithm II," *Structural and Multidisciplinary Optimization*, vol. 56, no. 4, pp. 885-901, 2017.
[44] **P. D. Justesen**, "Multi-objective optimization using evolutionary algorithms," *University of Aarhus, Department of Computer Science, Denmark*, 2009.

APPENDICES

APPENDIX A: Optimal Flywheel Design Parameters

APPENDIX B: Optimal Flywheel Shapes

APPENDIX C: Pareto Optimal Fronts

APPENDIX D: Convergence Speeds

APPENDIX A: Optimal Flywheel Design Parameters

Table A. 1 Solutions for ω_{max}=100000 rpm, h_{max}=0.01m, R_{thk}=0.1m

	N1	***N2***	***N3***	***N4***	***N5***	***N6***	***N7***	***N8***
h1 (m)	0.009997	0.009998	0.009999	0.009999	0.009974	0.009198	0.009571	0.00952
h2 (m)	0.009206	0.009257	0.009198	0.009195	0.009162	0.008614	0.009044	0.007087
h3 (m)	0.007997	0.008018	0.007909	0.007763	0.007753	0.007561	0.007796	0.004461
h4 (m)	0.007088	0.007082	0.006911	0.006674	0.006648	0.006662	0.006807	0.004097
h5 (m)	0.006417	0.006329	0.006047	0.005736	0.005714	0.005736	0.005707	0.003447
h6 (m)	0.005633	0.005454	0.005143	0.00469	0.004719	0.004682	0.004501	0.00257
h7 (m)	0.00556	0.004493	0.004185	0.003676	0.003741	0.003554	0.003345	0.002622
h8 (m)	0.008602	0.004058	0.003262	0.002824	0.002927	0.002627	0.002543	0.002517
h9 (m)	0.009894	0.006569	0.003584	0.002554	0.00253	0.002518	0.002529	0.002555
h10 (m)	0.009981	0.009975	0.00786	0.005331	0.005211	0.002626	0.002626	0.002633
h11 (m)	0.009884	0.009677	0.009578	0.009729	0.006338	0.00295	0.003005	0.002922
h12 (m)	0.009741	0.009741	0.00772	0.009768	0.003583	0.003055	0.003082	0.003062
m	11.06721	14.75849	69.02149	20.82489	1.831321	0.807992	0.083003	0.0285
Mat_in	3	3	3	3	3	3	3	1
Mat_out	2	2	2	1	1	1	1	1
Energy (J)	342609.6	320508.1	294145.6	260463.2	226600.3	185455.5	138978.6	80785.77
Mass (kg)	2.75237	2.229639	1.865225	1.52424	1.237147	0.980814	0.769899	0.563348

Table A. 2 Solutions for ω_{max}=100000 rpm, h_{max}=0.01m, R_{thk}=0.3m

	N1	***N2***	***N3***	***N4***	***N5***	***N6***	***N7***	***N8***
h1 (m)	0.009997	0.009999	0.01	0.009998	0.009999	0.00996	0.009999	0.009999
h2 (m)	0.008668	0.008609	0.008578	0.008529	0.008565	0.008682	0.008649	0.007552
h3 (m)	0.007412	0.00748	0.007291	0.007203	0.007161	0.007308	0.007322	0.005296
h4 (m)	0.006977	0.006948	0.00675	0.006735	0.006769	0.006885	0.006926	0.004497
h5 (m)	0.00652	0.006539	0.006051	0.005982	0.005979	0.006268	0.006211	0.003434
h6 (m)	0.005827	0.005607	0.00527	0.005006	0.00511	0.005192	0.00511	0.002971
h7 (m)	0.005955	0.004801	0.004345	0.003958	0.004105	0.003953	0.003862	0.002565
h8 (m)	0.009198	0.004276	0.003403	0.003012	0.003224	0.002861	0.002678	0.002549
h9 (m)	0.009986	0.007175	0.004189	0.002615	0.002636	0.00262	0.00257	0.002521
h10 (m)	0.009922	0.009959	0.008429	0.004761	0.004703	0.002773	0.002578	0.002539
h11 (m)	0.009859	0.009875	0.009674	0.008755	0.009083	0.003154	0.003104	0.003061
h12 (m)	0.009931	0.009982	0.008484	0.009859	0.009848	0.004214	0.003609	0.003638
m	6.909428	11.16721	33.5916	67.56266	1.979607	0.952134	0.116465	0.2893
Mat_in	3	3	3	3	3	3	3	1
Mat_out	2	2	2	2	1	1	1	1
Energy (J)	2385714	2227241	2043875	1820178	1567928	1293945	973148.6	577800.5
Mass (kg)	20.81985	16.82833	14.0494	11.52646	9.295744	7.33995	5.724058	4.106595

Table A. 3 Solutions for ω_{max}=100000 rpm, h_{max}=0.01m, R_{thk}=0.5m

	N1	***N2***	***N3***	***N4***	***N5***	***N6***	***N7***	***N8***
h1 (m)	0.01	0.01	0.01	0.009993	0.009999	0.009961	0.009297	0.008843
h2 (m)	0.00835	0.008382	0.008209	0.008425	0.008408	0.008366	0.008287	0.008412
h3 (m)	0.00704	0.007259	0.007214	0.006967	0.006946	0.007011	0.00718	0.005994
h4 (m)	0.006891	0.006928	0.006751	0.006528	0.006597	0.006766	0.006774	0.003672
h5 (m)	0.00636	0.006349	0.006119	0.005853	0.005963	0.006175	0.006095	0.003034
h6 (m)	0.005616	0.005566	0.005272	0.004932	0.005035	0.005153	0.004952	0.00264
h7 (m)	0.00594	0.004706	0.004248	0.003915	0.003998	0.003928	0.003747	0.002525
h8 (m)	0.009139	0.003904	0.003348	0.002937	0.003119	0.00279	0.002728	0.002513
h9 (m)	0.00993	0.005632	0.00338	0.002536	0.00256	0.002531	0.002531	0.002528
h10 (m)	0.009883	0.009883	0.006936	0.004102	0.004101	0.002571	0.002514	0.00251
h11 (m)	0.009947	0.009672	0.009898	0.007954	0.008126	0.002736	0.002707	0.002761
h12 (m)	0.009771	0.009829	0.009658	0.00979	0.009869	0.003103	0.002986	0.002993
m	14.40601	17.77186	12.34596	2.051551	1.965192	0.867057	0.093064	0.014278
Mat_in	3	3	3	3	3	3	3	1
Mat_out	2	2	2	3	1	1	1	1
Energy (J)	6187619	5676057	5184569	4581251	3948510	3195795	2408074	1375842
Mass (kg)	54.48748	41.76705	35.02224	28.80489	23.29472	18.2892	14.37762	10.26637

Table A. 4 Solutions for ω_{max}=100000 rpm, h_{max}=0.055m, R_{thk}=0.1m

	N1	***N2***	***N3***	***N4***	***N5***	***N6***	***N7***	***N8***
h1 (m)	0.054997	0.054997	0.054981	0.054981	0.054981	0.054236	0.053364	0.042958
h2 (m)	0.050663	0.050869	0.050868	0.050064	0.050113	0.050251	0.050113	0.024402
h3 (m)	0.043648	0.043706	0.04357	0.042711	0.042147	0.043374	0.042802	0.016931
h4 (m)	0.038625	0.038612	0.038167	0.036284	0.036156	0.037028	0.03507	0.01406
h5 (m)	0.034426	0.033742	0.032891	0.030356	0.030271	0.029537	0.027374	0.008308
h6 (m)	0.029888	0.028754	0.02699	0.02416	0.024109	0.020568	0.01811	0.004593
h7 (m)	0.025312	0.023542	0.021209	0.018159	0.017396	0.012822	0.010852	0.005708
h8 (m)	0.02901	0.018796	0.016327	0.012741	0.0122	0.007425	0.005877	0.002801
h9 (m)	0.052368	0.025628	0.012575	0.009204	0.008794	0.004307	0.003647	0.003968
h10 (m)	0.054268	0.050118	0.02558	0.012161	0.008943	0.004014	0.003514	0.00386
h11 (m)	0.051465	0.047848	0.050794	0.033362	0.024335	0.004732	0.002957	0.002598
h12 (m)	0.049408	0.044488	0.050724	0.046106	0.040779	0.0032	0.002933	0.002627
m	13.95955	29.9856	18.69943	1.661134	1.398606	0.67934	0.043106	0.120257
Mat_in	3	3	3	3	3	3	3	1
Mat_out	2	3	2	3	1	1	1	1
Energy (J)	1824014	1666258	1491514	1283016	1051515	794179.8	521922	141966.1
Mass (kg)	13.46751	10.88475	8.872438	7.026038	5.356852	3.804039	2.58271	1.108044

Table A. 5 Solutions for ω_{max}=100000 rpm, h_{max}=0.055m, R_{thk}=0.3m

	N1	***N2***	***N3***	***N4***	***N5***	***N6***	***N7***	***N8***
h1 (m)	0.054954	0.054982	0.054984	0.054901	0.054958	0.054285	0.054593	0.038596
h2 (m)	0.047135	0.047127	0.046987	0.046612	0.04696	0.046378	0.042894	0.04639
h3 (m)	0.039559	0.039559	0.039306	0.039319	0.038117	0.038364	0.035342	0.022342
h4 (m)	0.037145	0.037145	0.036336	0.036432	0.034544	0.035789	0.031234	0.009902
h5 (m)	0.034186	0.034083	0.03259	0.031692	0.028986	0.030728	0.026591	0.007121
h6 (m)	0.030284	0.029725	0.027746	0.025844	0.022475	0.023345	0.018783	0.004107
h7 (m)	0.025883	0.024231	0.022246	0.019262	0.015712	0.015662	0.012629	0.003027
h8 (m)	0.029292	0.019365	0.017061	0.014169	0.010202	0.009377	0.007332	0.003306
h9 (m)	0.0506	0.025574	0.013028	0.009963	0.006603	0.005604	0.004399	0.003718
h10 (m)	0.054696	0.048692	0.029824	0.013659	0.005679	0.004178	0.002724	0.002639
h11 (m)	0.05404	0.05409	0.054053	0.034001	0.015598	0.008813	0.00759	0.007738
h12 (m)	0.054708	0.054572	0.053273	0.046688	0.024939	0.01489	0.014757	0.014914
m	13.25964	13.20014	15.17922	20.27616	2.050398	0.74894	0.091584	1.428404
Mat_in	3	3	3	3	3	3	3	1
Mat_out	2	2	3	3	3	1	1	1
Energy (J)	12548878	11510526	10248927	8678543	6946126	5174495	3295585	817473.1
Mass (kg)	98.74953	80.67823	65.23886	51.44259	38.48097	27.64033	18.16475	7.12082

Table A. 6 Solutions for ω_{max}=100000 rpm, h_{max}=0.055m, R_{thk}=0.5m

	N1	***N2***	***N3***	***N4***	***N5***	***N6***	***N7***	***N8***
h1 (m)	0.054947	0.05497	0.054946	0.05488	0.054473	0.05487	0.046415	0.046473
h2 (m)	0.04563	0.045363	0.04517	0.045476	0.045524	0.045214	0.039588	0.047792
h3 (m)	0.040588	0.0393	0.039388	0.039281	0.039555	0.037571	0.027512	0.020458
h4 (m)	0.038444	0.037252	0.037451	0.037252	0.035839	0.034394	0.022702	0.011416
h5 (m)	0.036102	0.034086	0.033298	0.031675	0.030068	0.029348	0.019059	0.009184
h6 (m)	0.032641	0.029603	0.028176	0.025905	0.024551	0.022577	0.014706	0.007973
h7 (m)	0.028344	0.02464	0.022614	0.019623	0.018444	0.015422	0.010304	0.003793
h8 (m)	0.04091	0.019652	0.017125	0.014339	0.013525	0.009715	0.006635	0.003726
h9 (m)	0.053795	0.027527	0.013719	0.010069	0.009689	0.006115	0.003868	0.002737
h10 (m)	0.05343	0.05329	0.033533	0.018423	0.010245	0.004293	0.003288	0.003171
h11 (m)	0.053766	0.051712	0.052094	0.03305	0.03079	0.008962	0.005509	0.00533
h12 (m)	0.050257	0.048259	0.038761	0.032644	0.048607	0.01522	0.007468	0.00926
m	11.02684	26.14211	1.205364	18.70995	2.317076	1.209097	1.040283	0.012853
Mat_in	3	3	3	3	3	3	3	1
Mat_out	2	2	3	3	1	1	1	1
Energy (J)	33612774	30523317	27090683	22977868	18593346	13907145	8862658	2613594
Mass (kg)	284.322	218.1066	175.7507	138.7703	104.9874	75.46114	49.22997	20.38144

Table A. 7 Solutions for ω_{max}=100000 rpm, h_{max}=0.1m, R_{thk}=0.1m

	N1	***N2***	***N3***	***N4***	***N5***	***N6***	***N7***	***N8***
h1 (m)	0.099911	0.099893	0.099679	0.099664	0.099664	0.094272	0.097423	0.077895
h2 (m)	0.091597	0.092076	0.091594	0.090794	0.091011	0.086369	0.087532	0.036383
h3 (m)	0.0789	0.079028	0.07677	0.076535	0.075086	0.073321	0.072089	0.025736
h4 (m)	0.06912	0.06912	0.065986	0.064496	0.0618	0.062573	0.058553	0.024028
h5 (m)	0.06127	0.05994	0.056128	0.053189	0.050032	0.049398	0.043827	0.007445
h6 (m)	0.05326	0.050237	0.04619	0.040882	0.037787	0.035317	0.030479	0.011081
h7 (m)	0.047345	0.040498	0.035395	0.029929	0.026676	0.022094	0.017056	0.009501
h8 (m)	0.048112	0.031333	0.027224	0.020815	0.018544	0.01265	0.008689	0.00408
h9 (m)	0.061089	0.030196	0.020684	0.013691	0.015575	0.007076	0.004898	0.004032
h10 (m)	0.099206	0.068254	0.049546	0.013468	0.011944	0.005068	0.004074	0.00458
h11 (m)	0.097599	0.097634	0.09759	0.046559	0.018639	0.009829	0.006699	0.003491
h12 (m)	0.098938	0.0873	0.087089	0.080471	0.037823	0.01517	0.008493	0.003839
m	12.19079	27.44476	18.43328	17.79186	2.037185	0.51999	0.06391	10.812
Mat_in	3	3	3	3	3	3	1	1
Mat_out	2	2	1	3	1	1	1	1
Energy (J)	3178112	2867761	2529181	2150659	1744251	1293398	806238	169679
Mass (kg)	22.46677	17.80301	14.51521	11.37207	8.777766	6.184723	4.005988	1.645292

Table A. 8 Solutions for ω_{max}=100000 rpm, h_{max}=0.1m, R_{thk}=0.3m

	N1	***N2***	***N3***	***N4***	***N5***	***N6***	***N7***	***N8***
h1 (m)	0.099961	0.099946	0.099949	0.099946	0.099622	0.098923	0.095159	0.098301
h2 (m)	0.085923	0.08597	0.085122	0.085078	0.08522	0.083947	0.084396	0.066635
h3 (m)	0.072098	0.071786	0.071976	0.071691	0.070533	0.067465	0.066989	0.021883
h4 (m)	0.06862	0.067391	0.066921	0.065781	0.064555	0.059047	0.05914	0.017839
h5 (m)	0.062913	0.062068	0.060601	0.05831	0.05481	0.04791	0.048764	0.012914
h6 (m)	0.056866	0.05456	0.051978	0.048484	0.042741	0.034312	0.035053	0.009891
h7 (m)	0.06016	0.04558	0.041935	0.037073	0.030208	0.021671	0.022029	0.007957
h8 (m)	0.097393	0.041382	0.033252	0.02814	0.020297	0.012599	0.012599	0.004517
h9 (m)	0.097453	0.067174	0.031654	0.020222	0.013572	0.007192	0.007356	0.003696
h10 (m)	0.099542	0.098973	0.070607	0.032273	0.01118	0.004375	0.004431	0.004166
h11 (m)	0.099726	0.098209	0.09701	0.074425	0.048365	0.011073	0.009516	0.009415
h12 (m)	0.099694	0.099694	0.076981	0.098756	0.088342	0.01969	0.015497	0.011385
m	5.986657	18.07921	28.9178	3.625804	62.48419	1.478652	0.151302	0.012832
Mat_in	3	3	3	3	3	3	3	3
Mat_out	2	2	3	3	1	3	1	1
Energy (J)	23804800	21915907	19530546	16804215	13570089	9995642	6215508	1729591
Mass (kg)	209.2929	162.3488	129.4325	101.9602	76.1733	53.28427	33.50718	11.49889

Table A. 9 Solutions for ω_{max}=100000 rpm, h_{max}=0.1m, R_{thk}=0.5m

	N1	***N2***	***N3***	***N4***	***N5***	***N6***	***N7***	***N8***
h1 (m)	0.099771	0.099955	0.099982	0.099958	0.098741	0.099015	0.097837	0.060871
h2 (m)	0.081528	0.082066	0.081492	0.083141	0.082385	0.08323	0.080695	0.035514
h3 (m)	0.079118	0.072167	0.073226	0.070738	0.067751	0.068599	0.067192	0.023252
h4 (m)	0.07361	0.068084	0.06829	0.067528	0.062196	0.063207	0.062065	0.014944
h5 (m)	0.064395	0.061809	0.059904	0.058952	0.053501	0.053935	0.047966	0.010001
h6 (m)	0.056932	0.053495	0.050814	0.04982	0.040721	0.040483	0.034008	0.00755
h7 (m)	0.048963	0.044583	0.040397	0.039971	0.028694	0.026575	0.020874	0.008207
h8 (m)	0.054998	0.035466	0.032303	0.031657	0.018544	0.015512	0.012087	0.003518
h9 (m)	0.095968	0.047285	0.02351	0.026373	0.01206	0.009945	0.005803	0.002949
h10 (m)	0.098887	0.092757	0.050683	0.047258	0.012617	0.006591	0.005484	0.003595
h11 (m)	0.09886	0.098441	0.0992	0.085851	0.024864	0.00946	0.006383	0.004059
h12 (m)	0.097965	0.096706	0.088886	0.091898	0.029012	0.013718	0.008014	0.002708
m	15.34653	20.70815	6.29204	2.474604	1.998616	0.835241	0.545287	28.26684
Mat_in	3	3	3	3	3	3	1	1
Mat_out	2	2	3	1	3	1	1	1
Energy (J)	60480812	55169463	48544045	40800398	32367344	22831914	13590535	3311538
Mass (kg)	489.3514	392.0101	311.7773	244.9623	181.3183	123.0928	75.10881	23.32879

Table A. 10 Solutions for ω_{max}=10000 rpm, h_{max}=0.01m, R_{thk}=0.1m

	N1	***N2***	***N3***	***N4***	***N5***	***N6***	***N7***	***N8***
h1 (m)	0.002629	0.002516	0.002502	0.002553	0.002512	0.002516	0.002514	0.002727
h2 (m)	0.002664	0.002535	0.002573	0.002606	0.00256	0.002546	0.002549	0.002596
h3 (m)	0.002595	0.002599	0.002537	0.002536	0.002535	0.002581	0.002538	0.002526
h4 (m)	0.002941	0.002541	0.002595	0.002533	0.002532	0.002539	0.002518	0.002526
h5 (m)	0.002834	0.002577	0.00251	0.00251	0.002536	0.002503	0.002509	0.002507
h6 (m)	0.008584	0.00343	0.00255	0.002582	0.002504	0.002515	0.002517	0.002525
h7 (m)	0.009864	0.008518	0.00377	0.003103	0.002514	0.002522	0.002522	0.002522
h8 (m)	0.009969	0.009937	0.00935	0.006971	0.004174	0.002516	0.002538	0.00253
h9 (m)	0.00999	0.009997	0.009913	0.00985	0.00935	0.004883	0.002537	0.002522
h10 (m)	0.009994	0.009979	0.009996	0.00995	0.009908	0.009894	0.005324	0.002554
h11 (m)	0.009971	0.009949	0.009949	0.00998	0.009862	0.009775	0.009693	0.00254
h12 (m)	0.009915	0.009955	0.009976	0.009948	0.009957	0.009908	0.009761	0.002616
m	0.138793	0.25414	0.540556	1.686066	4.163559	7.140437	14.72534	81.60945
Mat_in	2	1	1	1	1	1	1	1
Mat_out	2	2	2	2	2	2	2	2
Energy (J)	14013	12857.51	11485.51	9935.252	8143.194	6247.912	4193.305	2070.759
Mass (kg)	3.037249	2.591338	2.181397	1.8148	1.444553	1.1055	0.789768	0.501595

Table A. 11 Solutions for ω_{max}=10000 rpm, h_{max}=0.01m, R_{thk}=0.3m

	N1	***N2***	***N3***	***N4***	***N5***	***N6***	***N7***	***N8***
h1 (m)	0.006318	0.006578	0.006425	0.00651	0.006696	0.006459	0.006631	0.006519
h2 (m)	0.004478	0.004323	0.004229	0.004344	0.004408	0.004373	0.004373	0.004255
h3 (m)	0.002554	0.002513	0.002516	0.00254	0.002556	0.002532	0.002543	0.002535
h4 (m)	0.002756	0.002584	0.002592	0.002547	0.002548	0.002536	0.002562	0.002592
h5 (m)	0.0028	0.002536	0.002533	0.002547	0.002523	0.00252	0.00255	0.002507
h6 (m)	0.007616	0.002846	0.00265	0.002522	0.002518	0.002536	0.002533	0.002518
h7 (m)	0.009723	0.005796	0.003622	0.002515	0.002513	0.002514	0.002514	0.002514
h8 (m)	0.009943	0.0095	0.009263	0.004379	0.00384	0.002518	0.00254	0.002557
h9 (m)	0.009988	0.009984	0.009922	0.009627	0.008475	0.004733	0.00255	0.002529
h10 (m)	0.009995	0.009998	0.009993	0.009885	0.00991	0.009727	0.005625	0.002571
h11 (m)	0.009979	0.009986	0.009983	0.009971	0.009989	0.009839	0.009861	0.006041
h12 (m)	0.009959	0.009976	0.009973	0.009919	0.009991	0.009987	0.009694	0.009897
m	0.03237	0.012871	0.904142	1.004649	4.066404	8.826095	14.60169	96.49318
Mat_in	3	1	1	1	1	1	1	1
Mat_out	2	2	2	2	2	2	2	1
Energy (J)	716262.4	657306	589744.8	512578.4	425799.5	323356.8	229812.5	125673.5
Mass (kg)	22.4837	18.97048	16.03684	13.34877	10.78112	8.153582	6.092306	4.060492

Table A. 12 Solutions for ω_{max}=10000 rpm, h_{max}=0.01m, R_{thk}=0.5m

	N1	***N2***	***N3***	***N4***	***N5***	***N6***	***N7***	***N8***
h1 (m)	0.007201	0.007169	0.007041	0.006254	0.007208	0.006374	0.006323	0.006192
h2 (m)	0.005778	0.005419	0.005173	0.004832	0.005916	0.005167	0.004705	0.0045
h3 (m)	0.005072	0.004259	0.003856	0.003392	0.004731	0.003717	0.0028	0.002735
h4 (m)	0.005044	0.004066	0.003519	0.002991	0.004318	0.003614	0.002543	0.002536
h5 (m)	0.005154	0.004021	0.003467	0.002767	0.003918	0.003261	0.002519	0.002516
h6 (m)	0.00891	0.003746	0.00326	0.00258	0.003389	0.002923	0.002509	0.002545
h7 (m)	0.00988	0.00558	0.002996	0.002531	0.002806	0.002682	0.002527	0.002528
h8 (m)	0.009941	0.009142	0.006088	0.003454	0.002816	0.002606	0.002637	0.00254
h9 (m)	0.009927	0.009933	0.00991	0.007299	0.006375	0.004044	0.002527	0.002522
h10 (m)	0.009984	0.009976	0.009694	0.009844	0.009957	0.008675	0.005607	0.002571
h11 (m)	0.009934	0.009949	0.009938	0.009796	0.009701	0.009913	0.009789	0.00312
h12 (m)	0.009966	0.00989	0.009737	0.009825	0.009922	0.009978	0.009336	0.003618
m	1.847348	2.485758	4.742256	4.529882	2.635422	8.369444	22.37864	93.1355
Mat_in	3	3	3	3	1	1	1	1
Mat_out	2	2	2	2	3	2	2	3
Energy (J)	4993024	4526263	4011825	3415251	2792462	2176101	1527519	765208.9
Mass (kg)	62.1934	51.1532	43.11447	35.33525	28.12241	21.53275	15.55842	9.973357

Table A. 13 Solutions for ω_{max}=10000 rpm, h_{max}=0.055m, R_{thk}=0.1m

	N1	***N2***	***N3***	***N4***	***N5***	***N6***	***N7***	***N8***
h1 (m)	0.004709	0.002537	0.002844	0.002596	0.002774	0.003868	0.002646	0.00254
h2 (m)	0.00332	0.002787	0.003104	0.003032	0.002945	0.003812	0.002989	0.003045
h3 (m)	0.002957	0.002865	0.002958	0.002817	0.002993	0.002891	0.002846	0.003058
h4 (m)	0.002844	0.002617	0.002579	0.00267	0.002768	0.002798	0.002678	0.002792
h5 (m)	0.015616	0.003319	0.002591	0.00278	0.002662	0.002625	0.002617	0.002585
h6 (m)	0.047569	0.007888	0.002683	0.002558	0.002596	0.002561	0.00257	0.002559
h7 (m)	0.054729	0.043145	0.010928	0.003256	0.002679	0.002726	0.002647	0.002678
h8 (m)	0.054843	0.054433	0.046236	0.01849	0.008894	0.002559	0.002691	0.002599
h9 (m)	0.05484	0.054864	0.054676	0.053287	0.037162	0.014547	0.002668	0.002607
h10 (m)	0.054896	0.054946	0.054974	0.053971	0.054878	0.047024	0.023939	0.003468
h11 (m)	0.054938	0.054771	0.05479	0.054861	0.053927	0.054764	0.053866	0.004866
h12 (m)	0.054954	0.054543	0.054539	0.054093	0.054856	0.052566	0.053435	0.004373
m	6.390069	3.316705	0.059858	0.076959	1.444148	3.210304	11.88625	66.82606
Mat_in	2	2	3	1	1	1	1	1
Mat_out	2	2	2	2	2	2	2	3
Energy (J)	76891.91	70134.65	61334.89	51295.13	40525.95	28607.13	16615.03	2584.08
Mass (kg)	16.28615	13.37086	10.7817	8.483829	6.393797	4.325462	2.484527	0.583485

Table A. 14 Solutions for ω_{max}=10000 rpm, h_{max}=0.055m, R_{thk}=0.3m

	N1	***N2***	***N3***	***N4***	***N5***	***N6***	***N7***	***N8***
h1 (m)	0.007686	0.010152	0.010079	0.010354	0.009854	0.007473	0.009941	0.009622
h2 (m)	0.007805	0.006159	0.005533	0.006892	0.006872	0.006145	0.006256	0.007281
h3 (m)	0.013134	0.004306	0.00328	0.003335	0.003703	0.00332	0.003493	0.004248
h4 (m)	0.006757	0.003364	0.002971	0.003034	0.002933	0.003006	0.003006	0.003219
h5 (m)	0.041791	0.005046	0.002809	0.002801	0.002617	0.002667	0.002638	0.002609
h6 (m)	0.054332	0.006957	0.003251	0.002652	0.002654	0.00259	0.002625	0.002516
h7 (m)	0.054745	0.044879	0.009168	0.002745	0.002745	0.002731	0.002707	0.002518
h8 (m)	0.054736	0.054646	0.04467	0.015555	0.006158	0.00276	0.002596	0.002625
h9 (m)	0.054901	0.054918	0.054569	0.051685	0.031024	0.014406	0.002551	0.002804
h10 (m)	0.054896	0.054851	0.054843	0.054707	0.054329	0.046984	0.023875	0.002654
h11 (m)	0.05488	0.054782	0.054712	0.054865	0.05359	0.054207	0.054524	0.014002
h12 (m)	0.054793	0.054718	0.054769	0.05439	0.054981	0.054995	0.051717	0.028546
m	0.364496	1.156249	0.82058	1.26365	0.910518	5.190041	16.53796	93.37141
Mat_in	3	3	3	3	1	1	1	1
Mat_out	2	2	2	2	2	2	2	2
Energy (J)	4016416	3672351	3225066	2714126	2125256	1498823	880776	213461.2
Mass (kg)	131.794	102.8906	81.96763	64.23568	47.79137	32.201	18.68307	5.819359

Table A. 15 Solutions for ω_{max}=10000 rpm, h_{max}=0.055m, R_{thk}=0.5m

	N1	***N2***	***N3***	***N4***	***N5***	***N6***	***N7***	***N8***
h1 (m)	0.038305	0.03257	0.032518	0.035599	0.034221	0.034419	0.018218	0.036357
h2 (m)	0.031271	0.030701	0.030446	0.025389	0.026203	0.025985	0.016435	0.015965
h3 (m)	0.02615	0.024378	0.022544	0.015694	0.018197	0.017518	0.013148	0.005594
h4 (m)	0.025484	0.021959	0.018006	0.015343	0.016196	0.0161	0.009646	0.005898
h5 (m)	0.027434	0.020025	0.01705	0.014086	0.013786	0.014017	0.009925	0.004806
h6 (m)	0.045645	0.018758	0.015749	0.013022	0.012048	0.012012	0.008162	0.004168
h7 (m)	0.05372	0.0247	0.014406	0.011804	0.010189	0.009638	0.007318	0.003344
h8 (m)	0.052212	0.05098	0.025577	0.014089	0.008693	0.00765	0.006457	0.0034
h9 (m)	0.054646	0.054305	0.053915	0.037108	0.020769	0.010912	0.005879	0.00469
h10 (m)	0.054598	0.054938	0.053938	0.05475	0.053202	0.036281	0.023391	0.009431
h11 (m)	0.05459	0.054385	0.054579	0.053885	0.053092	0.054559	0.051321	0.0168
h12 (m)	0.054519	0.054516	0.053198	0.054784	0.053468	0.050809	0.049931	0.008169
m	2.047518	6.081637	5.216366	11.303	0.561621	2.227039	21.4306	18.58938
Mat_in	3	3	3	3	1	1	1	1
Mat_out	2	2	2	2	3	3	3	1
Energy (J)	27005814	24248158	21118988	17691379	14111086	10328146	6296482	1998452
Mass (kg)	333.5622	269.7723	221.9286	179.2429	137.9191	99.39877	59.72442	22.11112

Table A. 16 Solutions for ω_{max}=10000 rpm, h_{max}=0.1m, R_{thk}=0.1m

	N1	***N2***	***N3***	***N4***	***N5***	***N6***	***N7***	***N8***
h1 (m)	0.011305	0.007011	0.005972	0.003214	0.004431	0.003068	0.002842	0.003199
h2 (m)	0.003785	0.006713	0.005693	0.003833	0.003613	0.003803	0.003803	0.00366
h3 (m)	0.009377	0.004202	0.004131	0.00297	0.003655	0.003794	0.003393	0.003375
h4 (m)	0.003732	0.004744	0.00278	0.00278	0.002872	0.002937	0.002699	0.002824
h5 (m)	0.076267	0.004955	0.002655	0.002708	0.002667	0.00264	0.002682	0.00264
h6 (m)	0.0954	0.020975	0.002988	0.003107	0.002726	0.003113	0.002646	0.002682
h7 (m)	0.098786	0.08866	0.024335	0.005211	0.003196	0.00289	0.002744	0.002702
h8 (m)	0.099813	0.099211	0.092049	0.040846	0.016238	0.003321	0.002809	0.002949
h9 (m)	0.099869	0.099804	0.098372	0.097825	0.07139	0.029703	0.003223	0.002869
h10 (m)	0.09989	0.09989	0.099842	0.097075	0.099009	0.094796	0.041498	0.004547
h11 (m)	0.099658	0.099625	0.099866	0.099339	0.099089	0.097658	0.098045	0.005333
h12 (m)	0.099801	0.099503	0.099798	0.09975	0.098622	0.09687	0.095242	0.002515
m	0.161589	0.116891	0.012511	0.176847	1.414022	4.590124	12.04433	23.95386
Mat_in	2	2	1	3	1	1	1	1
Mat_out	2	2	2	2	2	2	2	2
Energy (J)	142719.6	130098.9	113833.9	95121.31	74406.3	52500.44	28673.26	3157.444
Mass (kg)	31.58163	25.17001	20.06106	15.688	11.61095	7.787832	4.129105	0.676502

Table A. 17 Solutions for ω_{max}=10000 rpm, h_{max}=0.1m, R_{thk}=0.3m

	N1	***N2***	***N3***	***N4***	***N5***	***N6***	***N7***	***N8***
h1 (m)	0.035633	0.018833	0.008597	0.012287	0.010382	0.009263	0.009287	0.008859
h2 (m)	0.024516	0.010882	0.006383	0.005877	0.006014	0.006871	0.006475	0.006106
h3 (m)	0.018565	0.00486	0.00486	0.003643	0.002568	0.004732	0.00355	0.003238
h4 (m)	0.016375	0.004059	0.003797	0.0033	0.003991	0.003666	0.003036	0.003455
h5 (m)	0.036409	0.004503	0.003125	0.002961	0.002777	0.002917	0.002931	0.002652
h6 (m)	0.026352	0.007541	0.003711	0.002801	0.002774	0.002783	0.002771	0.002795
h7 (m)	0.086824	0.040852	0.009686	0.003229	0.002637	0.002664	0.002649	0.002702
h8 (m)	0.099223	0.094781	0.05684	0.01816	0.002649	0.00272	0.002696	0.002551
h9 (m)	0.09986	0.098215	0.098355	0.080367	0.035246	0.017473	0.002571	0.002708
h10 (m)	0.099658	0.099827	0.098729	0.099705	0.098355	0.068885	0.034377	0.003125
h11 (m)	0.099649	0.099744	0.099851	0.097414	0.09709	0.099533	0.090368	0.004169
h12 (m)	0.098673	0.09981	0.09884	0.099893	0.099711	0.097149	0.097477	0.005592
m	0.395008	1.274709	1.416011	2.307976	1.254096	3.293479	23.48055	9.064955
Mat_in	2	3	3	3	3	1	1	1
Mat_out	2	2	2	2	2	2	2	2
Energy (J)	6877187	6223165	5414281	4496437	3486719	2450424	1300842	156996.6
Mass (kg)	203.9012	164.5035	132.2802	103.0068	75.57156	51.25535	26.67113	4.897945

Table A. 18 Solutions for ω_{max}=100000 rpm, h_{max}=0.1m, R_{thk}=0.5m

	N1	***N2***	***N3***	***N4***	***N5***	***N6***	***N7***	***N8***
h1 (m)	0.083881	0.079674	0.091832	0.040989	0.086774	0.053703	0.060627	0.060178
h2 (m)	0.065481	0.065076	0.064582	0.036008	0.062737	0.042843	0.038004	0.040284
h3 (m)	0.052724	0.046306	0.039995	0.03327	0.039322	0.030015	0.019776	0.009243
h4 (m)	0.055474	0.039602	0.03402	0.028179	0.036058	0.025281	0.015384	0.008421
h5 (m)	0.052721	0.038171	0.031175	0.026947	0.032526	0.022698	0.014804	0.006029
h6 (m)	0.087437	0.035648	0.030185	0.022972	0.027715	0.018827	0.013022	0.005812
h7 (m)	0.096459	0.045277	0.027051	0.022466	0.022401	0.016092	0.011811	0.003785
h8 (m)	0.098723	0.093921	0.045059	0.022889	0.017976	0.012269	0.012245	0.003184
h9 (m)	0.099009	0.099048	0.09714	0.065561	0.037728	0.015012	0.008543	0.007314
h10 (m)	0.099714	0.099679	0.097108	0.09967	0.097164	0.062672	0.040504	0.005898
h11 (m)	0.098661	0.098387	0.099128	0.096167	0.096486	0.095394	0.085563	0.020556
h12 (m)	0.09775	0.096602	0.095031	0.098837	0.097173	0.069965	0.084349	0.039206
m	1.060954	3.217532	4.464153	9.602644	1.84631	2.055591	33.10418	33.31889
Mat_in	3	3	3	3	1	1	1	1
Mat_out	2	2	2	2	3	3	3	1
Energy (J)	49856468	44578335	38181641	31679594	24660569	17203539	9895784	2264529
Mass (kg)	622.793	498.4896	403.258	321.592	242.7247	165.4665	95.30208	26.30013

APPENDIX B: Optimal Flywheel Shapes

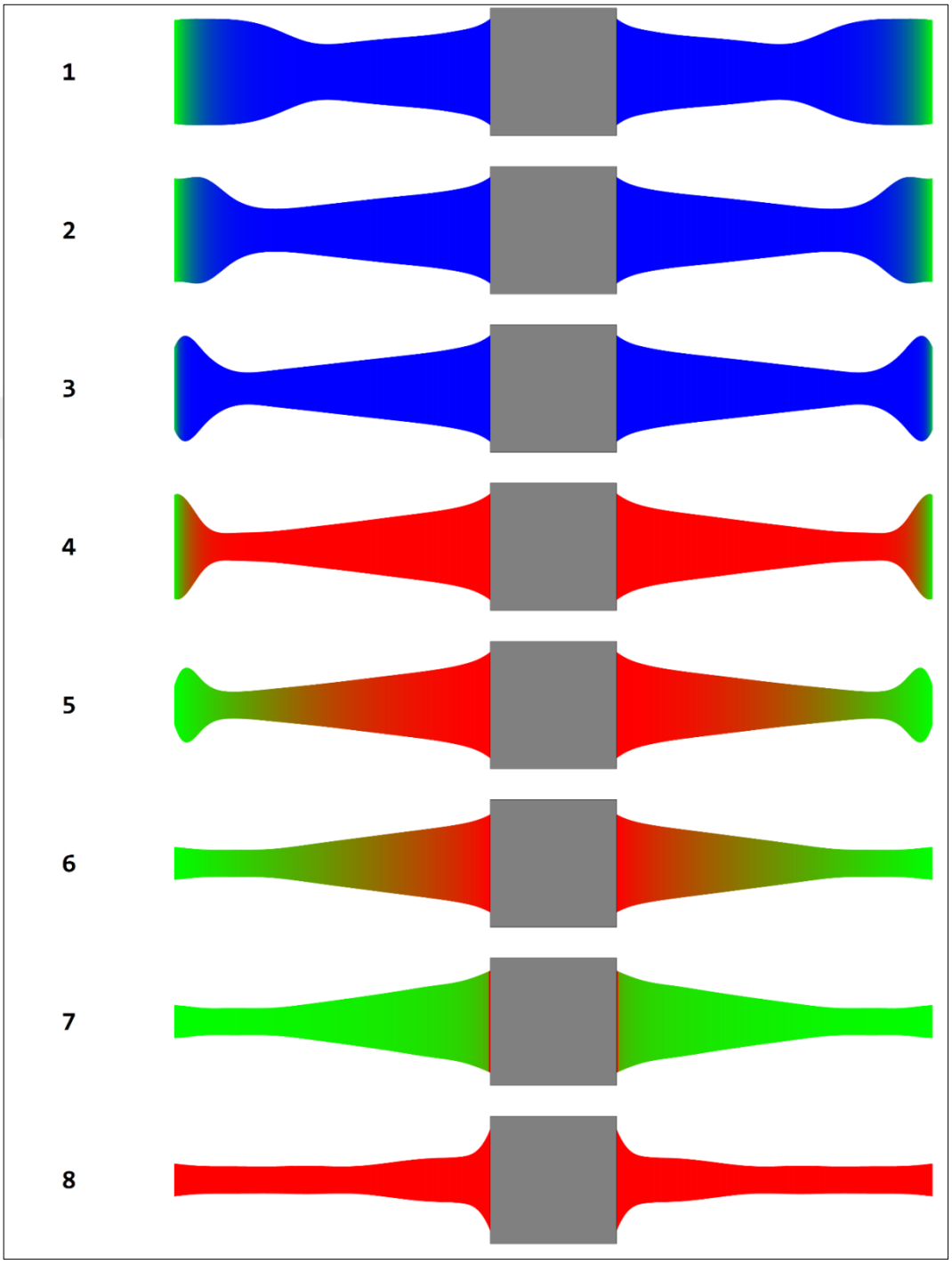

Figure B. 1 Optimal Designs for ω_{max}=100000 rpm, h_{max}=0.01m, R_{thk}=0.1m

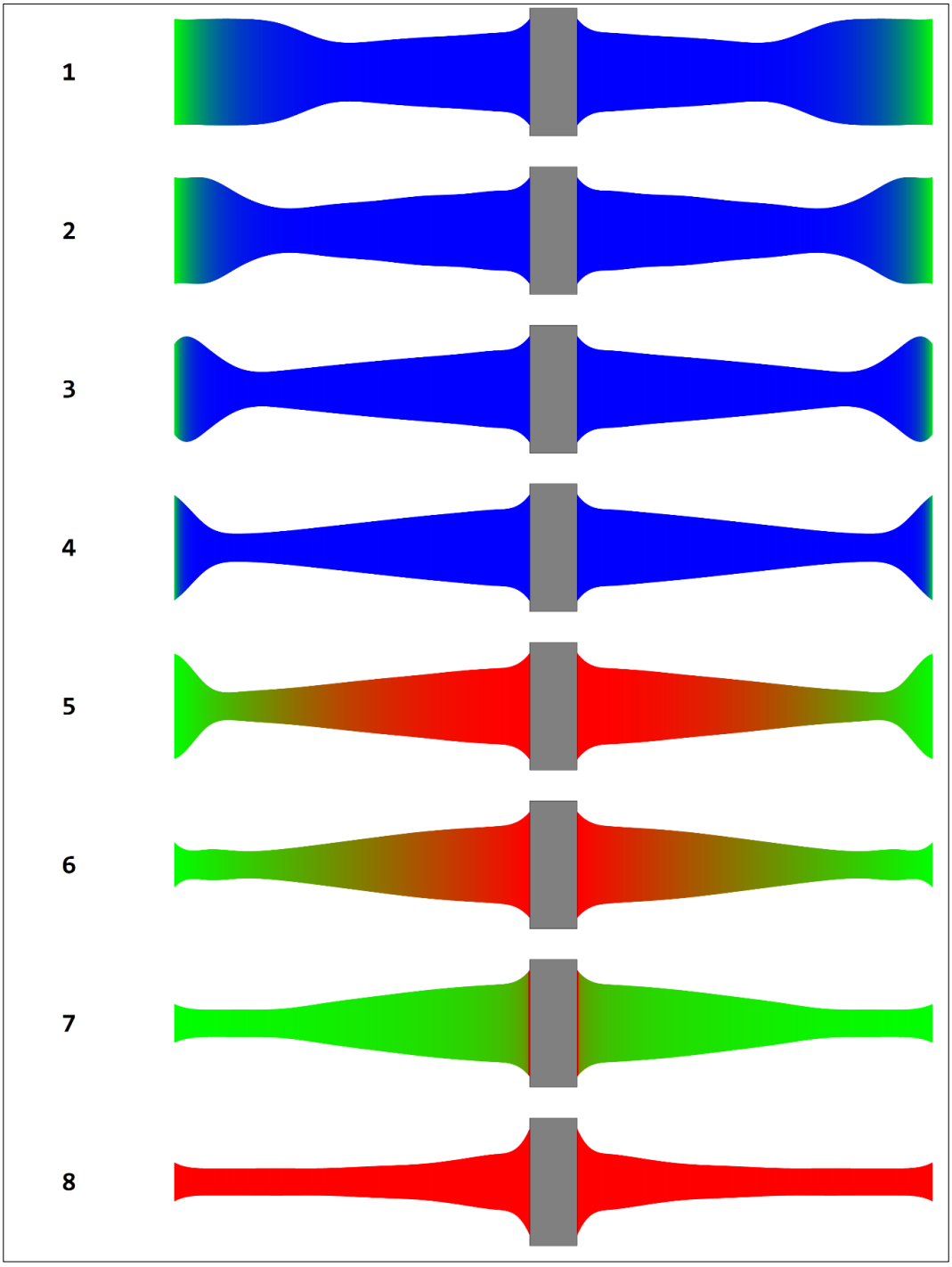

Figure B. 2 Optimal Designs for ω_{max}=100000 rpm, h_{max}=0.01m, R_{thk}=0.3m

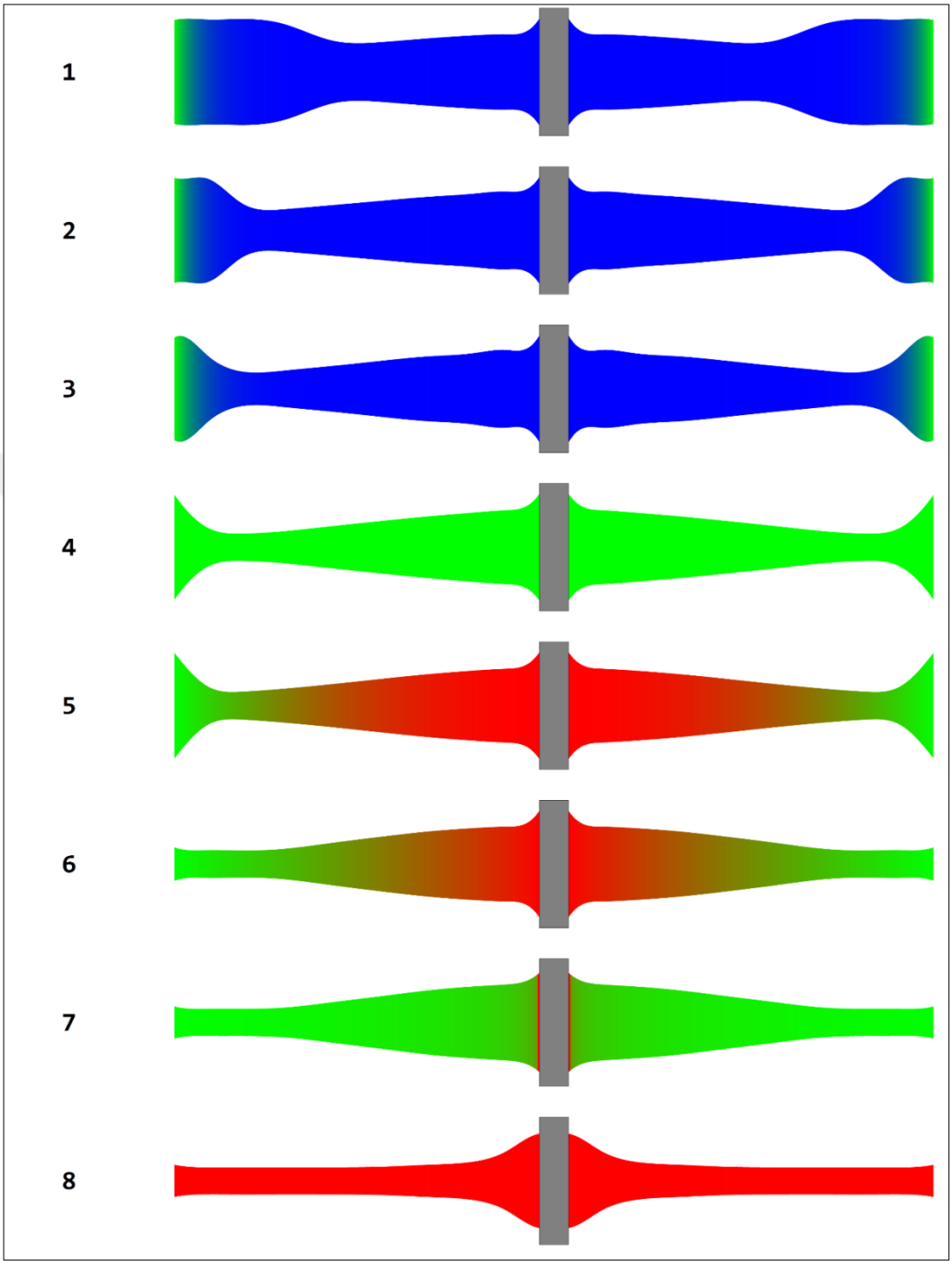

Figure B. 3 Optimal Designs for ω_{max}=100000 rpm, h_{max}=0.01m, R_{thk}=0.5m

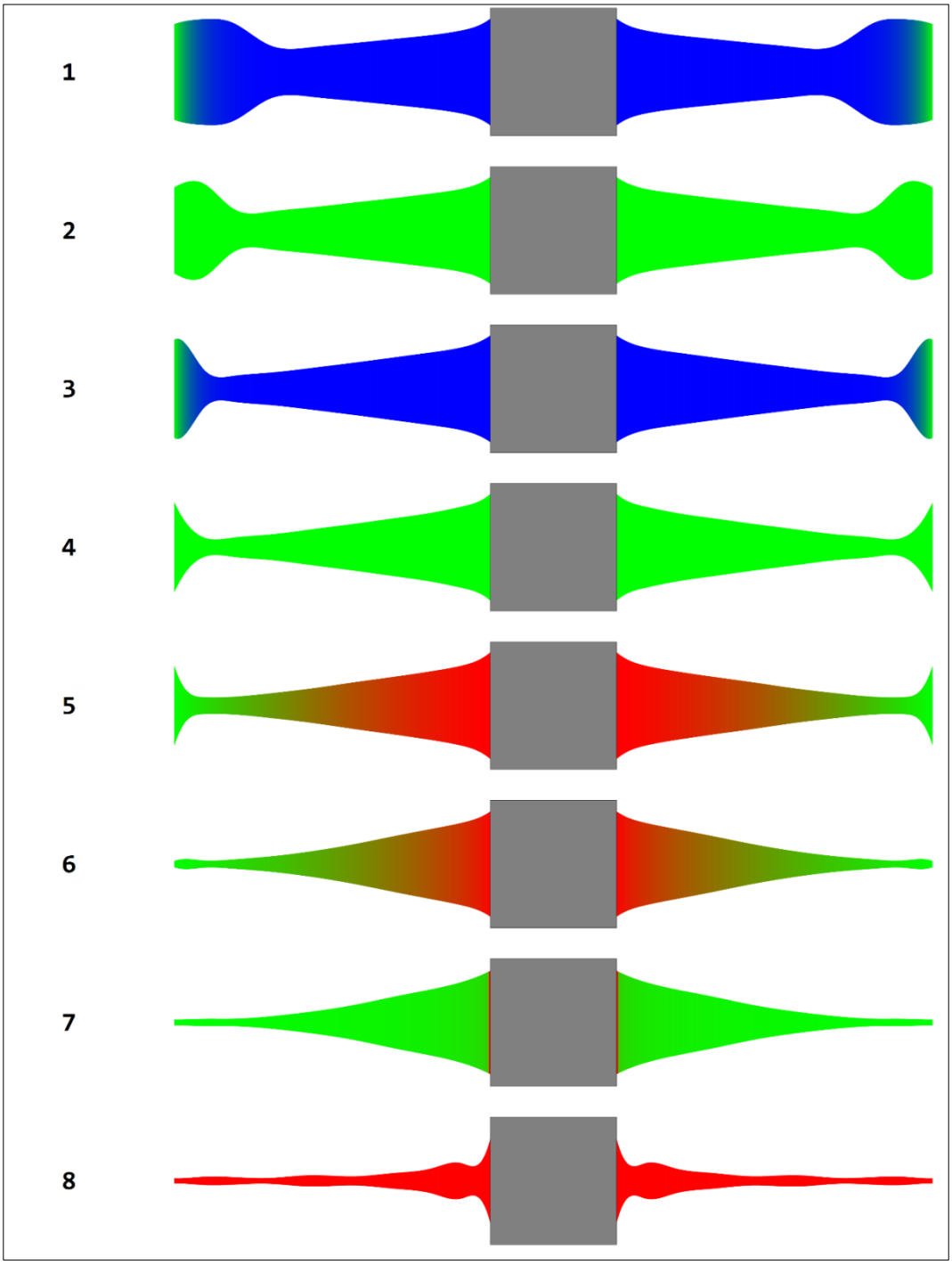

Figure B. 4 Optimal Designs for ω_{max}=100000 rpm, h_{max}=0.055m, R_{thk}=0.1m

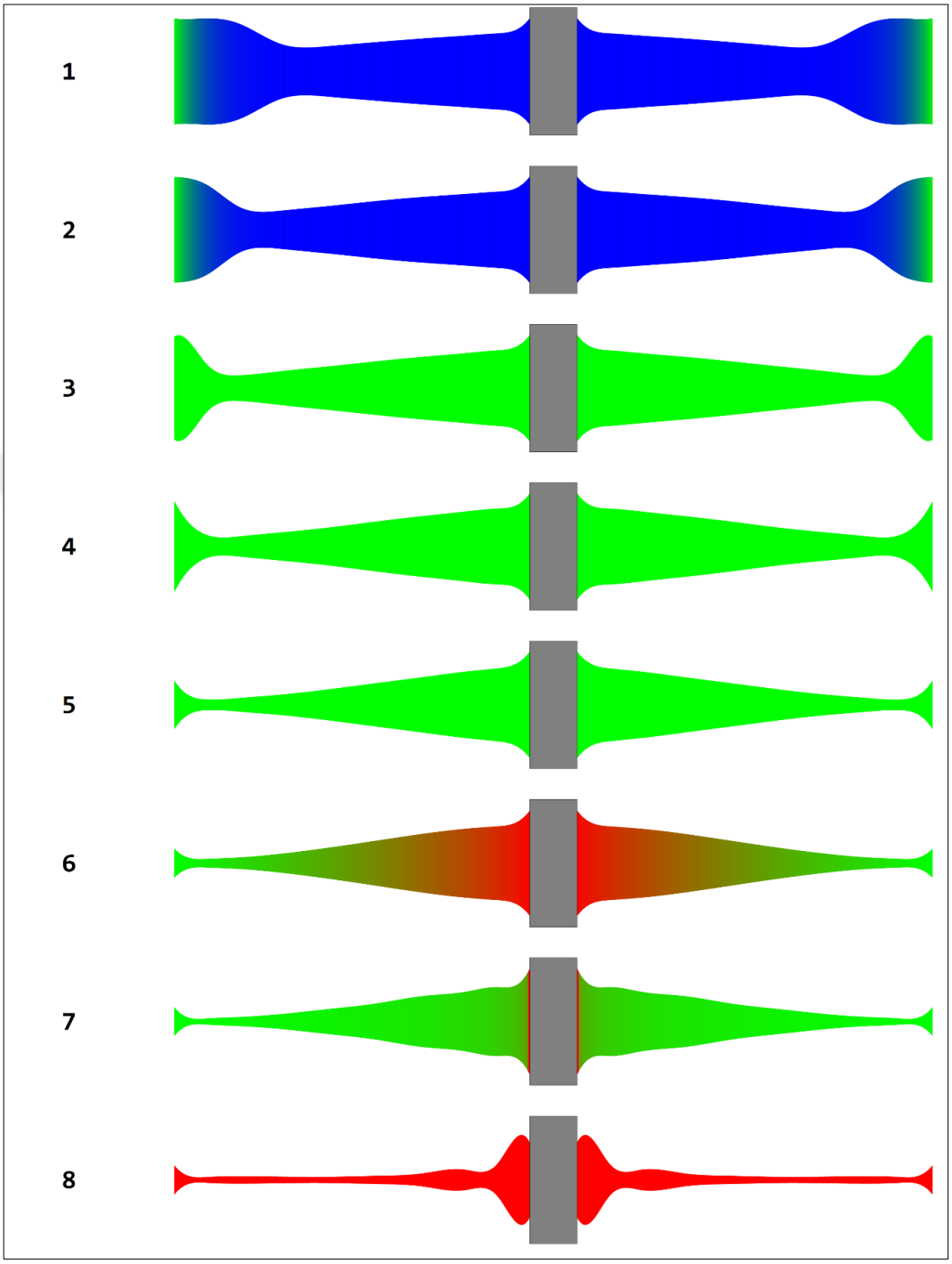

Figure B. 5 Optimal Designs for ω_{max}=100000 rpm, h_{max}=0.055m, R_{thk}=0.3m

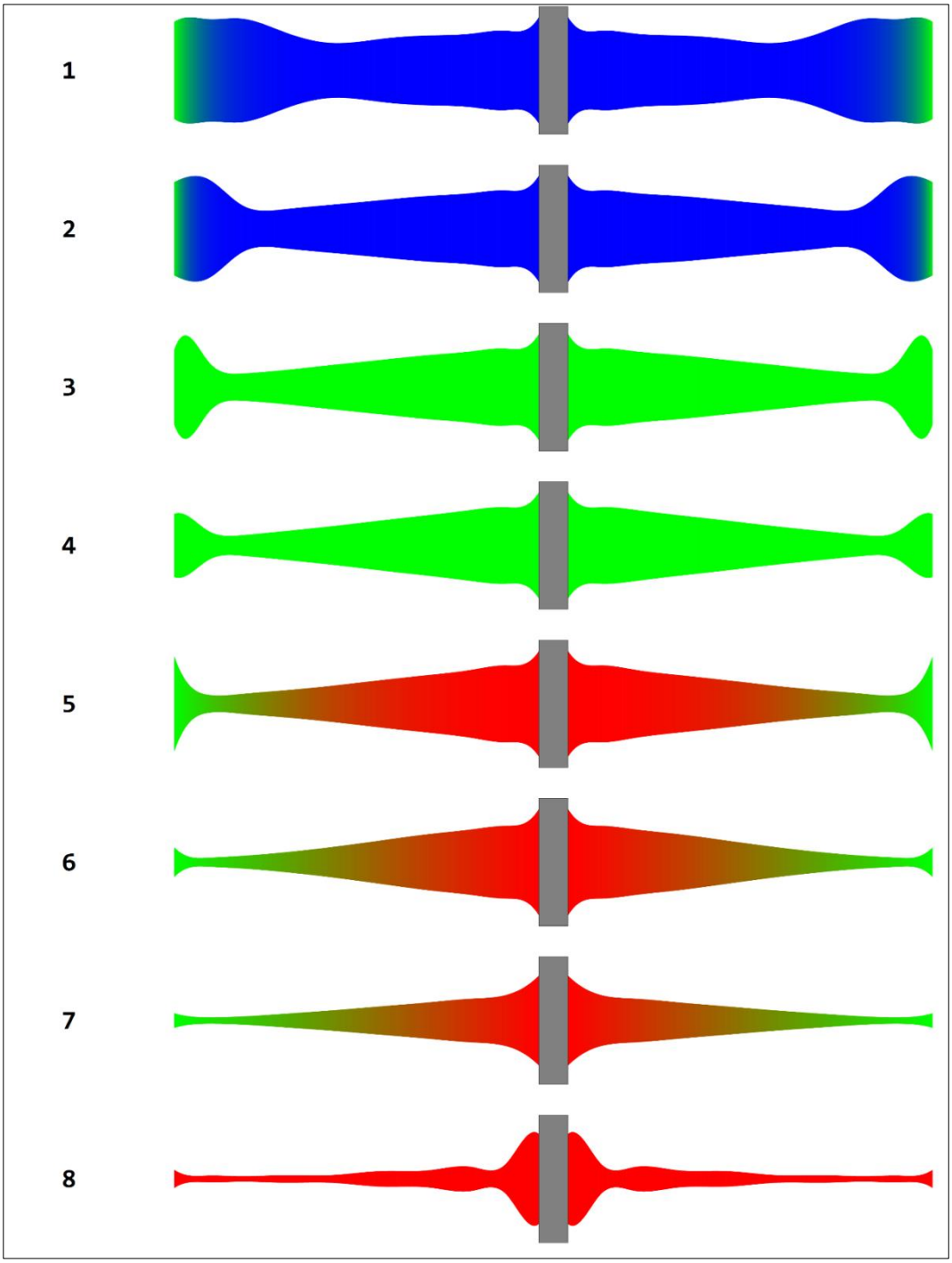

Figure B. 6 Optimal Designs for ω_{max}=100000 rpm, h_{max}=0.055m, R_{thk}=0.5m

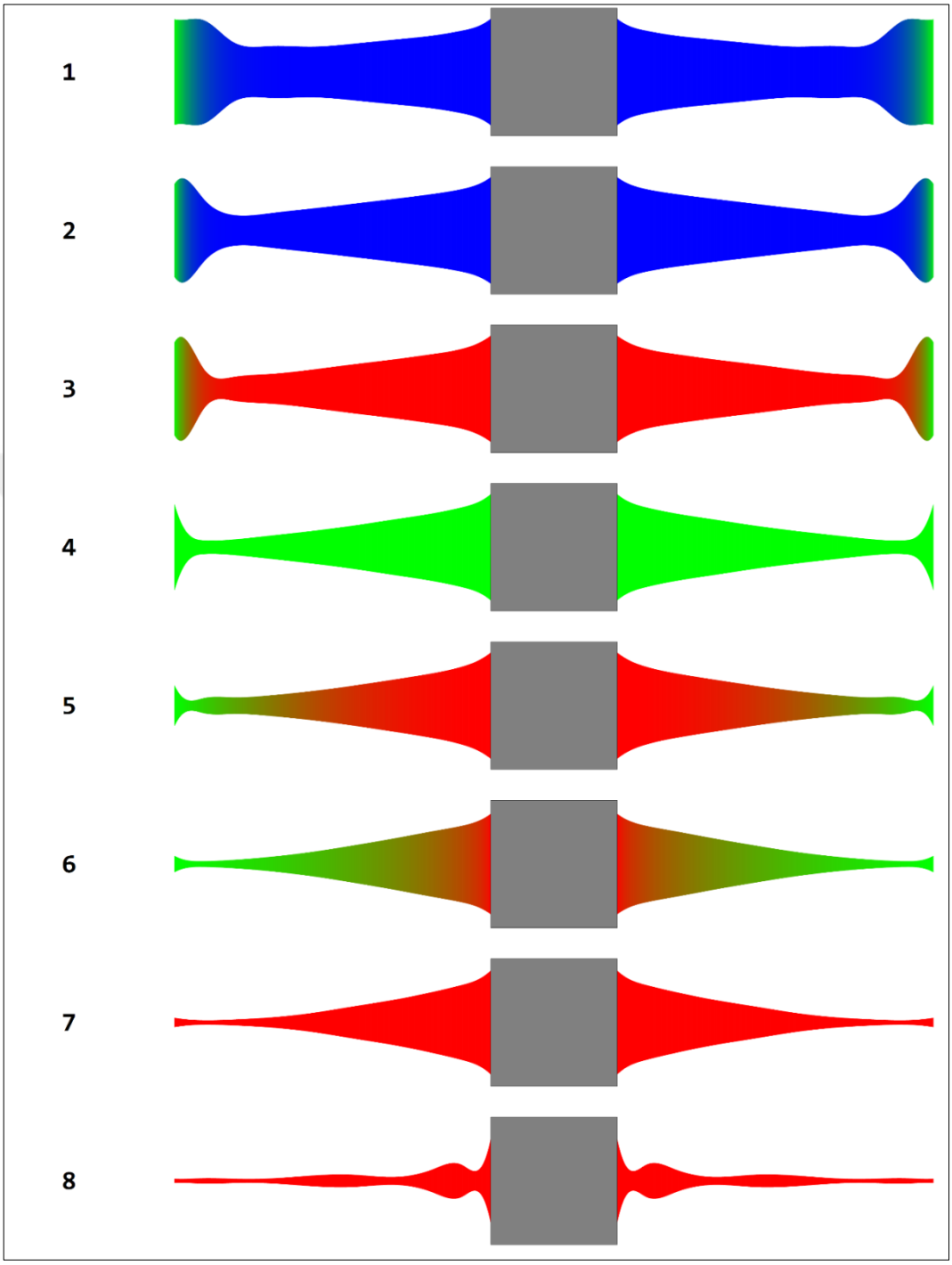

Figure B. 7 Optimal Designs for ω_{max}=100000 rpm, h_{max}=0.1m, R_{thk}=0.1m

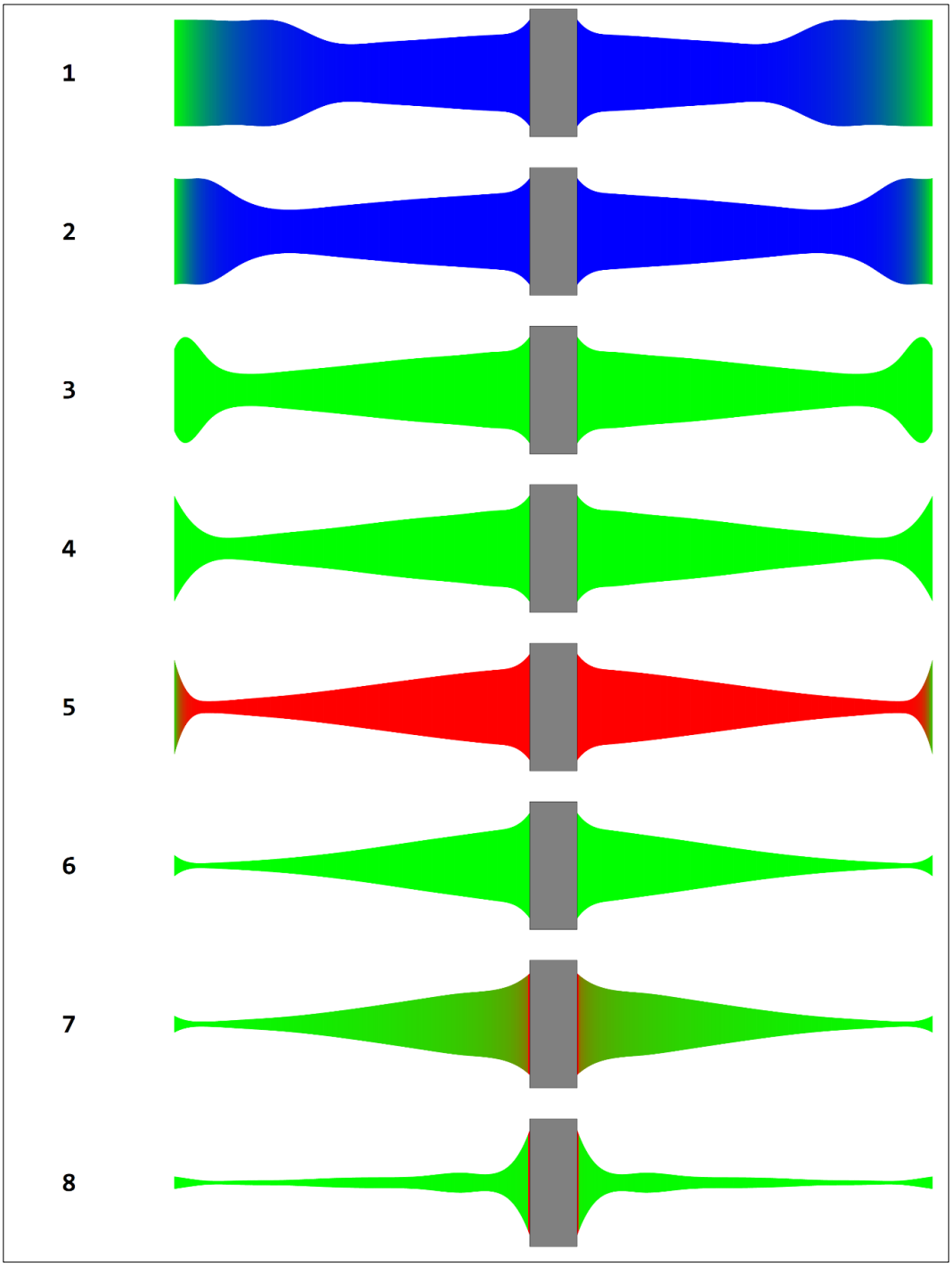

Figure B. 8 Optimal Designs for ω_{max}=100000 rpm, h_{max}=0.1m, R_{thk}=0.3m

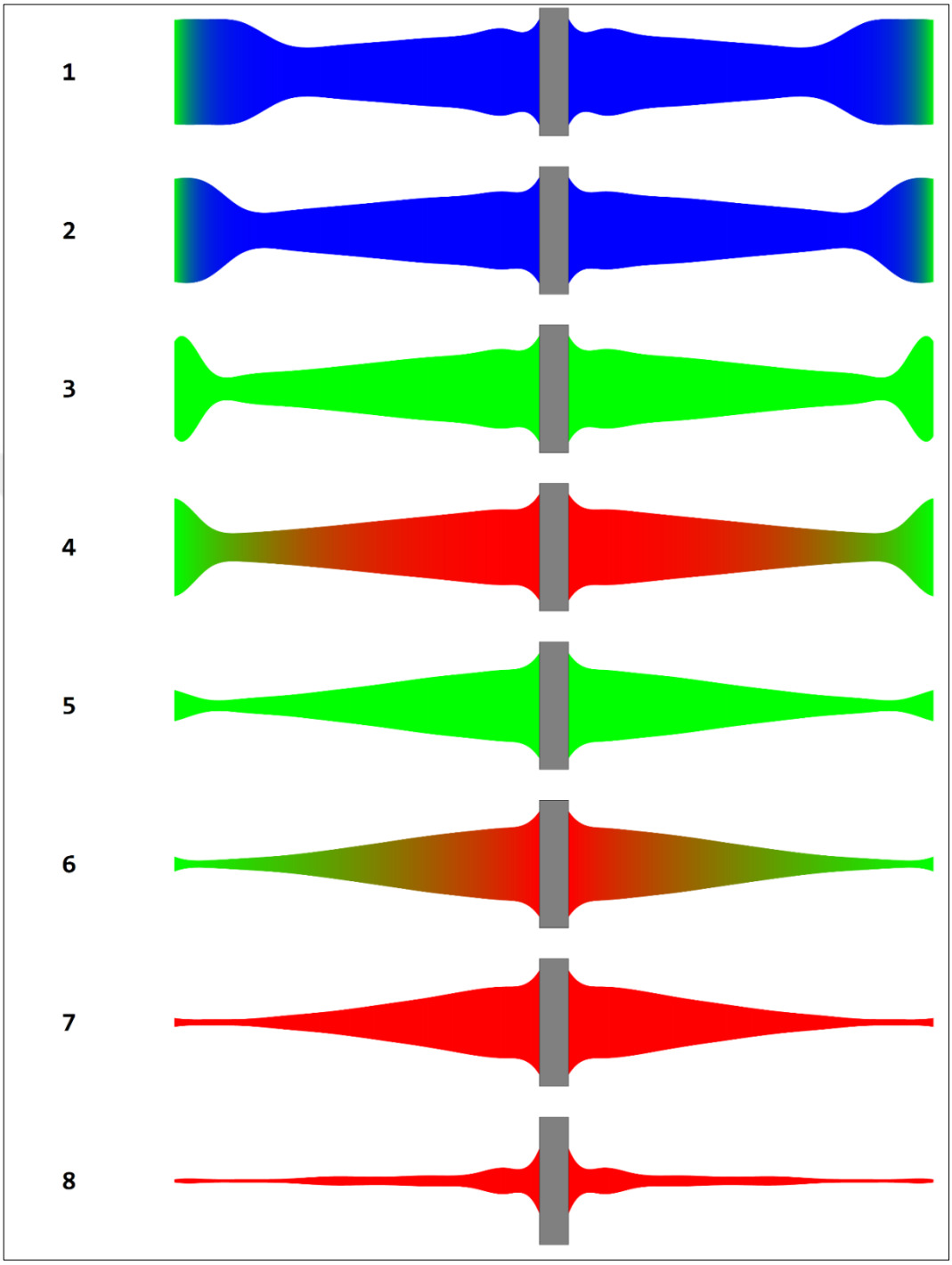

Figure B. 9 Optimal Designs for ω_{max}=100000 rpm, h_{max}=0.1m, R_{thk}=0.5m

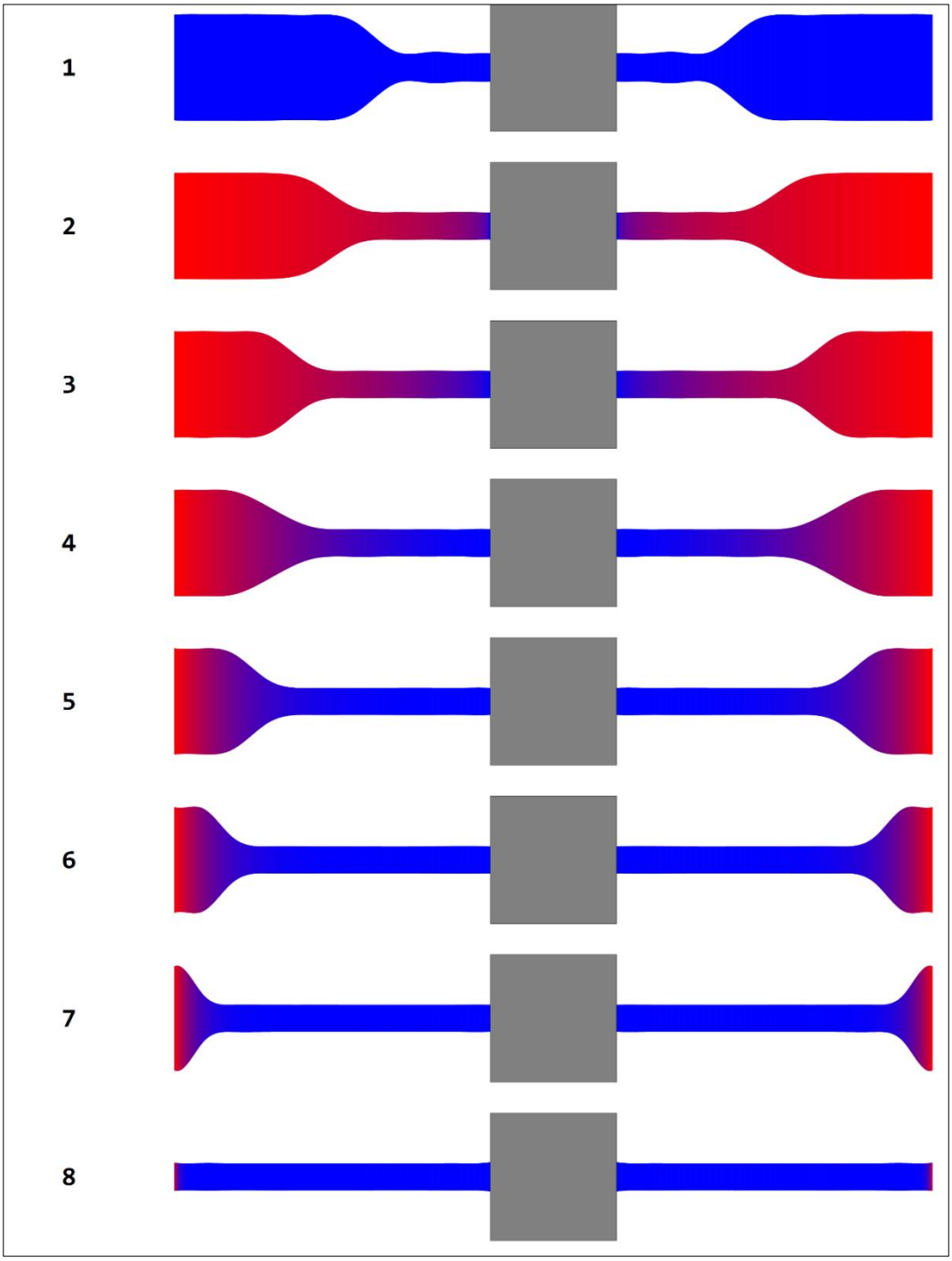

Figure B. 10 Optimal Designs for ω_{max}=10000 rpm, h_{max}=0.01m, R_{thk}=0.1m

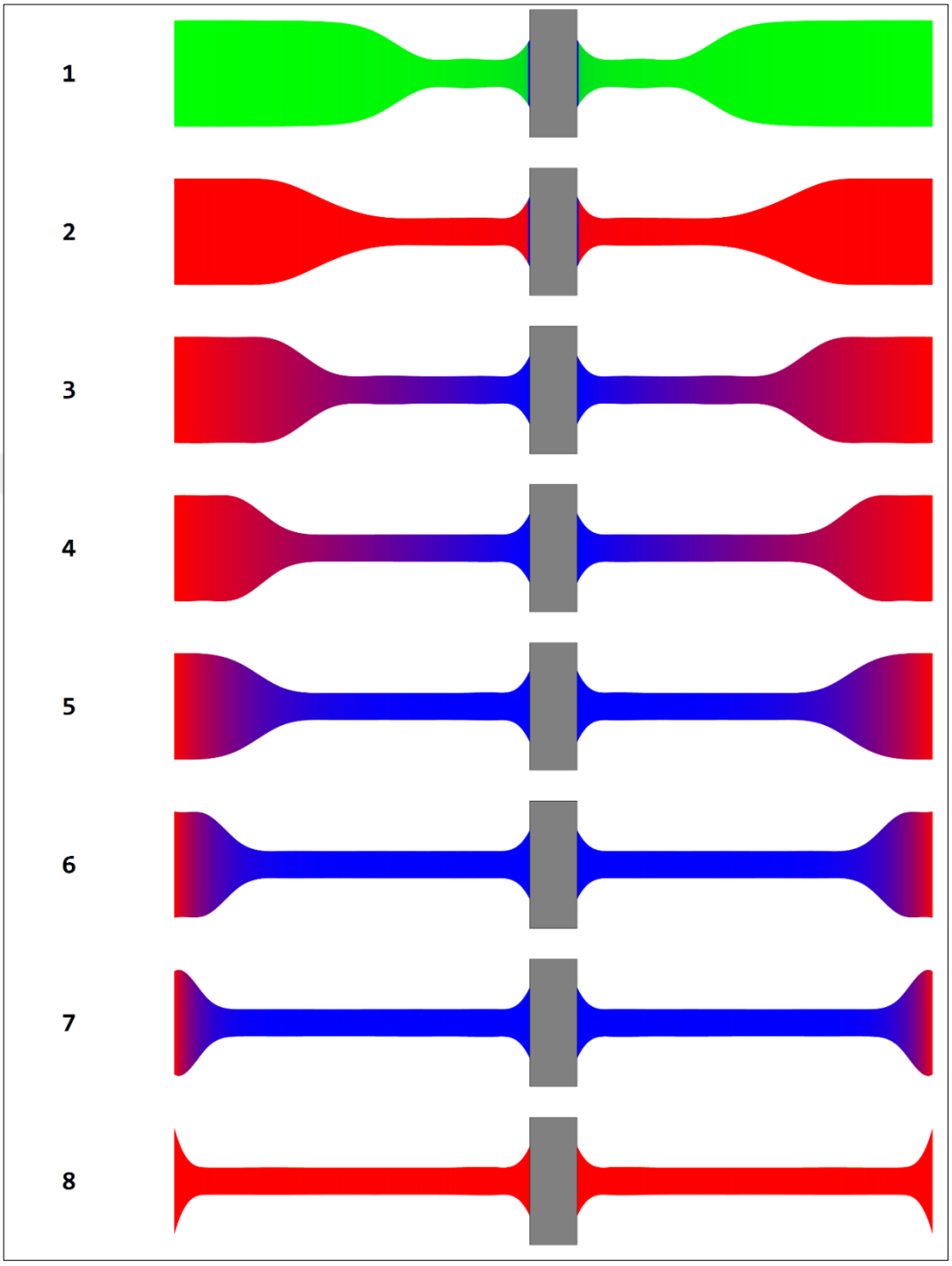

Figure B. 11 Optimal Designs for ω_{max}=10000 rpm, h_{max}=0.01m, R_{thk}=0.3m

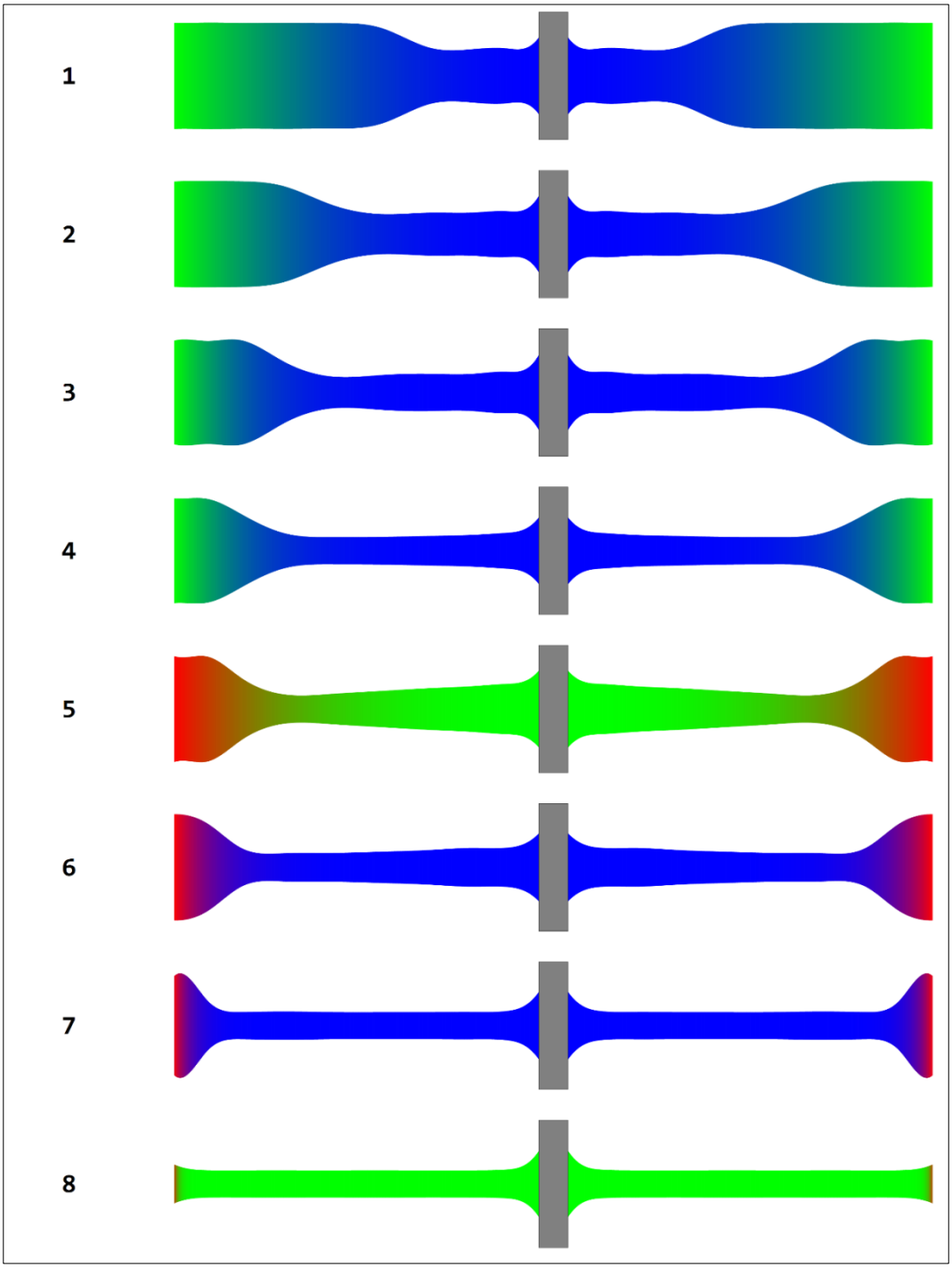

Figure B. 12 Optimal Designs for ω_{max}=10000 rpm, h_{max}=0.01m, R_{thk}=0.5m

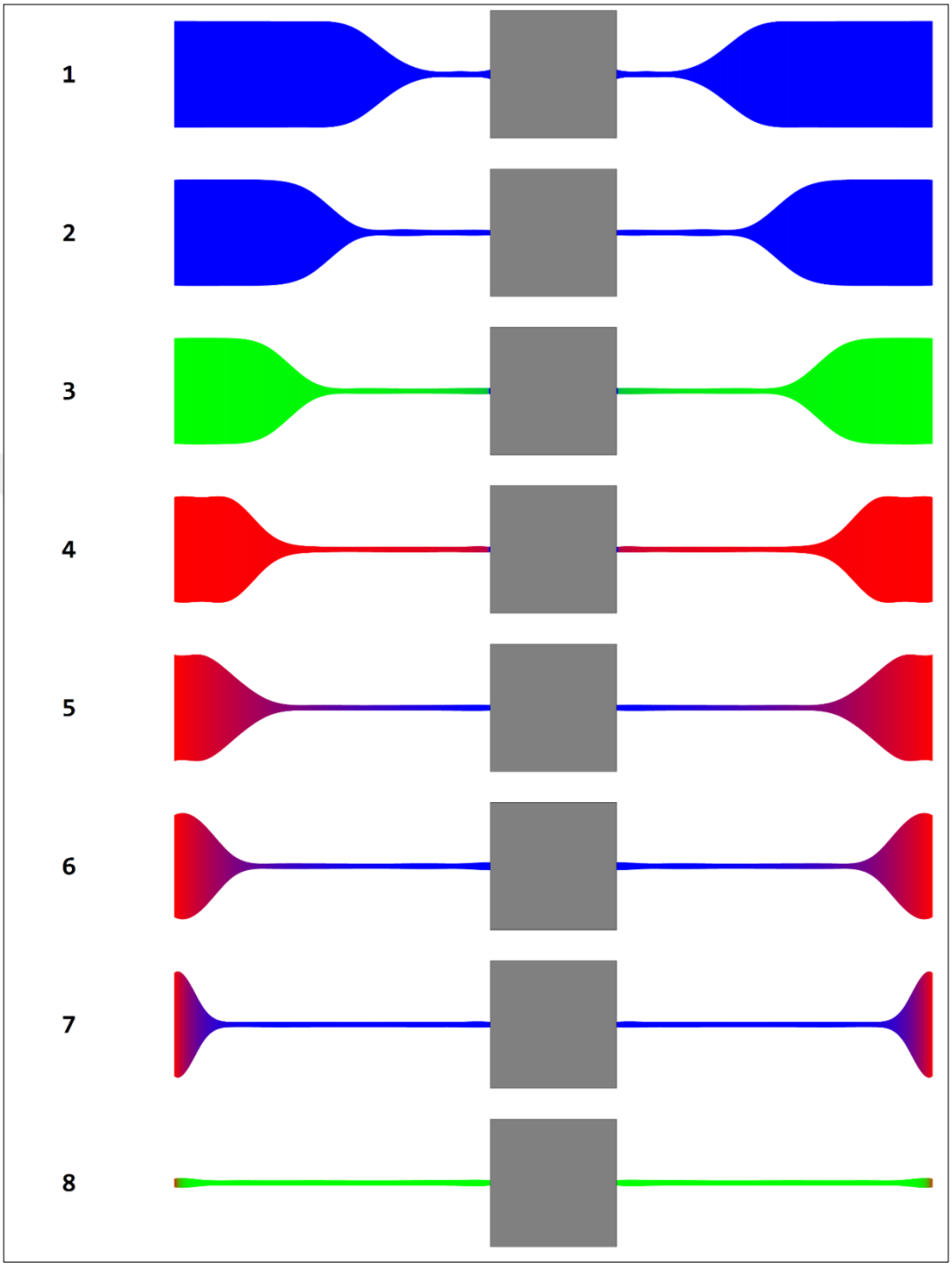

Figure B. 13 Optimal Designs for ω_{max}=10000 rpm, h_{max}=0.055m, R_{thk}=0.1m

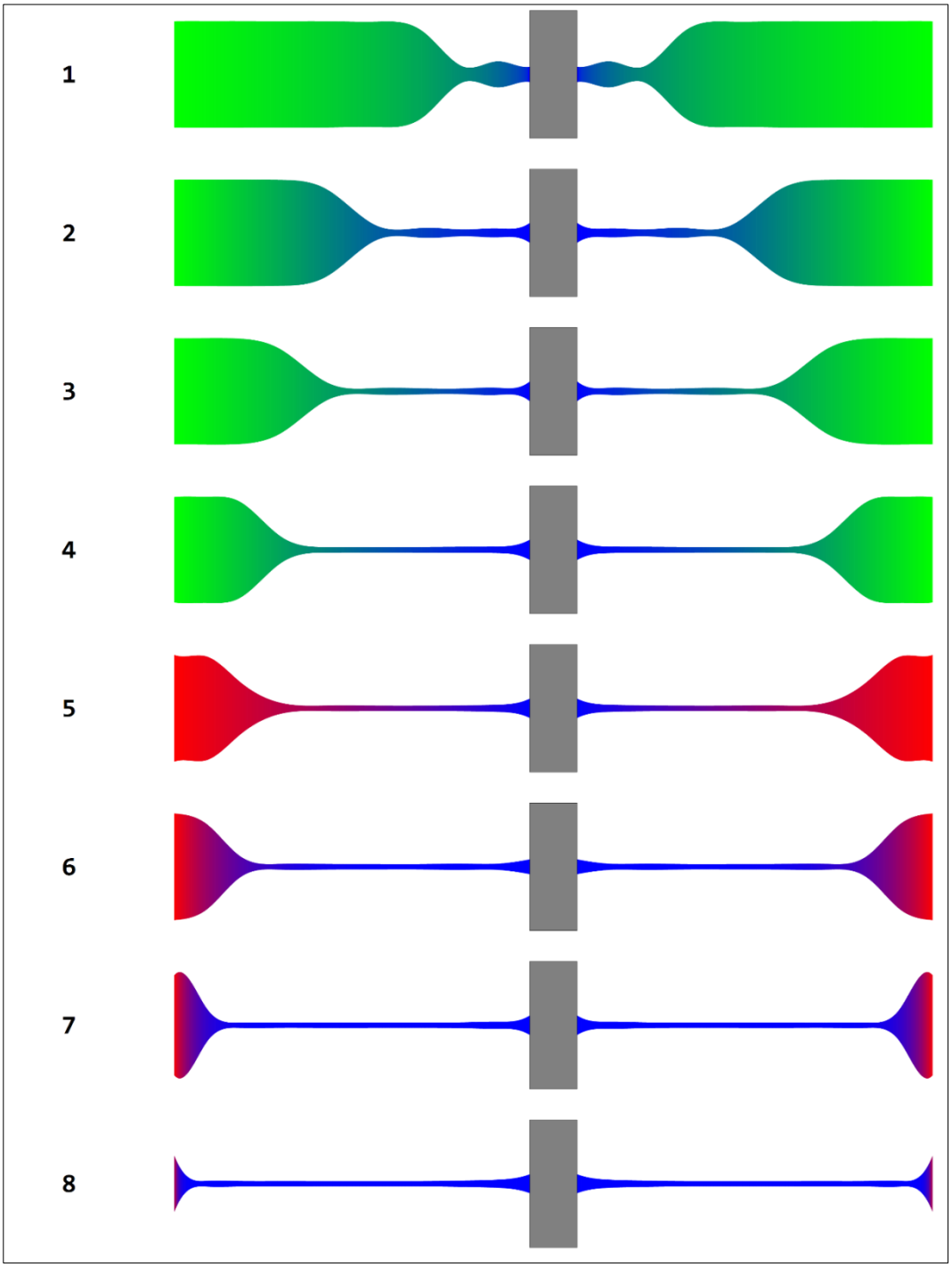

Figure B. 14 Optimal Designs for ω_{max}=10000 rpm, h_{max}=0.055m, R_{thk}=0.3m

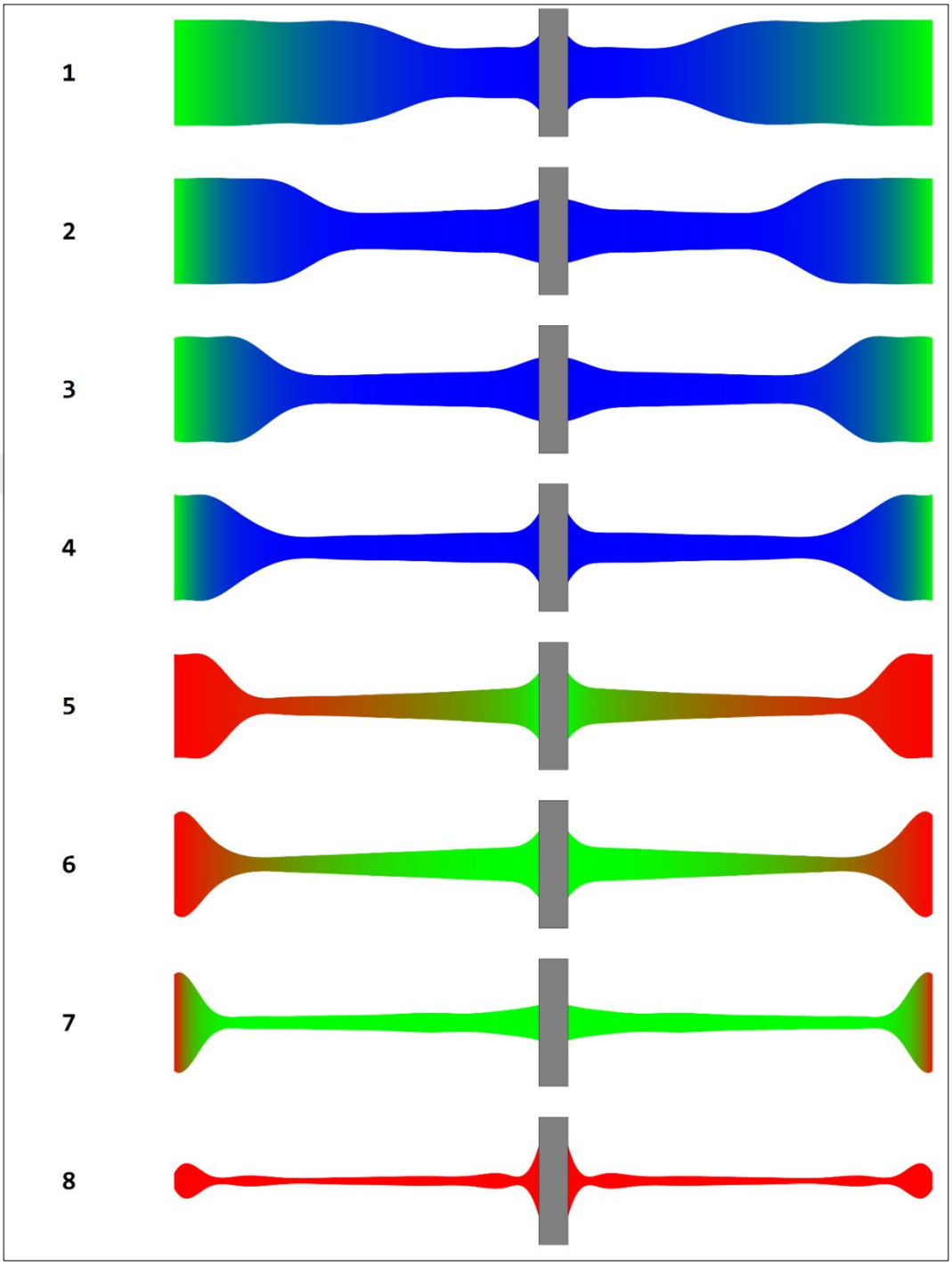

Figure B. 15 Optimal Designs for ω_{max}=10000 rpm, h_{max}=0.055m, R_{thk}=0.5m

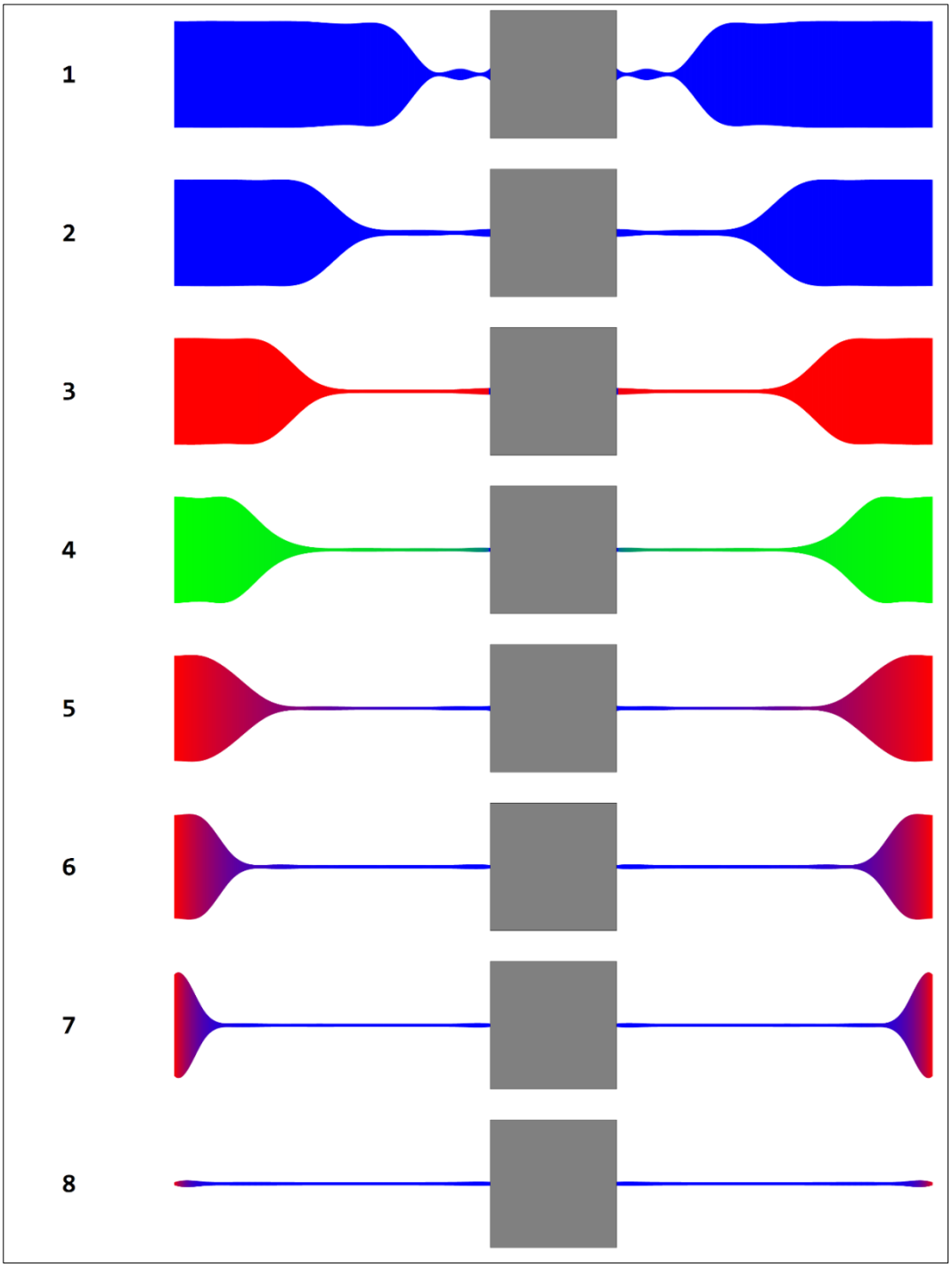

Figure B. 16 Optimal Designs for ω_{max}=10000 rpm, h_{max}=0.1m, R_{thk}=0.1m

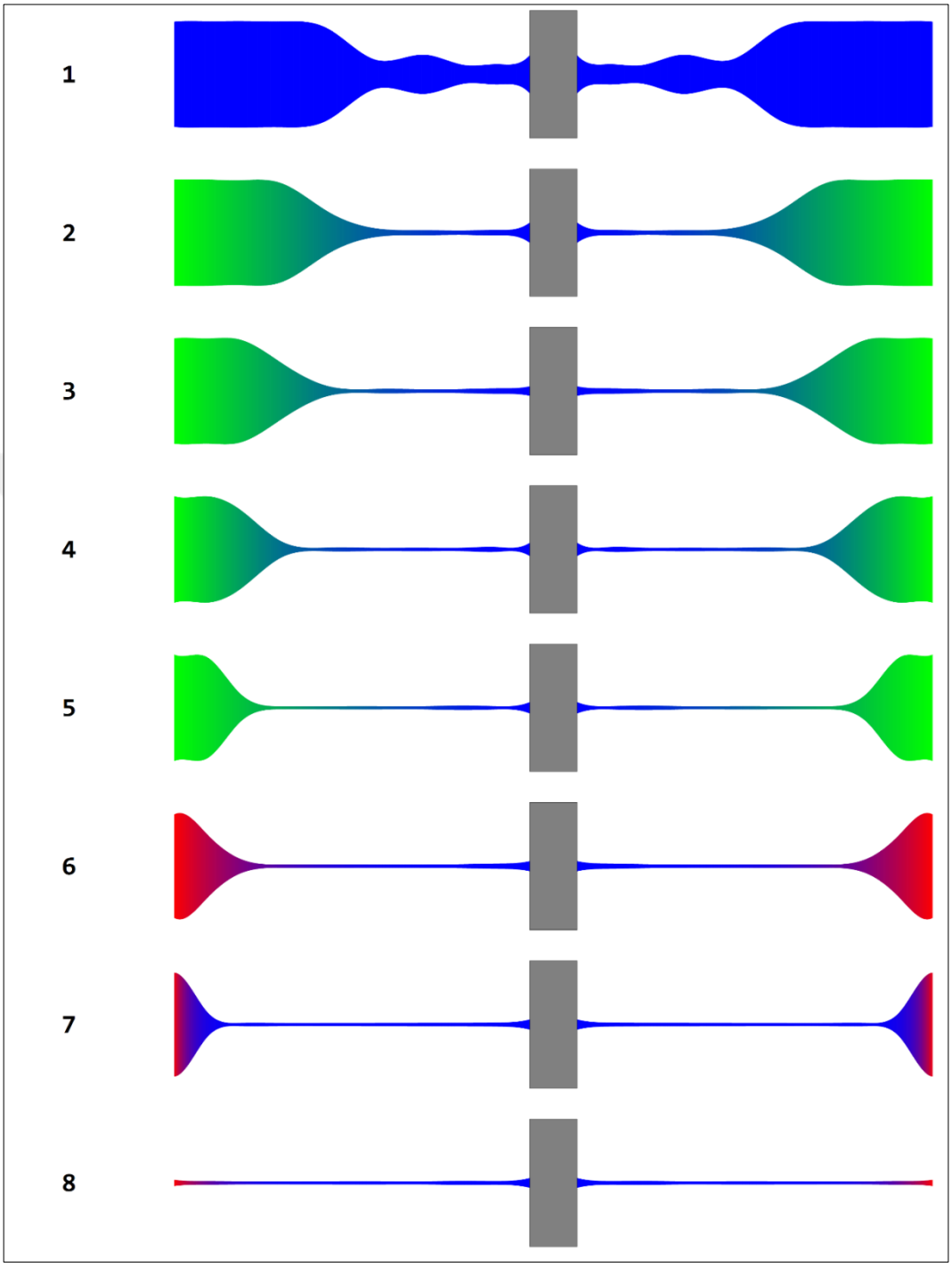

Figure B. 17 Optimal Designs for ω_{max}=10000 rpm, h_{max}=0.1m, R_{thk}=0.3m

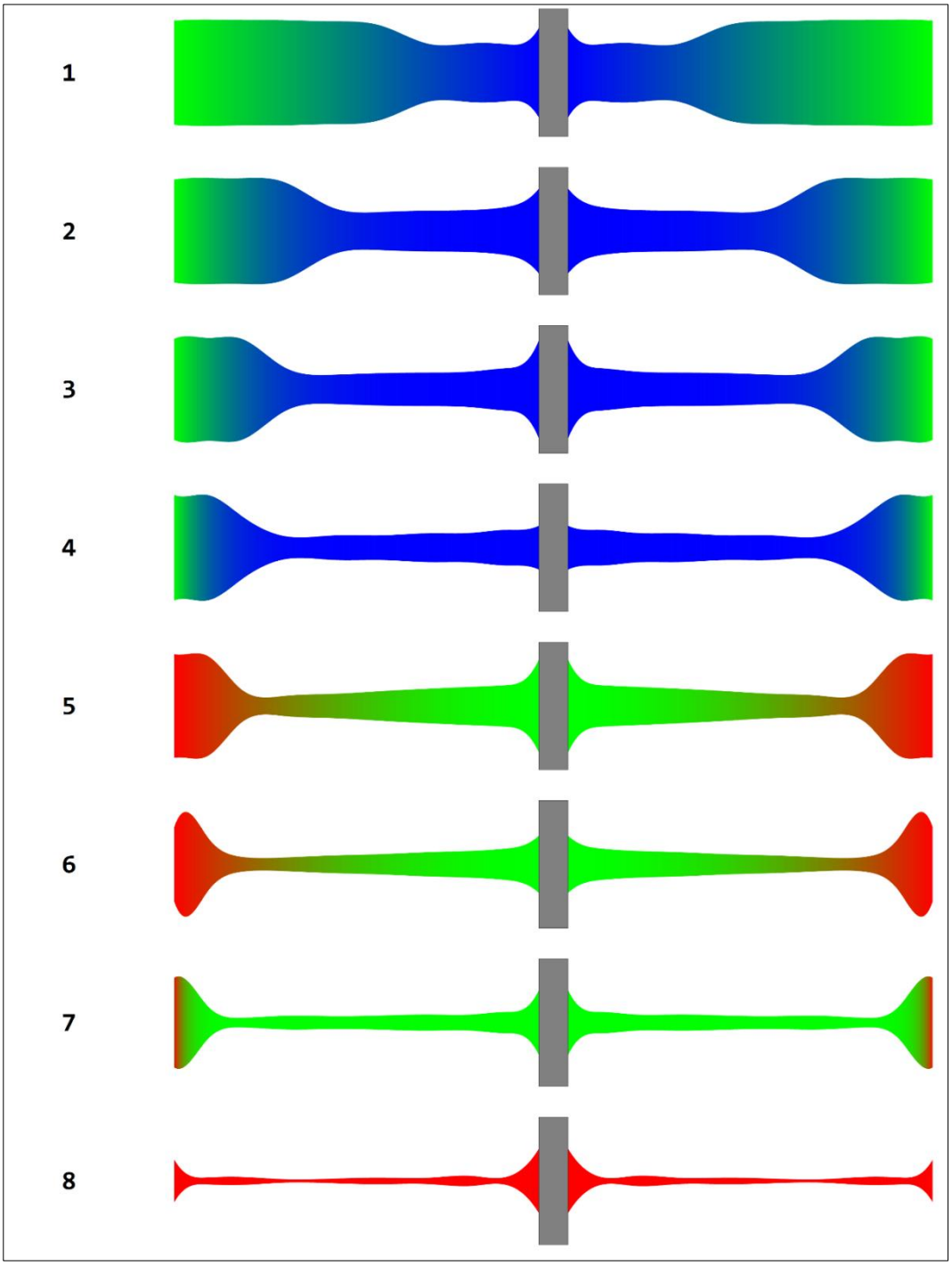

Figure B. 18 Optimal Designs for ω_{max}=10000 rpm, h_{max}=0.1m, R_{thk}=0.5m

APPENDIX C: Pareto Optimal Fronts

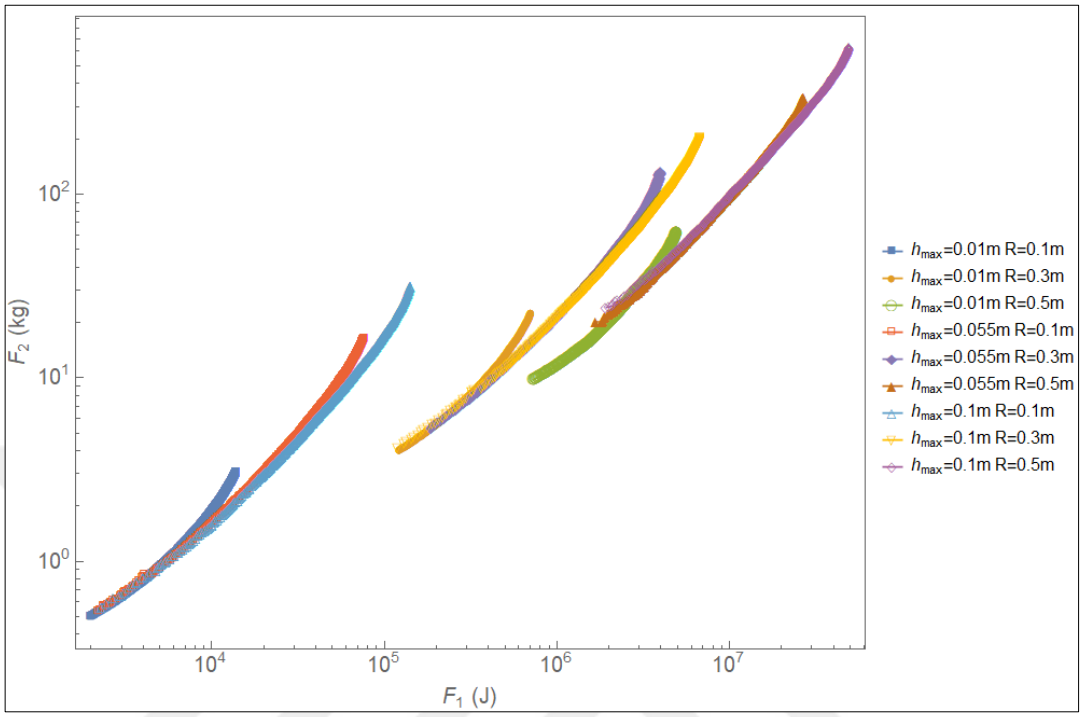

Figure C. 1 Pareto optimal front for ω_{max}=10000 rpm

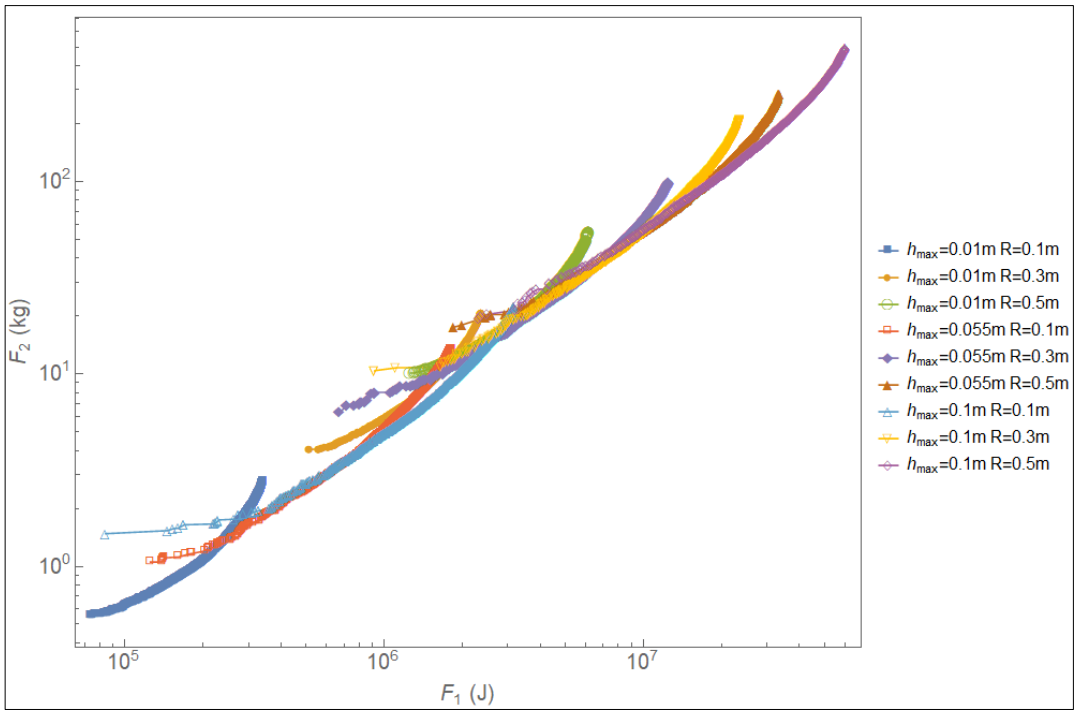

Figure C. 2 Pareto optimal front for ω_{max}=100000 rpm

APPENDIX D: Convergence Speeds

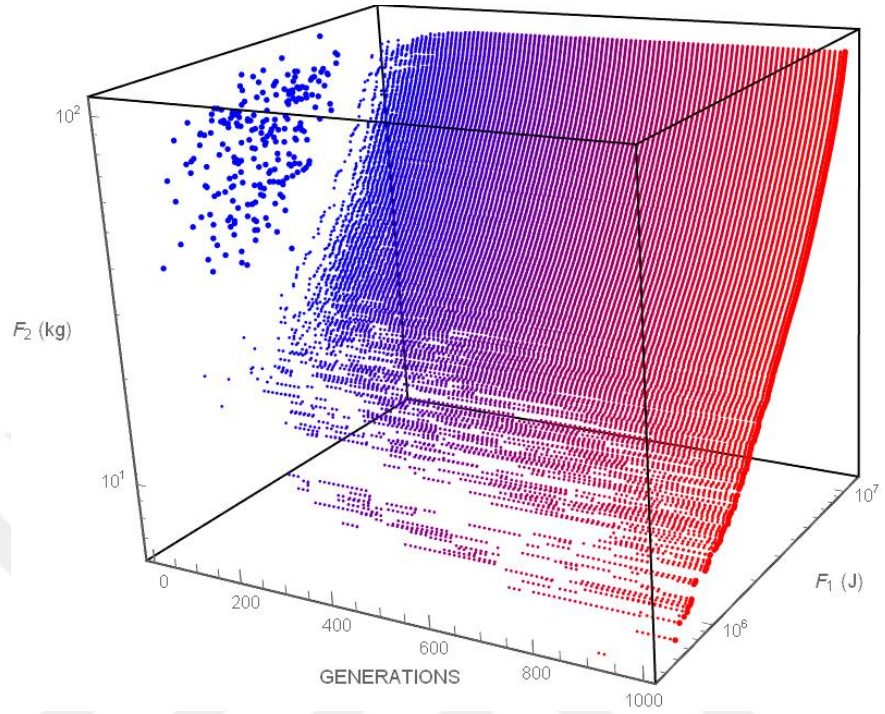

Figure D. 1 Speed of convergence for ω_{max}=100000 rpm

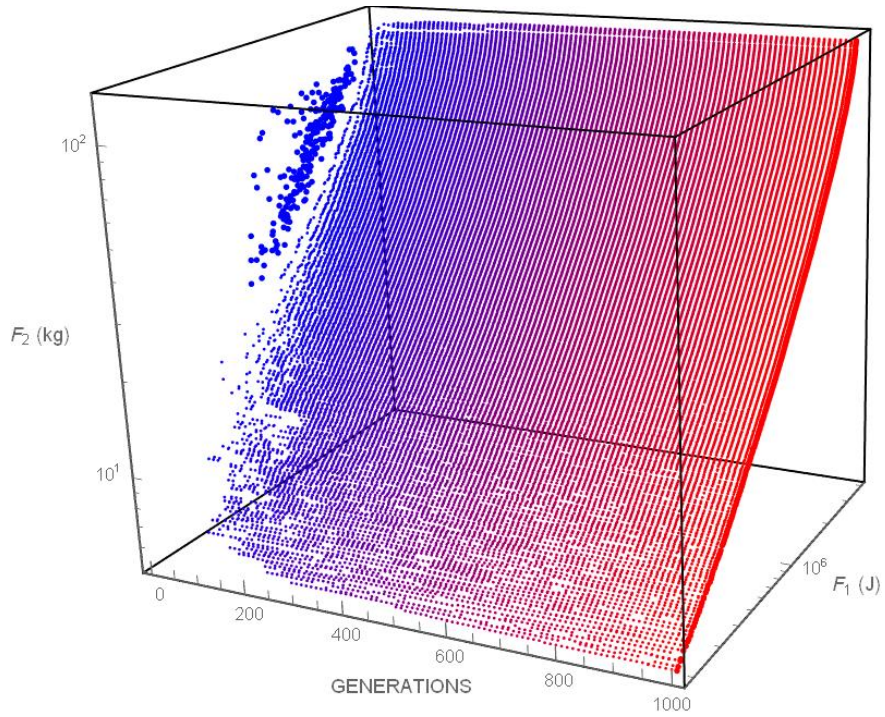

Figure D. 2 Speed of convergence for ω_{max}=10000 rpm

CIRRICULUM VITAE

Name Surname **:** Alper Uyar

Place and Date of Birth **:** Eskişehir, 10/01/1980

E-Mail **:** alper_uyar@yahoo.com

EDUCATION

- **High School** **:** 1997, Eskişehir Fen Lisesi
- **B.Sc.** **:** 2002, ITU Aeronautical Engineering
- **M.Sc.** **:** 2005, OGU Engineering Management

PROFESSIONAL EXPERIENCE AND REWARDS:

- 2014- …. (current job): GE Aviation, Design Engineer
- 2007- 2014 : TEI, Design Engineer
- 2002-2007 : FORD Otosan, Method Engineer

US Patent for a Bearing Support Apparatus (Co-inventor) for a Gas Turbine.

https://www.google.ch/patents/US8727632